Arild Helseth

Modelling Reliability of Supply and Infrastructural Dependency in Energy Distribution Systems

Thesis for the degree of philosophiae doctor

Trondheim, March 2008

Norwegian University of Science and Technology
Faculty of Information Technology,
Mathematics and Electrical Engineering
Department of Electric Power Engineering

NTNU

Norwegian University of Science and Technology

Thesis for the degree of philosophiae doctor

Faculty of Information Technology,
Mathematics and Electrical Engineering
Department of Electric Power Engineering

ISBN 978-82-471-7748-8 (printed version)
ISBN 978-82-471-7751-8 (electronic version)
ISSN 1503-8181

Doctoral theses at NTNU, 2008:87

Printed by NTNU-trykk

Acknowledgements

This thesis documents the results of my research performed at the Electric Power Systems Group of the Norwegian University of Science and Technology (NTNU), lasting from September 2004 to March 2008.

I would like to express my gratitude to a number of people who have contributed in various ways to the completion of this thesis. First of all I would like to thank my supervisor Professor Arne T. Holen for guiding me through this work. He has always been supportive and inspiring in his ideas and advice, while keeping a critical eye on the scientific results. I have greatly appreciated the flexible and self-responsible way of working under his supervision, allowing me to explore various fields of energy system modelling.

I would like to thank Gerd Kjølle and Einar Jordanger at SINTEF Energy Research who have, together with Prof. Holen, established an arena for multi-disciplinary energy system research through the research project *Sustainable Energy Distribution Systems*. Various project workshops and meetings have provided useful input to this thesis.

I greatly appreciated the cooperation with Gaudenz Koeppel from ETH Zürich. Our scientific discussions and exchange of ideas significantly contributed to Chapter 5 of this thesis.

In 2006 I spent three months at INESC Porto, in an inspiring and pleasant environment. I am grateful to Professor Vladimiro Miranda who made this visit possible.

I also want to thank my colleagues at the power systems group for providing a good atmosphere, making this period an enjoyable time.

Most of all I thank my family; my parents Mariann and Nils for always supporting me, and in particular my wife Elisabeth Kristin, for her love and understanding throughout these years.

Trondheim, March 2008
Arild Helseth

Abstract

This thesis presents methods and models for assessing reliability of supply and infrastructural dependency in energy distribution systems with multiple energy carriers. The three energy carriers of electric power, natural gas and district heating are considered.

Models and methods for assessing reliability of supply in electric power systems are well documented, frequently applied in the industry and continuously being subject to research and improvement. On the contrary, there are comparatively few examples of formal reliability assessment models and methods applied to natural gas and district heating systems. This work aims at contributing to bridge this gap, considering the structural, operational and physical similarities and differences between the systems. A method for evaluating the reliability of supply in natural gas distribution systems is presented, based on state-of-the-art reliability calculations from the electric power domain. Furthermore, a novel modelling approach incorporating pipeline storage in reliability evaluation of high-pressure natural gas pipeline systems is presented.

Parallel energy infrastructures depend on each other at different levels, two of which are addressed in this work. First, by introducing a second energy carrier in an area dominated by electric power, the type of energy end-uses served by the electric power system is affected. An optimisation problem is formulated, finding the optimal allocation of switchgear in an electric power distribution system. It is shown how changes in energy end-uses cause changes in the expected customer interruption costs, which in turn affects the optimisation problem. Second, the dependency of district heating systems on electric power is modelled. Network models for the two systems are coupled, and the consequences of higher-order power system failures are quantified for both systems.

The methods and approaches presented in this thesis are demonstrated by use of simple examples, and applied to test networks and case studies.

Contents

Acknowledgements **iii**

Abstract **v**

1 Introduction **1**
1.1 Background and Motivation 1
1.2 The SEDS Project 2
1.3 Objective 3
1.4 Main Contributions 3
1.5 List of Publications 4
1.6 Thesis Outline 5
1.7 Network Modelling Notation 6

2 Electric Power Distribution Systems **9**
2.1 Reliability Modelling and Hierarchical Levels 9
2.2 Distribution System Operation 11
2.3 Switchgear and System Protection 11
2.4 Basic Reliability Indices 12
2.4.1 Without Load Transfer 13
2.4.2 With Load Transfer 14
2.4.3 With Load Transfer and Network Constraints 14
2.5 Analytical Simulation 16
2.5.1 A Two-Stage Restoration Procedure 17
2.6 Energy End-uses and Customer Interruption Costs 19
2.6.1 Energy End-uses 19
2.6.2 Customer Interruption Costs 20
2.6.3 Load Duration Curves 21
2.7 Optimal Allocation of Switchgear 22
2.7.1 Application to Test Systems 23

3 Natural Gas Distribution Systems **25**
3.1 Reliability Modelling and Hierarchical Levels 25
3.2 Previous Studies 27
3.3 Unwanted Events 27
3.4 Component Failures 28
3.4.1 Regulator Station 28
3.4.2 Pipeline 28
3.5 Valve Allocation 29
3.6 Operator Response to Failures 30
3.7 Reliability Modelling 31
3.7.1 Test System I 31
3.7.2 Test System II 32

4 District Heating Systems **35**
4.1 Reliability Modelling and Hierarchical Levels 35
4.2 Previous Studies 36
4.3 Component Failures 37
4.4 Describing Thermal Power Flow 38
4.4.1 Changes in Pressure and Temperature 39
4.4.2 Steady-State Response to Failures 40
4.5 A Network Flow Model 41
4.6 Controlling Thermal Power Flow 43
4.7 A Simplified Thermal Power-Flow Model 44
4.7.1 Example: A Simple Test System 45
4.7.2 Applicability of the Simplified Model 47

5 Pipeline Storage **49**
5.1 Introduction 49
5.2 Previous Studies 50
5.3 Storage in Natural Gas Pipelines 51
5.4 Survival Time 52
5.4.1 Example: Survival Time of a Pipeline 53
5.5 Markov Approach for Pipeline Storage 54
5.5.1 Storage Failure Rate 54
5.5.2 Markov Model 55
5.5.3 Assumptions 55
5.5.4 Reliability Indices 57
5.5.5 Model Extensions 57
5.6 Modelling Storage in Pipeline Networks 58
5.6.1 Example: Network Storage 59
5.7 Application to District Heating Systems 60

6 Closure **63**
6.1 Summary 63
6.2 Potential Applications 64
6.3 Concluding Comments 65
6.4 Future Work 66

A Flow in Pipeline Networks **67**
A.1 Introduction 67
A.2 Nodal Formulation 68
A.3 Loop Formulation 69
A.4 Newton Loop-node Method 70

B Publications **73**
B.1 Publication A 75
B.2 Publication B 85
B.3 Publication C 93
B.4 Publication D 103

Bibliography **113**

List of Acronyms

AOS	Automatically Operated Switch
CB	Circuit Breaker
DHS	District Heating System
DSO	Distribution System Operator
ECOST	Expected Customer Interruption Cost
EPDS	Electrical Power Distribution System
EPS	Electrical Power System
GA	Genetic Algorithm
HLI	Hierarchical Level I
HLII	Hierarchical Level II
HLIII	Hierarchical Level III
LDC	Load Duration Curve
LV	Low Voltage
MOS	Manually Operated Switch
MOV	Manually Operated Valve
MRS	Measuring and Regulating Station
MTTF	Mean Time To Failure
MV	Medium Voltage
NGDS	Natural Gas Distribution System
NGS	Natural Gas System
NO	Normally Open Point/Switch

pu	Per Unit
ROV	Remotely Operated Valve
RS	Regulator Station
SCDF	Sector Customer Damage Function
SEDS	Sustainable Energy Distribution Systems

List of Symbols

B	Number of branches
D_i	Thermal power demand at node i
G_i	Thermal power production at node i
$I_{b,max}$	Maximum current for branch b
I_b	Current in branch b
L_i	Load demand at node i
N	Number of nodes
P^t	Thermal power
$P^t_{b(i,j)}$	Thermal power flow in pipeline b
P_i	Electric power demand at node i
P^t_{curt}	Curtailed thermal power
Q	Mass flow
ST_{ij}	Survival time of pipeline b_{ij}
S_{ij}	Storage in pipeline b_{ij}
T	Temperature
U_i	Average annual outage time for load point i
V_{ij}	Total gas volume in pipeline b_{ij}
V^{min}_{ij}	Minimum gas volume in pipeline b_{ij}
V^s_{ij}	Storage gas volume in pipeline b_{ij}
V_i	Voltage at node i
V_{min}	Minimum voltage
ΔT	Temperature differential
λ_b	Failure rate of component b
λ_i	Average interruption rate of load point i
λ_s	Storage failure rate
λ_{PL}	Pipeline leakage failure rate
λ_{PR}	Pipeline rupture failure rate
λ_{RS}	Regulator station failure rate
λ_u	Upstream failure rate

μ_s	Storage repair rate
μ_u	Upstream repair rate
ζ_i	Interruption cost for the customer sector at load point i
p_{init}	Initial pressure
p_{min}	Minimum pressure
pr	Probability
r_i	Average outage time for load point i
r_{ib}	Interruption duration at load point i due to failure of component b

Chapter 1

Introduction

1.1 Background and Motivation

Large parts of today's energy infrastructure was constructed during the second half of the 20^{th} century. In Norway, development of the hydropower industry has strongly influenced the current energy infrastructure. Unlike the general case for most European countries, Norway has traditionally met most of its stationary energy demand with electricity, including the demand for space heating and hot-tap water. Cheap and abundant access to electric power has to a certain degree suppressed the need for other energy sources and infrastructures. However, after the deregulation of the Norwegian electricity market in the 1990s, the increase in installed electric power generation capacity was less than the increase in load demand. This changing pattern was mainly due to low electricity prices during the period, together with the fact that the national energy companies were no longer obliged to meet the load growth. Currently, Norway is a net importer of electricity in normal hydrological years. The situation has led to a strong emphasis on establishing parallel energy infrastructures to decrease our dependency on electricity.

Reliability of supply has become an important planning criterion when maintaining and reinforcing the electric power infrastructure. Reliability assessment methodologies are well documented in the literature [1–3] and are continuously being subject to research and improvement [4]. On the contrary, there are comparatively few examples of formal reliability assessment

models and methods applied to natural gas and district heating systems. Why is this so?

First, there is a relation between size and impact. It is clear that the electric power system is and will be the largest of these infrastructures, transporting the most energy and reaching the most consumers. Being the backbone of most nations' energy systems, comparison of methods, benchmarks and failure statistics regarding the electric power system is exchanged between researchers and practitioners across the world. Second, electricity covers certain customer end-uses that are not easily covered by other energy carriers. Apparent examples are lighting and computerised systems. Our society has become particularly sensitive to short-duration interruptions of supply to these end-uses. Natural gas and district heating systems normally only cover a subset of all energy end-uses, and one may argue that customers are less vulnerable to interruptions of supply to these.

However relevant, these arguments do not exclude the need for methods to estimate the level of reliability in natural gas and district heating systems as well. After all, the basic goal of these systems is the same; to supply customers with energy as economically as possible and with an acceptable degree of quality and reliability of service.

Another aspect influencing the need for models and methods concerns the rules and regulations that apply to the different energy carriers. As an example from the power system domain, several countries have estimated the costs associated with customer interruptions. In Norway, a specific regulation scheme is applied, adjusting the revenue of the network companies in accordance with the customers' interruption costs [5]. This scheme is intended to guide network companies arriving at an optimal level of reliability. Appropriate regulations generally provide an incentive to treat reliability of supply as an important criterion in the planning process, which in turn boosts the need for accurate reliability assessment methods.

1.2 The SEDS Project

This work is a contribution to the research project *Sustainable Energy Distribution Systems* (SEDS). The SEDS project was initiated in 2002 and is conducted by SINTEF Energy Research and the Department of Electric Power Engineering at the Norwegian University of Science and Technology.

The major objective of the SEDS project is to develop methods and models that allow several energy sources and carriers to be optimally integrated with the existing electric power system. Particular emphasis is placed on distribution systems and integration of distributed energy sources, from a technical, economical and environmental point of view.

The SEDS project emphasise on the following energy carriers:

- Electric power
- Natural gas
- District heating

Furthermore, as the project concerns local (or regional) energy planning, the geographical system-boundary typically encompasses a municipality, a suburban area or a city.

1.3 Objective

This work adheres to the SEDS-project framework. Thus, the distribution systems considered and their system boundaries are basically as described in Section 1.2.

The objective of this work is to present and discuss different methods and models for assessing:

a) Reliability of supply in energy distribution systems

b) Dependency between energy distribution systems

1.4 Main Contributions

This work presents methods suitable for assessing the reliability of supply and infrastructural dependency in energy distribution systems with multiple energy carriers. These methods were tested by applying network models of

electric power, natural gas and district heating systems. More precisely, the main contributions can be summarised as follows:

- A method for finding the optimal allocation of switchgear in an electric power distribution system subject to changes in energy end-uses supplied by the system. Changes in energy end-uses cause changes in the expected customer interruption costs, which in turn affect the optimisation problem. Such changes typically occur in areas where a second energy carrier is introduced along with the existing electric power system to serve energy demand. The novel part in this method is the incorporation of changes in energy end-uses in the optimisation problem.
- A conventional approach for quantifying reliability of supply in electric power distribution systems applied to natural gas distribution systems. Structural and operational similarities between the two systems justify the novel application of this approach.
- A method suitable for assessing the dependency of a district heating system on supply from the electric power system. Network models of the two systems are coupled and the dependency is explicitly modelled. This method differs from other published material in the way consequences of power system failures are quantified for the energy supply as a whole. A simplified thermal power-flow model intended for contingency evaluation in the district heating system was developed and applied along with this method.
- A novel Markov-based method for quantifying the impact of pipeline storage on the reliability of supply in pipeline energy systems. The concept of storage failure rate is introduced.
- Several basic examples are presented to demonstrate the modelling approaches and discuss the simplifying assumptions. In addition, most of the presented models are applied to larger test systems or case studies.

1.5 List of Publications

The main contributions of this thesis are presented in Publications A-D listed below. These publications are presented in Appendix B.

- **Publication A:** A. Helseth and A. T. Holen. Impact of Energy End-use and Customer Interruption Cost on Optimal Allocation of Switchgear in Constrained Distribution Networks. *IEEE Transactions on Power Delivery*, accepted for future publication.
- **Publication B:** A. Helseth and A. T. Holen. Reliability Modeling of Gas and Electric Power Distribution Systems; Similarities and Differences. In *Proc. of 9th International Conference on Probabilistic Methods Applied to Power Systems*, Stockholm, Sweden, 2006.
- **Publication C:** A. Helseth and A. T. Holen. Structural Vulnerability of Energy Distribution Systems; Incorporating Infrastructural Dependencies. Accepted for presentation at *16th Power Systems Computation Conference*, Glasgow, Scotland, 2008.
- **Publication D:** A. Helseth and G. Koeppel. Pipeline Storage and its Impact on Reliability of Supply in Pipeline Energy Systems. *Reliability Engineering & System Safety*, in review.

Besides, the following two publications are early, and slightly different, versions of publications A and D:

- A. Helseth and A. T. Holen. Impact of Energy End-use on Optimal Allocation of Switchgear in Radial Distribution Networks. In *Proc. of 3rd International Symposium on Modern Electric Power Systems*, Wrocław, Poland, 2006.
- A. Helseth and G. Koeppel. Storage Potential in Pipelines and its Impact on Reliability of Supply. In *Proc. of the European Safety and Reliability Conference*, Stavanger, Norway, 2007.

1.6 Thesis Outline

Publications A-D, as listed in Section 1.5, are introduced in Chapters 2 - 5. The energy distribution systems of electric power, natural gas and district heating are addressed in Chapters 2, 3 and 4, respectively. These chapters discuss the essential structural and operational topologies of each system, focusing on similarities and differences between the systems which are relevant for the presented models and methods.

It should be noted that the chapters do not fully summarise the findings in the publications. They rather serve as introductions to their associated publication, without reproducing the case-study results in the publications. Some of the chapters also contain supplemental material and examples. Thus, it is recommended to read each chapter and its associated publication in conjunction. A brief description of each chapter is given below.

Chapter 2: concerns the electric power distribution system and serves as a background for Publication A. A method for finding optimal allocation of switchgear is presented.

Chapter 3: concerns the natural gas distribution system and serves as a background and supplement to the reliability evaluation approach presented in Publication B.

Chapter 4: concerns the district heating system and describes a thermal power-flow model suitable for contingency analysis as performed in Publication C.

Chapter 5: concerns pipeline storage in natural gas pipeline systems and its impact on reliability of supply. This chapter serves as a background and supplement to Publication D.

Chapter 6: concludes the thesis by summarising the major achievements, discussing potential applications and suggesting possible future work.

1.7 Network Modelling Notation

The purpose of this section is to introduce the basic network modelling notation used throughout this thesis.

The topology of an energy distribution system can be represented by a graph $\mathcal{G}$ comprising a set of nodes $\mathcal{N}$ and branches $\mathcal{B}$. A branch connects a pair of distinct nodes.

Nodes are indexed i and branches b in the subsequent chapters, and there are N nodes and B branches in the sets $\mathcal{N}$ and $\mathcal{B}$, respectively.

$$i \in \mathcal{N} = \{1, ..., i, ..., N\}$$
$$b \in \mathcal{B} = \{1, ..., b, ..., B\}$$

The graph $\mathcal{G}$ represents only the topology of a distribution system, and gives no further information about its elements. When adding additional, quantitative information to the graph, it is referred to as a network.

Lines, cables, pipelines, compressors, pumps, valves and switches are typical representations and subclasses of a branch.

Load points, junctions and generators are typical representations and subclasses of a node. Load point nodes are in a subset $\mathcal{N}_L \subseteq \mathcal{N}$. Similarly, electric and thermal power generation nodes are in a subset $\mathcal{N}_G \subseteq \mathcal{N}$.

Chapter 2

Electric Power Distribution Systems

Publication A

The first part of this chapter provides a perspective on reliability modelling in electric power distribution systems. First, the hierarchical levels commonly applied in reliability evaluation of electric power systems are presented. The scope is then narrowed to the distribution system and the modelling techniques and assumptions applied in Publication A are explained. It is described how the impact of changes in energy end-use on customer interruption costs was quantified in Publication A.

2.1 Reliability Modelling and Hierarchical Levels

Today's electric power systems (EPS) are complex interconnected systems commonly being divided into four major parts; generation, transmission, distribution and loads. Fig. 2.1 illustrates the interrelation of the various networks and the connection of generators and loads. The transmission system is used to transfer large amounts of energy from the main generation area to major load centres. The extra-high voltage (EHV) and the high voltage (HV) levels are considered parts of the transmission system. In Fig. 2.1, the distribution systems comprise two different voltage levels, the medium voltage (MV) and low voltage (LV). The HV and MV networks provide

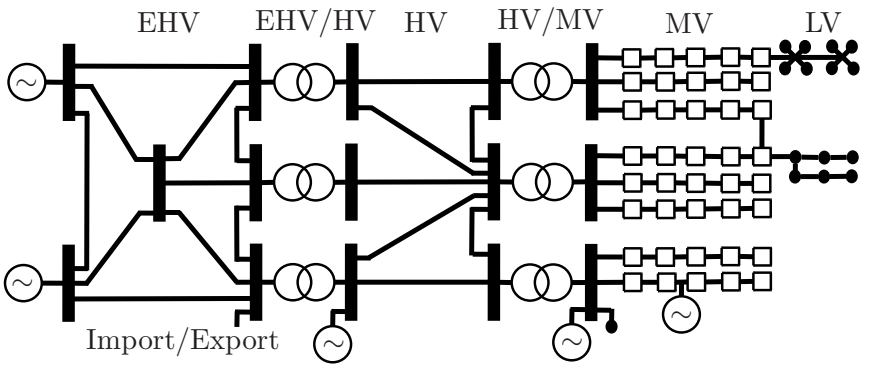

Figure 2.1: Illustration of an electrical power system (□ = MV/LV substation and • = load point).

supplies direct to large customers, but the vast majority of customers are connected at LV and supplied via MV/LV substations.

Techniques for power system reliability analysis are normally categorised in terms of their application to different parts of the power system [6]. The power system may be divided in three different functional zones, relating to generation, transmission and distribution facilities. Reliability studies are conducted within functional zones or within a hierarchical level. Hierarchical levels are combinations of zones as described in [6] and shown in Fig. 2.2. Hierarchical level I (HLI) is only concerned with the generation facilities, hierarchical level II (HLII) includes both generation and transmission facilities and hierarchical level III (HLIII) includes all functional zones. Assessing the reliability of the entire power system as one single entity would be exhaustive and make meaningful data interpretation difficult. Therefore, studies aimed at HLIII are normally performed for the distribution functional zone only. In case a complete HLIII study is wanted, results from reliability studies at HLII may serve as input to reliability studies in the distribution functional zone [2].

Failures of facilities in the generation and transmission functional zones may cause widespread system consequences. For this reason, a majority of the research effort has been aimed at improving techniques for reliability assessment of HLI and HLII. Comparatively, distribution systems have received less attention. However, the fact that distribution facilities have greater average effect on loss of supply to customers than generation and transmission facilities, necessitates accurate reliability assessment techniques for this

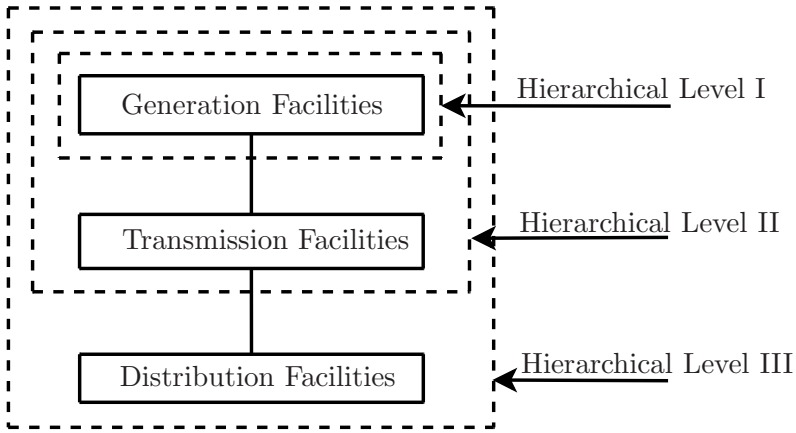

Figure 2.2: Functional zones and hierarchical levels.

domain as well.

The remaining part of this chapter concerns radially operated Electric Power Distribution Systems (EPDS) at MV level. First, some basic operational concepts and modelling techniques are discussed.

2.2 Distribution System Operation

The structural topology of an EPDS varies from the pure radial system in rural areas to highly meshed systems in urban areas. Most distribution system operators (DSOs) choose to operate the system radially. Considering power losses and voltage drops, it would be beneficial to apply a meshed operational topology whenever possible. However, as protection arrangements are simpler, voltage control is easier and fault levels are lower, the preferred operational topology is normally the radial one [7]. The techniques applied in the remainder of this chapter are aimed at radially operated EPDSs.

2.3 Switchgear and System Protection

A wide variety of switchgear and protective devices may be applied in an EPDS. Below is a brief and general introduction to the devices considered

in Publication A, and the assumptions regarding their locations.

Consider the EPDS radial shown in Fig. 2.3, containing fuses (f_1-f_3), a circuit breaker (CB) and switches (s_1-s_5). Fuses are overcurrent protection devices. Once a fuse has melted and operated due to a downstream fault, it requires replacement before the protected branch can carry load again. It is assumed that no fuse has switchgear located downstream of it. A circuit breaker has the ability to break fault currents and is located at the sending end of each branch leaving the HV/MV substation.

Two types of switches are considered; the automatically[1] operated (AOS) and the manually operated switch (MOS). An AOS will automatically isolate a permanently faulted section of a distribution circuit once an upstream circuit breaker has interrupted the fault current. In contrast, the MOS requires the presence of a repair crew in order to be operated. It is clear that an EPDS containing AOSs will provide faster failure isolation and network reconfiguration than would be the case for MOSs. However, as neither of these has the ability to break fault currents, the type of switch will not influence the frequency of interruptions experienced by customers.

2.4 Basic Reliability Indices

The system shown in Fig. 2.3 illustrates a simple EPDS radial. The radial receives power from an HV/MV substation to feed load points L_A-L_C. These load points represent the aggregation of loads connected to the underlying LV network, downstream MV/LV transformers t_a-t_c. EPDS cables and lines are either classified as terminal or primary branches. Terminal branches (a-c) have no downstream connected MV cables or lines and are equipped with fuses at their sending ends. Primary branches (1-3) are not directly connected to MV/LV transformers and may have switches at both their sending and receiving ends.

The reliability assessment procedure is based on the following assumptions:

- only first-order permanent failures are considered;

[1] Automatic switches could be replaced with remote controlled switches in the presented method. One could loosely speak of one fast (automatic or remote control) and one slow (manual control) switch.

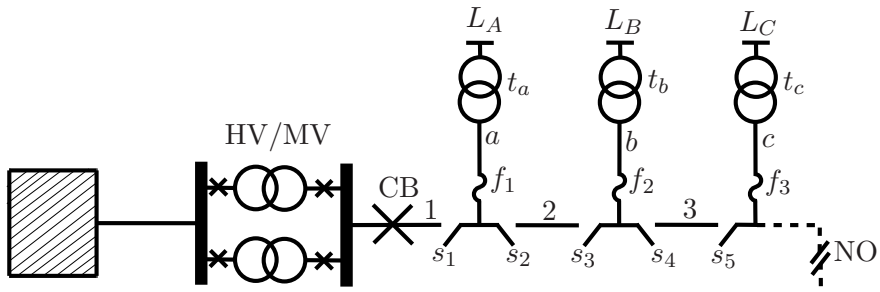

Figure 2.3: An electric power distribution system radial.

- all switchgear is fully reliable and properly coordinated.

2.4.1 Without Load Transfer

Consider the radial in Fig. 2.3 without any load transfer possibilities. In case the primary branch labelled 2 fails, the CB will open and de-energise the entire radial, interrupting supply to all load points. Subsequently, the switches s_2 and s_3 are used to isolate the faulted branch. Now CB is reset and supply to L_A is restored. L_B and L_C will not have their supply restored before branch 2 has been repaired.

For EPDS radials similar to the one in Fig. 2.3, the basic reliability parameters of average interruption rate λ_i, average annual outage time U_i and average outage time r_i for each load point i are found directly from (2.1).

$$\lambda_i = \sum_{\alpha \in \mathcal{S}_1} \lambda_\alpha + \sum_{\beta \in \mathcal{S}_2} \lambda_\beta \tag{2.1a}$$

$$U_i = \sum_{\alpha \in \mathcal{S}_1} \lambda_\alpha r_\alpha + \sum_{\beta \in \mathcal{S}_2} \lambda_\beta s \tag{2.1b}$$

$$r_i = \frac{U_i}{\lambda_i} \tag{2.1c}$$

where:

$\mathcal{S}_1$ = set of components upstream from load point i
$\mathcal{S}_2$ = set of primary branches downstream from load point i
$\lambda_{\{\alpha,\beta\}}$ = average failure rate of component $\{\alpha, \beta\}$
r_α = repair time of component α
s = sectionalising time

2.4.2 With Load Transfer

Now we assume that it is possible to supply all load connected to the radial through an adjacent radial by closing a normally open switch (NO), as illustrated with the dotted line in Fig. 2.3. Equations (2.1) still apply, but the sets $\mathcal{S}_1$ and $\mathcal{S}_2$ need to be redefined for each load point as follows. $\mathcal{S}_1$ will now comprise the set of components downstream the fuse protecting the terminal branch serving load point i. Evaluating L_B, $\mathcal{S}_1$ will contain components b and t_b. $\mathcal{S}_2$ will contain all primary branches on the radial, i.e. branches 1-3. Consequently, the average interruption rates will not be affected by the inclusion of a load transfer possibility, but the average annual outage times will decrease for all load points.

2.4.3 With Load Transfer and Network Constraints

In some cases, the ability to transfer load to another radial can be limited due to network constraints. Nodal voltages and branch currents must be within a predefined range in order to sufficiently supply customers and avoid equipment damages. For each load point i and each branch b, the voltages and currents must meet their corresponding minimum (V_{min}) and maximum ($I_{b,max}$) constraints in (2.2). In order to control that network constraints are not violated, an algorithm for computing the power flow in radial EPDS was applied, as described in [8].

$$\forall i \in \mathcal{N}_L : \; V_i \geq V_{min} \tag{2.2a}$$
$$\forall b \in \mathcal{B} : \; I_b \leq I_{b,max} \tag{2.2b}$$

Treating network constraints in a reliability model is not straightforward and depends, among other things, on utility practises and available switchgear. Consider a permanent failure of branch 1, as illustrated in Fig. 2.4. In

case load transfer capability is sufficient to supply loads L_A-L_C, CB and s_1 will open to isolate the faulted branch, and NO will close to transfer load. All load points are backfed until the faulted branch has been repaired and the normal system configuration is restored. However, if this load transfer will violate constraints in (2.2), alternative switch operations should be sought. In the further analysis load is always cut at the receiving end of the overloaded radial. Thus, we look for the closest switch downstream s_1, which is s_2, and re-evaluate the constraints assuming s_2 open. If the constraints are not violated this time, load points L_B and L_C are backfed, whereas L_A stays disconnected until branch 1 has been repaired. Compared to the case with no load transfer restrictions, branch 1 will be moved from set $\mathcal{S}_2$ to $\mathcal{S}_1$ for load point L_A. Thus, L_A will experience an increase in average annual outage time. The basic reliability parameters for the remaining load points will not change.

In this work, constraints were considered absolute, i.e. they cannot be violated. In practise, network constraints are not always treated as absolute requirements. For example, in case the voltage magnitude of L_A in Fig. 2.4 is marginally less than V_{min}, it is difficult to predict whether the DSO would strictly adhere to the constraint by not backfeeding L_A.

Customers must be prioritised if constraints are violated when transferring load. In principle, there are many possible strategies for prioritising load [2, 9], and some of them are listed below.

- cut load to customers with interruptible contracts;
- supply the maximum possible load without violating constraints;
- reduce load proportionally at all load points that can affect the overload;
- cut load at the receiving end of the overloaded radial.

Partial supply to aggregated load points was not considered in this work; thus, load points were either supplied or not supplied at all.

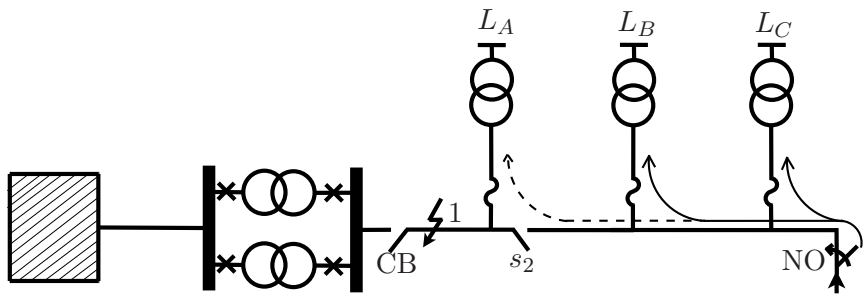

Figure 2.4: Illustration of switch operations and branch power flows subject to the failure of branch 1 and a subsequent system reconfiguration.

2.5 Analytical Simulation

In this section the reliability assessment procedure applied in Publication A is presented. The procedure is valid for any combination of AOSs and MOSs, given that the placement of switches adheres to the previously stated assumptions.

Rather than defining the cut sets $\mathcal{S}_1$ and $\mathcal{S}_2$ for each load point, it is possible to assess the impact of failures and accumulate load point indices sequentially. This technique, often referred to as analytical simulation, is intuitive and capable of capturing detailed physical and operational characteristics of the EPDS [3, 10]. The basic steps of the analytical simulation technique are outlined below.

1. Select a component b with failure rate λ_b

2. Simulate the system's response to the failure of b and compute the impact on all load points

3. Weight the impacts by λ_b

4. Repeat the steps until the failure of all components have been simulated

2.5.1 A Two-Stage Restoration Procedure

In the applied EPDS network model, both lines and transformers were modelled as branches. A two-stage restoration procedure was implemented, as described in [11] and outlined below. Interrupted load points are classified in sets $\mathcal{S}_A$, $\mathcal{S}_B$ and $\mathcal{S}_C$, depending on the interruption duration. First, a limited set of load points are restored by using the available AOSs. These load points experience an interruption of duration equal to the automatic sectionalising time and belong to $\mathcal{S}_A$. Second, additional load points are restored by using the available MOSs. These load points experience an interruption of duration equal to the manual sectionalising time and belong to $\mathcal{S}_B$. Load points which are not restored before the faulted component has been repaired belong to $\mathcal{S}_C$.

Fig. 2.5 shows a flow chart of the restoration procedure, focusing on the automatic restoration. A faulted branch b with nodes (ii, jj) is selected. First, an upstream search is performed from node ii. In case a fuse is found upstream b, it operates and all load points downstream the fuse belong to $\mathcal{S}_C$, while the remaining load points are not interrupted. In case there are no fuses upstream b, the circuit breaker will de-energise the faulted line and all load points on the radial are interrupted. The upstream search will also look for the AOS closest to ii and restore upstream load points by opening this. In case there is a load transfer possibility through a normally open point controlled by an AOS (AOS_{LT}) downstream jj, the downstream restoration part of the algorithm starts. A downstream search from node jj of the faulted branch is initiated, looking for the closest AOS (AOS_{DS}). If any AOS_{DS} is identified, a power flow analysis is performed, assuming AOS_{LT} closed and AOS_{DS} open. If the network constraints are met, AOS_{LT} is closed and AOS_{DS} is opened, otherwise a new downstream search is initiated to find the next AOS_{DS}.

Once the automatic response has finished, it is possible to identify the load points belonging to $\mathcal{S}_A$. Load points on the faulted radial which have not had their supply restored yet, will either belong to $\mathcal{S}_B$ or $\mathcal{S}_C$, depending on the manual restoration.

It should be noted that the algorithm illustrated in Fig. 2.5 only considers single load transfer options. A procedure including multiple transfer options would be more elaborate, requiring a method for prioritising the transfer option with the highest available capacity.

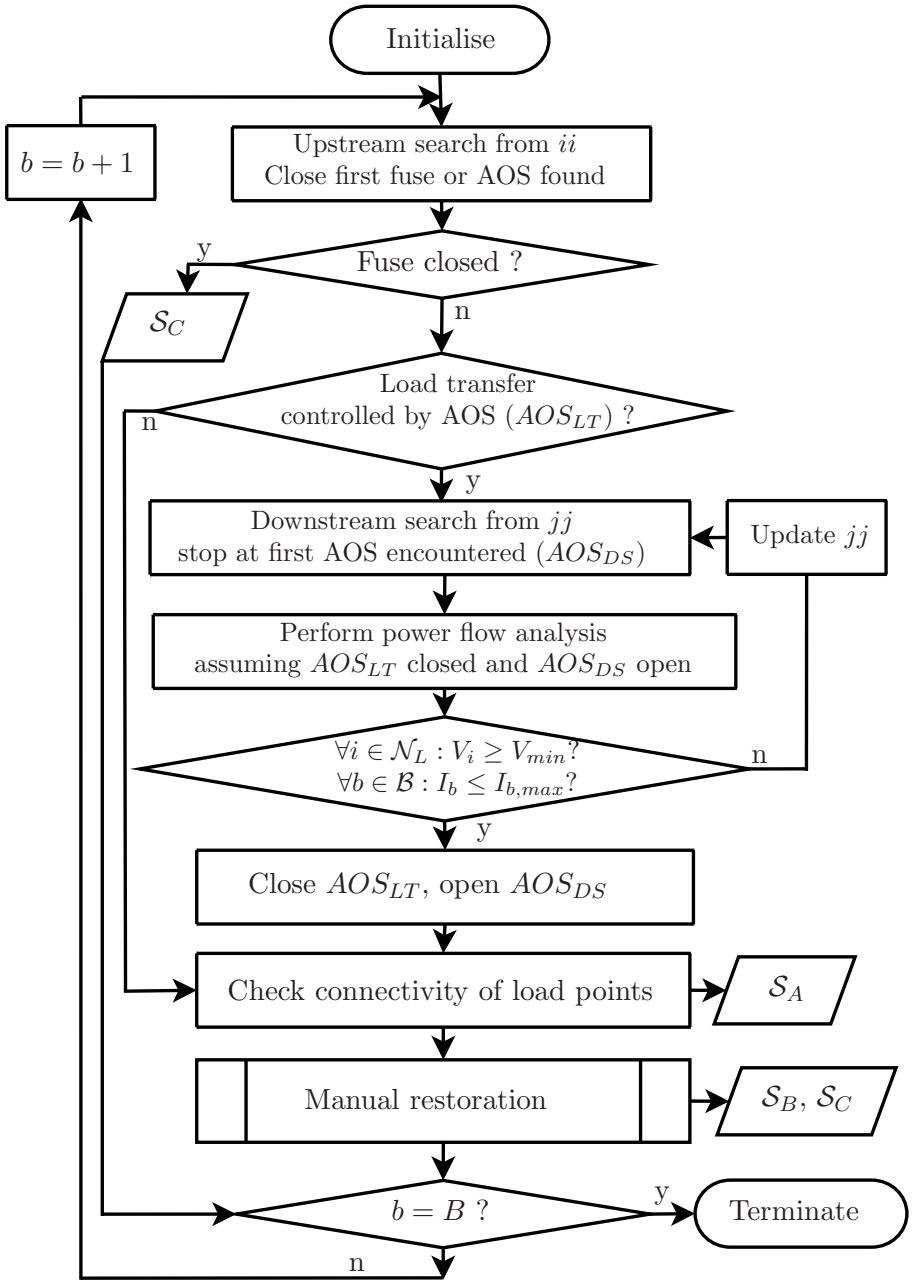

Figure 2.5: Flowchart of the automatic restoration stage.

2.6 Energy End-uses and Customer Interruption Costs

So far, a conventional approach for finding the basic reliability parameters in an EPDS has been presented. In this section it is shown how the expected customer interruption costs can be found based on results from the analytical simulation approach. It is elaborated how changes in energy end-uses will impact expected customer interruption costs. This chapter summarises the novel part of the method presented in Publication A.

2.6.1 Energy End-uses

Energy end-uses are often categorised, separating between space heating, hot-tap water, cooling, lighting, fans and pumps, computers, etc. Alternative energy carriers, such as district heating and natural gas, are able to cover some of the same energy end-uses as electricity. Other end-uses can only be covered by electricity. In the further discussion end-uses are aggregated in two major categories:

End-use category:	*Covered by:*
Electricity specific	electricity
Flexible	any energy carrier

Consider an area where all energy end-uses are covered by electricity. By introducing a second energy carrier, such as natural gas or district heating, some of the flexible end-uses initially served by the EPDS will be gradually decoupled and served by the new energy carrier.

Will this shift in magnitude and type of demand affect the optimal level of investments in EPDS reliability-enhancing projects? Intuitively, a relief in demand for electric power will lead to decreased interruption consequences since less power has to be transported to the customers. Thus, the optimal level of investment in reliability will decrease, compared to the case where electricity serves all end-uses. Furthermore, a relief in load demand on a tightly constrained EPDS radial may improve the reconfiguration capability, resulting in reliability improvements without additional investments. On the other hand, customer surveys reveal that the electricity specific

end-uses tend to have a higher associated cost of interruption. These conflicting momentums are all considered when finding the expected customer interruption costs in the presented optimisation method.

2.6.2 Customer Interruption Costs

Different customer sectors apply electricity for different end-uses. Surveys from various countries show that each customer sector will evaluate the loss of supply differently, depending on the interruption duration and the type of end-uses the customer sector typically cover by electricity [12].

One way to monetise reliability of supply is to introduce a specific, sector-dependent interruption cost that is independent of interruption duration. Such costs are applied in several countries, including Norway [5, 12]. The expected customer interruption cost (ECOST) can then be found as:

$$\text{ECOST} = \sum_{b \in \mathcal{B}} \lambda_b \sum_{i \in \mathcal{N}_L} P_i \zeta_i r_{ib} \tag{2.3}$$

where:

λ_b	=	failure rate of component b, in year^{-1}
P_i	=	average power consumption at load point i, in kW
ζ_i	=	interruption cost for the customer sector at load point i, in €/kWh
r_{ib}	=	interruption duration at load point i due to failure of component b, in hours

The two loops in (2.3) represent the analytical simulation approach described in section 2.5, where r_{ib} is determined based on the classification of each load point (in sets $\mathcal{S}_A - \mathcal{S}_C$).

For more detailed system planning, it is believed that the non-linear profile of interruption costs as a function of interruption duration should be accounted for. Such profiles are conveniently displayed in a sector customer damage function (SCDF). SCDFs are created by aggregating the cost functions of individual customers in the same customer sector. By incorporating such functions, equation (2.3) may be reformulated to (2.4).

$$\text{ECOST} = \sum_{b \in \mathcal{B}} \lambda_b \sum_{i \in \mathcal{N}_L} P_i \zeta_i(r_{ib}) \tag{2.4}$$

where:
$\zeta_i(r_{ib})$ = interruption cost for the customer sector at load point i due to failure of component b, in €/kW

The SCDFs provide important information about the costs customers associate with the inability to perform their activities. It was shown in Publication A that the type of activities, or end-uses, performed by a customer will influence the customer damage function.

Consider a load point i where all energy end-uses are covered by electricity and where the SCDF $\zeta_i(r)$ reflects the interruption costs. Suppose that a second energy carrier is introduced and takes over supply of the flexible end-uses at this load point. Results from a survey among Norwegian customers indicate that the interruption costs associated with electricity specific end-uses are different from the interruption costs associated with flexible end-uses [13]. Therefore, it is likely to believe that the true SCDF for this load point can be represented by a function $\zeta_i^{new}(r)$ which is different from $\zeta_i(r)$. Applying $\zeta_i^{new}(r)$ in (2.4) will affect the ECOST. Publication A holds a more detailed presentation of SCDFs and data from the Norwegian survey in [13].

2.6.3 Load Duration Curves

In EPDSs with constrained capacity, power flow studies will reveal whether the network constraints are met before system reconfigurations are performed. Estimates of reconfiguration capability are normally based on system peak load, and thus, contributes to a conservative estimate of network reliability [2]. For more detailed reliability studies, load duration curves (LDCs) may be applied. An LDC comprises load data plotted in a descending order of magnitude, where each load level has a corresponding probability of occurrence. Incorporating such load variations in (2.4), leads to (2.5).

$$\text{ECOST} = \sum_{k \in K} pr_k \sum_{b \in \mathcal{B}} \lambda_b \sum_{i \in \mathcal{N}_L} P_{i,k} \zeta_i(r_{ib}) \tag{2.5}$$

where:
K = number of steps on the LDC
pr_k = probability of load step k
$P_{i,k}$ = power consumption at load point i for load step k, in kW

Decoupling the flexible end-uses from the EPDS will not only reduce the demand for electricity, but also alter the profile of the LDC [14]. Generally, the LDC related to flexible end-uses has a lower utilisation time[2] than is the case for electricity specific end-uses. In order to provide an accurate measure of reconfiguration capability, different LDCs were applied for load points covering all end-uses and those covering electricity specific end-uses only.

2.7 Optimal Allocation of Switchgear

In this section it is briefly discussed how expected customer interruption costs can be included in an optimisation procedure for finding the optimal allocation of switches in a radially operated EPDS. By performing this type of study, a network company can analyse whether the amount, location and type of switches is appropriate according to the end-uses served by the system. The major findings from the case studies in Publication A and [15] are restated at the end of this section.

Finding the optimal allocation of switchgear in radially operated EPDS is a complex problem which has been addressed by several authors [16–22]. The problem may be classified as a combinatorial optimisation problem having a non-linear and non-differentiable objective function. Various techniques have been applied to solve the optimisation problem, e.g. dynamic programming [16], binary programming [17], simulated annealing [18], direct search [19] and genetic algorithms [20–22].

The applied optimisation procedure is based on a genetic algorithm (GA). The objective function is formulated in 2.6, where ECOST for an EPDS serving a predefined set of end-uses and having a given combination of switches is found from (2.5). ICOST is the total annualised capital cost for the selected set of switches.

$$\text{Minimise: } \text{ECOST} + \text{ICOST} \tag{2.6}$$

[2] utilisation time is defined as the ratio between annual energy and maximum power demands.

2.7.1 Application to Test Systems

The suggested method was tested on the EPDSs connected to buses 5 and 6 of the Roy Billinton Test System (RBTS) described in [23,24]. Two different supply scenarios were assumed:

1. All energy end-uses are supplied by electricity at all load points.
2. All energy end-uses are supplied by electricity at some selected load points, and only the electricity specific end-uses at others.

The optimal allocation of switches was found for both scenarios. Scenario 2 was first tested using the same SCDFs and LDCs as for scenario 1. Then the SCDFs and LDCs were adjusted as described in Section 2.6, and scenario 2 was retested.

The results generally indicated that the amount of switches allocated in the test systems decreases when decoupling the flexible end-uses. However, by using customer interruption costs and load duration curves adjusted according to the electricity specific end-use, the reduction is not as evident as found when using aggregated data. Furthermore, it was found that changes in SCDFs have a more significant impact on the results than changes in LDCs.

Chapter 3

Natural Gas Distribution Systems

Publication B

This chapter summarises and supplements the content of Publication B, where a reliability evaluation approach well known from the electric power domain was applied to natural gas distribution systems.

First, the structural similarities between natural gas and electric power systems are discussed. Subsequently, the most important components in natural gas distribution systems and their possible failure modes are addressed. The impact of valve allocation and system operation on reliability of supply is elaborated. Finally, a test-system study is presented, supplementing the case study in Publication B.

3.1 Reliability Modelling and Hierarchical Levels

Fig. 3.1 illustrates an onshore natural gas system (NGS). In such systems, gas is transported from the source (S) to the consumers through a network of pipelines operated at different pressure levels. The transmission system is characterised by few pipelines covering large distances at high operating pressures. Compressor stations (C) are used to maintain the desired pressure in the transmission network. As an interface between the transmission

and the distribution system, a measuring and regulating station (MRS) meters the gas and reduces its pressure so that it is suitable for distribution purposes. It should be noted that the system presented in Fig. 3.1 is rather simple, as it depends on one source and one transmission pipeline only.

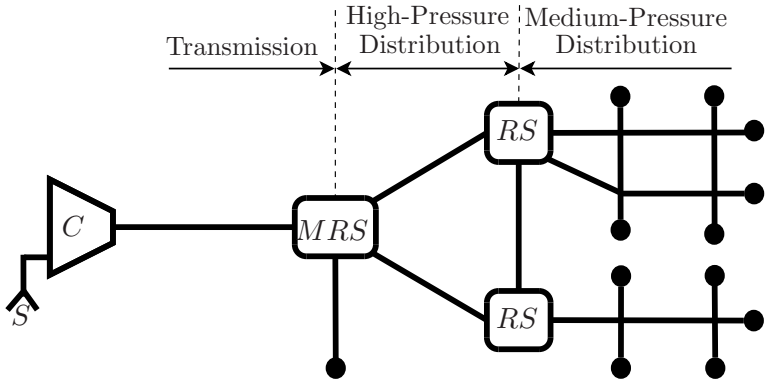

Figure 3.1: Illustration of a natural gas system (• = load point).

There are some obvious analogies between EPSs and NGSs. For example the fact that voltages and pressures are step-wise reduced on the pathway from the transmission system to the customers. For both systems, generators and sources are mainly located at high voltage and pressure level and load is connected at low voltage and pressure. Realising these structural similarities, [25] suggested organising reliability models applied to NGSs in functional zones and hierarchical levels similar to the ones applied in the EPS domain. The following three functional zones were suggested:

1. Gas production, gathering and processing facilities
2. Gas transmission facilities
3. Gas distribution facilities

The presented work and the further discussion in this chapter is concerned with reliability methods applicable in functional zone 3. The system boundary is defined such that MRSs are not encompassed, assuming fully reliable supply from these stations. The natural gas distribution system (NGDS) will normally comprise two or three subsystems, operating at different pressure levels. A regulator station (RS) provides the interface between subsystems. In Fig. 3.1 two subsystems are shown; the high-pressure and the

medium-pressure distribution system. A reliability analysis can be performed considering both subsystems combined as well as either one individually, as discussed in Section 3.4.

3.2 Previous Studies

Reliability evaluation of natural gas production and transmission facilities has been investigated in several publications, such as [25–29]. Authors [27–29] performed Monte Carlo simulations to assess the availability of sufficient compression facilities in the transmission system to meet the consumer load. A method for minimising loss of supply due to transmission pipeline failures was presented in [26]. These publications all concern the natural gas transmission system, considering the downstream distribution systems as aggregated load points. On the contrary, this chapter focus on the NGDS and treats upstream supply from the transmission system as fully reliable.

3.3 Unwanted Events

There are basically two unwanted events in NGSs; gas escape and customer interruptions. Uncontrolled release of natural gas or loss of pressure in the system can cause unsafe situations due to the potential explosive mixture of gas and air. This may be contrasted with electricity, where, in the event of loss of supply, the system itself is considered safe. Thus, when gas leaks from the system, and the leak is considered severe, the component causing the leak will be isolated, which in turn may cause customer interruptions. The system operator will always prioritise to minimise gas escape in critical situations. Therefore, in some cases this objective is followed at the cost of less reliable supply to the end-users.

Available failure statistics are primarily concerned with causes to gas escape, and do not address customer interruptions. It is indicated that pipeline incidents contribute most frequently to gas escape at both transmission [30] and distribution level [31].

3.4 Component Failures

The components in an NGDS may be grouped as regulator stations, pipelines and valves. In the further study it is assumed that all valves are fully reliable. A brief discussion on regulator station and pipeline failures is presented below.

3.4.1 Regulator Station

A regulator station will normally have two parallel and redundant processing lines, each comprising a rather complex setup of valves and pressure regulating devices. A typical setup is presented in Publication B. In the following, a regulator station failure describes the state when the station is not capable of supplying gas to the underlying distribution system. The corresponding failure rate was simply set to λ_{RS}. For detailed reliability studies of regulator stations, the reader should refer to other sources, such as [32].

In case the reliability study encompasses both the high and medium-pressure NGDSs, the regulator station will be within the system boundary. Alternatively, studies can be focused on either of the subsystems alone, using the regulator station as an aggregated load point or upstream source, respectively. Thus, in terms of reliability modelling, the regulator station can be treated analogous to substations in the EPDS.

3.4.2 Pipeline

A pipeline incident may be defined as any event leading to gas escape from the pipeline. It is separated between a pipeline incident and a pipeline failure, as the DSO's response to pipeline incidents will vary depending on the severity of the incident. Pipeline incidents are classified as follows:

- Minor leakage
- Leakage
- Rupture

In case of a minor leakage, the pipeline can be repaired while carrying load. Thus, the pipeline is not taken out of service, and supply to customers is not interrupted. For leakages, described by a pipeline leakage failure-rate λ_{PL}, the pipeline itself is isolated for repair. However, it is assumed that the leakage does not affect gas flow before the pipeline has been isolated. In case of a rupture, described by a pipeline rupture failure-rate λ_{PR}, all supply pathways to the faulted pipeline are shut off as fast as possible. For the further analysis, only leakages and ruptures are considered pipeline failures. It should be stressed that the classification of pipeline incidents in this work is done to separate between the different operator responses to these incidents.

3.5 Valve Allocation

Proper allocation of valves is essential for secure and reliable operation of the NGDS. Valves are installed along the NGDS to allow fault isolation and network reconfiguration. Valves are automatically, remotely or manually operated, depending on pressure level and operating philosophy. In this work it was differentiated between the remotely operated valve (ROV) and the manually operated valve (MOV). Valve allocation follows the practise adopted in Norway [33]; valves in the high-pressure NGDS and at the sending end of pipelines leaving the regulator stations are ROVs. The remaining valves are MOVs. The medium-pressure NGDS shown in Fig. 3.2 exemplifies this layout. The system comprises pipelines 1-9, valves v_1-v_5 and load points L_A- L_D. Valves v_1 and v_2 are ROVs, whereas v_3-v_5 are MOVs.

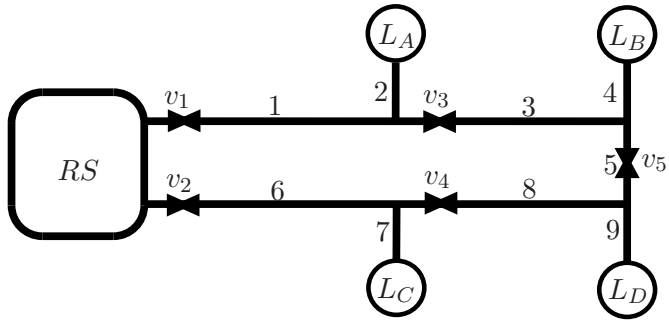

Figure 3.2: Valve allocation in a medium-pressure natural gas distribution system.

3.6 Operator Response to Failures

In case a pipeline fails, the fault is isolated by use of either valves or clamps. Clamps are used to squeeze off the faulted pipeline segment, and it is assumed just as fast to use as MOVs for fault isolation. In either case, the repair crew has to be physically present at the fault location. In case of a leakage, it is assumed that only the faulted pipeline is isolated. In case of a rupture, the closest ROV or set of ROVs are used to isolate the fault from the source(s).

The medium-pressure NGDS shown in Fig. 3.2 has a meshed structural topology. The reliability of supply to consumers may depend on whether the system is operated with an open or closed loop. By closing the valve v_5 under normal operation, the system is radially operated.

In case any of the pipelines on the upper radial in Fig. 3.2 (pipelines 1-4) ruptures, v_1 is closed to limit gas escape. Load points L_A and L_B are interrupted, but load points L_C and L_D are not interrupted since the flow in the lower radial is not affected by the failure response. If the system was operated as a loop by keeping v_5 normally open, the DSO would have to close both v_1 and v_2 to limit gas escape, and thus all load points would be interrupted.

In the case of leakages, the operational topology will not affect reliability of supply. Consider a leakage in pipeline 1. There are no significant changes in gas flow. Technically, the pipeline could be operated while repairing the leakage, but should be isolated for safety reasons. In case v_5 is normally closed, it is assumed that this valve has been opened before pipeline 1 is isolated. Thus, load point interruptions only occur in case the reconfiguration capability is insufficient to backfeed load points L_A and L_B.

The advantage of meshed operation is a better pressure distribution throughout the system and, consequently, the possibility to reduce energy needed for compression upstream the NGDS. On the other hand, larger parts of the NGDS may have to be isolated in case of pipeline ruptures. The argumentation has obvious analogies to the EPDS. Energy losses and voltage drops are reduced when operating the system as a loop, but radial operation is often said to be safer and provide a more reliable system operation. So should valve v_5 be normally open or closed? It seems like industrial practises vary, and there is no obvious answer to this question [33, 34].

Unlike the EPDS, which is extensively equipped with fuses for rapid isolation of failures, there are usually no valves which automatically isolate faulted network segments in the medium-pressure NGDS [35]. Thus, in case v_5 is normally closed, the rupture of any pipeline on a given radial will interrupt the load points connected to that particular radial.

3.7 Reliability Modelling

As discussed in the previous sections, there are structural and operational similarities between EPDSs and NGDSs, and both systems are constructed to provide reliable supply to the customers. However, to the author's knowledge, no comprehensive reliability model has been previously presented and applied to NGDS.

Publication B presents an approach for assessing reliability of supply in NGDSs, following the steps of the analytical simulation approach described in Section 2.5. The model was inspired by similar models applied to EPDSs and water distribution systems [10, 36].

Steady-state simulations of flows and pressures were incorporated in the approach to evaluate network constraints. It was generally assumed that gas storage does not affect reliability of supply at distribution system level. The impact of storage in transmission systems is addressed in Chapter 5. A load point interruption was defined as an event where the load point pressure is lower than a predefined minimum pressure p_{min}. Pipeline constraints, such as maximum flow velocity, were not considered. A detailed description on how to compute pipeline flows and nodal pressures in complex gas networks comprising valves and regulators is provided in Appendix A.

The reliability model was tested on two test systems.

3.7.1 Test System I

A simple, fictitious NGDS test system was presented in Publication B, similar to the one shown in Fig. 3.2. Load point reliability indices were found both for radial and meshed system operation. The case study in Publication B considered regulator station failures and pipeline ruptures. Violations of

network constraints were treated by cutting load at the receiving end of the overloaded radial.

Incorporating pipeline leakages in the model is straightforward. For each selected pipeline, both the response to a leakage and to a rupture must be simulated and weighted by failure rates λ_{PL} and λ_{PR}, respectively.

3.7.2 Test System II

Analysis of a second test system is presented below to supplement the case study in Publication B. The test system is shown in Fig. 3.3, being a medium-pressure NGDS operated with open loops. Pipeline lengths and diameters as well as load data and nodal numbers are taken from [37]. Each node represents either a junction or a load point. The system is fed through one single regulator station, and the operating pressure is set to 4.0 bar. It is assumed that valves in the test system are MOVs, except from the ROV v shown in Fig. 3.3.

In case a pipeline in the system ruptures, v is closed and all load points are interrupted. Similarly, if the regulator station fails, all load points are interrupted. For simplicity, these failures are omitted in the further study, and only pipeline failures in terms of leakages are considered. A pipeline leakage failure-rate of $\lambda_{PL} = 0.1$ (km $\times$ year)$^{-1}$ is assumed. Furthermore, it is assumed that each faulted pipeline may be manually isolated and that the repair time is identical for all pipelines. Only first-order failures are considered and upstream supply is considered fully reliable.

When simulating the system's response to a selected failure (step 2 in the analytical simulation procedure outlined in Section 2.5), the following steps are undertaken:

a) Isolate the faulted pipeline (by use of MOVs or clamps)

b) Evaluate pressures at all load points

c) Register interruptions for load points not meeting the pressure requirement p_{min}

Note that the procedure does not include any operator action to curtail load in case the pressure requirement is violated. Consequently, the calcu-

lated indices are pessimistic. The load curtailment algorithm presented in Chapter 4 could be applied to this problem.

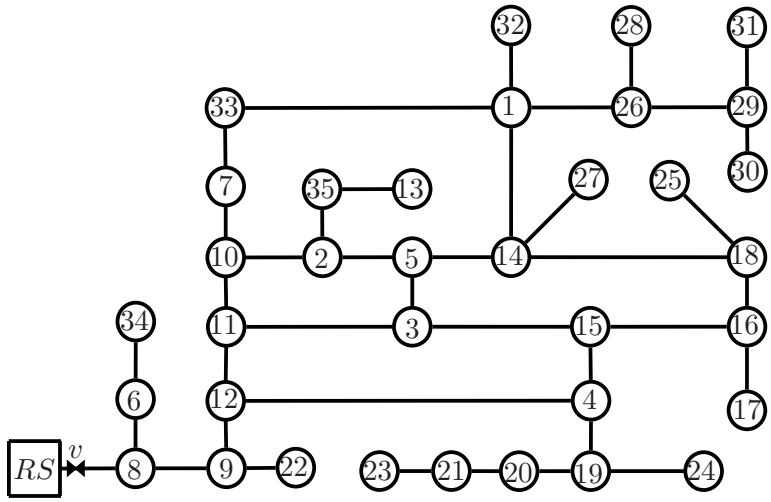

Figure 3.3: An NGDS test system.

Table 3.1 presents the average interruption rates found for five selected load points in Fig. 3.3. Three different minimum pressure levels were used: 2.0, 1.5 and 1.0 bar. The fifth column holds the pressure values (p_{init}) for the system in its normal state. As expected, the load points experiencing the lowest p_{init} are the ones benefiting the most, in terms of reduced average interruption rate, when decreasing p_{min}.

Table 3.1: Average interruption rates for some selected load points.

	Average interruption rate [year^{-1}]			p_{init} **[bar]**
Load pt	p_{min} =2.0 bar	p_{min} =1.5 bar	p_{min} =1.0 bar	–
1	0.293	0.255	0.244	2.15
3	0.244	0.244	0.244	2.44
7	0.279	0.250	0.244	2.20
24	0.264	0.264	0.256	2.55
28	0.363	0.320	0.309	2.13

Chapter 4

District Heating Systems

Publication C

This chapter serves as an introduction to Publication C, introducing the basic network structure and operational principles of a district heating system. A simplified thermal power-flow model is presented together with its underlying assumptions. The model is suitable for evaluating the district heating system's steady-state response to failures, and is applied to a test system presented at the end of the chapter.

District heating systems depend on electricity from the electric power system for proper operation. Publication C presents a method for assessing this dependency, building on the thermal power-flow model described in this chapter.

4.1 Reliability Modelling and Hierarchical Levels

In contrast to the EPS and the NGS, the district heating system (DHS) is considerably less geographical widespread. Transporting hot water over long distances is not a viable option when considering technical and economical constraints. For this reason, DHSs are normally located within the boundaries of a city or a local municipality.

The following system description is based on a DHS comprising two separate

distribution circuits, referred to as the primary and the secondary distribution system. A primary distribution system is illustrated in Fig. 4.1. The system comprises thermal power production units TP_1 and TP_2, pumps PU_1-PU_4 and heat exchanger stations HE_1-HE_4. A network of pipelines connects production units and heat exchangers. In each heat exchanger, the water in the primary distribution system is heat exchanged with water in a secondary distribution circuit to supply customers at a lower pressure and temperature. Large customers are occasionally connected directly to the primary distribution system.

Analogous to the different voltage and pressure levels in the EPS and NGS, larger DHSs are normally split into subsystems operating at different pressure and temperature levels. Pressures and temperatures are reduced stepwise as thermal power is transported from the production units to the customers. However, unlike flow in an NGS, the flow medium in a DHS is physically separated between subsystems.

As for the EPS and NGS, it is possible to split the DHS in three functional zones, grouping thermal power production, transmission and distribution facilities. The primary distribution system may be considered a transmission system, treating the heat exchangers as aggregated load points. As this work concerns the primary distribution system, it may be seen as an HLII-study; the combined analysis of the functional zones of thermal power production and primary distribution system facilities.

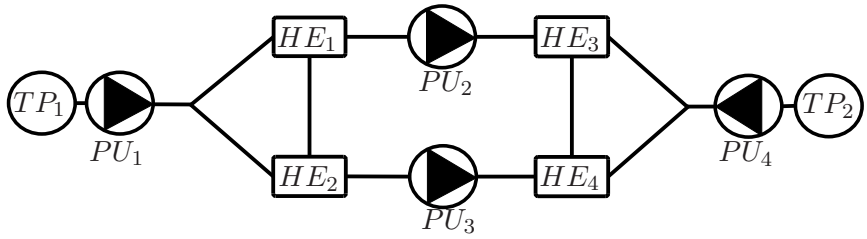

Figure 4.1: Illustration of a district heating system.

4.2 Previous Studies

Few authors have presented studies on reliability of supply in DHSs. The topic is generally addressed in [38, 39]. Two methods previously applied to

DHSs are discussed in [39]; fault tree analysis and the loss of load method. Fault tree analysis was aimed at components and subsystems within the DHS, finding the respective failure probabilities. The loss of load method is an HLI-study, finding the loss of load probability given production unit failure-rates and load distributions in the DHS. This method assumes a perfect network connecting production units and loads.

A series of publications propose different models for assessing the reliability and availability of the DHS in Turin, Italy [40–44]. A cut-set approach was presented in [40], incorporating failures of thermal power production units, pipelines, valves and heat exchangers in meshed DHSs. However, the presented reliability model did not take into account the physical flows in the DHS. A later publication presented a Monte Carlo approach applied to the same network [44]. The hydraulic and thermal responses from the DHS were included in the Monte Carlo simulations, analysing water flow and thermal power flow separately. To the author's knowledge, this approach did not incorporate the possibility to curtail and prioritise load, and was primarily aimed at radially operated networks.

4.3 Component Failures

The work presented in Publication C is not a reliability analysis of the coupled EPDS and DHS, but rather a study of the two systems' vulnerability to failures in the EPDS. The dependency of the DHS on electric power[1] was modelled as illustrated in Fig. 4.2. The EPDS network model is represented by a branch b_{EPDS} having a load point node i. This node stores a pointer to possible connected DHS nodes, in this case node j. In case i is interrupted, j is set to a faulted mode, and DHS consequences are quantified.

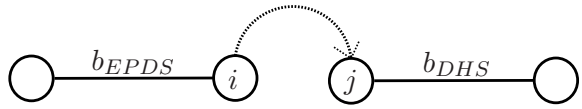

Figure 4.2: Modelling the district heating system's dependency on electric power.

[1] The term electric power is used when referring to electric power from the EPS in this chapter.

This chapter only concerns the district heating part of the material presented in Publication C. Thus, we are mainly concerned with what happens when node j is faulted rather than the EPDS failures causing j to reach its faulted mode. In the following, only DHS node failures are treated and loss of electric power is considered the only failure cause.

Two component types are considered dependent on electricity:

- Pumps
- Thermal power production units

Pumps are usually driven by electricity and therefore depend on electricity. It is not as easy to generalise the dependency of thermal power production units on electricity. Some of these units, such as electric boilers and heat pumps, have obvious dependencies, while others need electricity to perform auxiliary functions. It was assumed that pumps and thermal power generation units fail to operate if they do not receive electric power from the EPS. Both pumps and production units may have a dedicated back-up system for electric power supply, or the DSO may have mobile back-up units. The possibility of applying such back-up solutions was not modelled, but could be added as a cold stand-by switching system.

Consider the DHS in Fig. 4.1. As the system has several production units and pumps, it is not immediately clear if a single component failure will result in insufficient supply to any of the heat exchangers. Thus, the system's response to such failures should be simulated to evaluate the resulting consequences. For this reason, a thermal power-flow model was formulated, as described in the following sections.

4.4 Describing Thermal Power Flow

Studying the changes in thermal power flow due to component failures in a DHS involves both pressure and temperature dynamics. Procedures for simulating thermal power flow in DHSs normally take advantage of the fact that changes in pressure are distributed significantly faster throughout the system than temperature changes. By assuming a quasi-dynamic condition between mass flow and temperature, the mass flow can be found indepen-

dently from the temperature distribution and the temperatures are updated later on by assuming constant mass flow [45–47].

For the purpose of evaluating the consequences of nodal failures in a DHS, a simplified power-flow model was developed. This model fully decouples the pressure and temperature responses, considering the steady-state solution only. As a first step to describe this model and its assumptions, consider the flow in the simple DHS in Fig. 4.3.

4.4.1 Changes in Pressure and Temperature

Fig. 4.3 illustrates a simple DHS with primary and secondary distribution systems. The primary distribution system to the left of the heat exchanger HE has a thermal power production unit TP and a pump PU_P. To the right of the heat exchanger, water is circulated in a secondary distribution system by means of a pump PU_S, serving a single load.

The thermal power flow, in terms of changes in temperatures and pressures through the primary distribution system, is described below. This description relies on two assumptions:

1. Isothermal flow through pipelines and pumps (constant temperature)
2. Isobar flow through production units (constant pressure)

Starting at point a in Fig. 4.3, water is circulated in the indicated direction at a pressure p_a and temperature T_a. Flowing through the production unit and reaching point b, the temperature increases whereas the pressure is assumed constant. Subsequently, pressure increases and temperature is assumed constant as water is drawn through the pump between points b and c. Flowing through the pipeline between points c and d, pressure decreases while temperature does not change. Thermal power is supplied to the secondary distribution system in the heat exchanger, and both temperature and pressure decrease between points d and e. Summing up, the pressure gain added by the pump PU_P is lost in the pipeline flow (supply-return) and through the heat exchanger. The temperature gain added by the production unit TP is lost in the heat exchanger.

The thermal power P^t exchanged from the primary to the secondary distri-

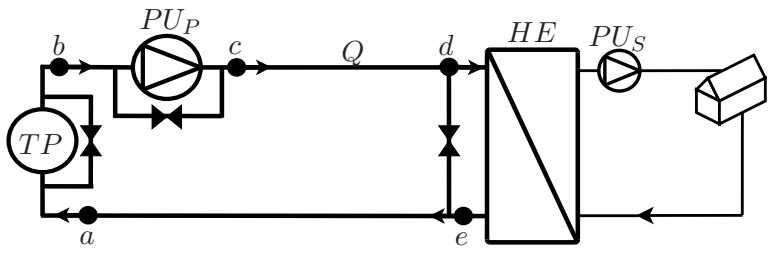

Figure 4.3: Temperature and pressure variations in a simple district heating system.

bution system through the heat exchanger is expressed as:

$$P^t = C_p \times Q \times \Delta T \tag{4.1}$$

where all variables refer to the primary distribution system side of the heat exchanger and:

C_p	=	Heat capacity of water
Q	=	Mass flow through heat exchanger
ΔT	=	Difference between heat exchanger inlet and outlet temperature

4.4.2 Steady-State Response to Failures

Three components in Fig. 4.3 fail to operate when loosing electric power supply; PU_P, TP and PU_S. It is briefly outlined how the system responds to such failures. For simplicity we assume that the components are bypassed when faulted.

If PU_P fails, the component is bypassed so that $p_b = p_c$. The mass flow Q quickly reaches zero, as do thermal power supply to the heat exchanger.

If TP fails in Fig. 4.3, the component is bypassed so that $T_a = T_b$. Changes in temperature are closely related to the flow of the circulating water. Assuming that Q is kept constant by PU_P, the time it takes before supply falls short of demand at the heat exchanger depends on the circulation speed and the distance between b and d. The dynamic changes in temperature subject to the failure of TP is discussed in Section 5.7 and Publication D. The steady-state solution in this case is obvious; ΔT eventually reaches zero, and there is no thermal power supply to the heat exchanger.

Being physically separated from the mass flow in the primary distribution system, the mass flow in the secondary distribution system depends on the pumping power of PU_S. Thus, if PU_S fails, the load in Fig. 4.3 will loose supply. In the further study, this is referred to as a failure of the aggregated load point, and HE is bypassed to reduce load in the primary distribution system.

4.5 A Network Flow Model

A general formulation of thermal power flowing in a DHS may be obtained by applying a conventional network flow model, explicitly considering thermal power flow rather than temperatures and pressures. In this type of model, the thermal power flow is described by conservation laws only. Network flow models have been applied in investigations related to optimisation of multi-carrier energy systems in [48, 49].

The model should be able to handle situations where production capacity does not meet demand, i.e. where supply to loads must be curtailed to fulfil the conservation law. In this study, emphasis was put on minimising the global consequences of DHS failures. Component failure and repair rates are not treated here, and the consequences are simply described in terms of curtailed thermal power P^t_{curt} in the system. Other relevant system indices, e.g. indices related to the number and type of consumers having their supply interrupted could easily be incorporated in the presented model.

The following linear programming formulation will find the minimum curtailed thermal power:

MIN.:

$$P^t_{curt} = \sum_{i \in \mathcal{N}_L} (1 - x_i) D_i \tag{4.2a}$$

S.T.:

$$\sum_{j:b(j,i)\in\mathcal{B}} P^t_{b(j,i)} - \sum_{j:b(i,j)\in\mathcal{B}} P^t_{b(i,j)} + G_i - x_i D_i = 0 \qquad \forall i \in \mathcal{N} \tag{4.2b}$$

$$|P^t_b| \leq P^t_{b,max} \qquad \forall (i,j) \in \mathcal{B} \tag{4.2c}$$

$$G_i \leq G_{i,max} \qquad \forall i \in \mathcal{N}_G \tag{4.2d}$$

$$0 \leq x_i \leq 1 \qquad \forall i \in \mathcal{N}_L \tag{4.2e}$$

Where x_i is the ratio between supplied thermal power and total demand at load-point node i. Restriction (4.2b) describes the thermal power balance at each node. $P^t_{b(i,j)}$ denotes thermal power flow in the pipeline connecting nodes i and j, being constrained by (4.2c). G_i and D_i denote thermal power production and demand at node i, respectively, where G_i is constrained by its maximum power $G_{i,max}$ in (4.2d). The network flow model relies on a set of underlying assumptions:

Sufficient nodal pressures: The formulation does not consider the physical law linking mass flow and pressure. Thus, the model relies on the assumption that there is sufficient pressure at all load nodes.

Lossless flow: Pipeline flow is isothermal. Thus, temperature is reduced only when the water flows through heat exchangers at the aggregated load points. In practise, heat losses will depend on several physical parameters, such as mass flow and outdoor air temperature.

Steady-state: The network flow problem describes the system at steady-state. Transient changes in thermal power flow due to failures and redispatch of production units and pumps are not considered.

Although applicable for general investigations of system behaviour, the network flow model was not considered appropriate for analysing the consequences of nodal failures, due to its inability to deal with deactivation and failure of pumps. For this reason, it was decided to make some assumptions regarding thermal power-flow control in DHSs, in order to arrive at a more accurate model.

4.6 Controlling Thermal Power Flow

It is possible to control the thermal power flow in a DHS by predefining the mass flow L through each heat exchanger and production unit, as illustrated in Fig. 4.4. L has a positive reference out of the supply network. G is the injected thermal power and D is the consumed thermal power, so that $\{G, D\} \propto |L|$. This control principle is based on a constant temperature differential ΔT at each load point and production unit. Initially, water is flowing through all heat exchangers and into the return pipeline network at a constant rate. Conversely, water is injected into the supply pipeline network through the production units at a constant rate. Thus, at steady-state, the mass balance in (4.3) is always fulfilled.

$$\sum_{i \in \mathcal{N}} L_i = 0 \tag{4.3}$$

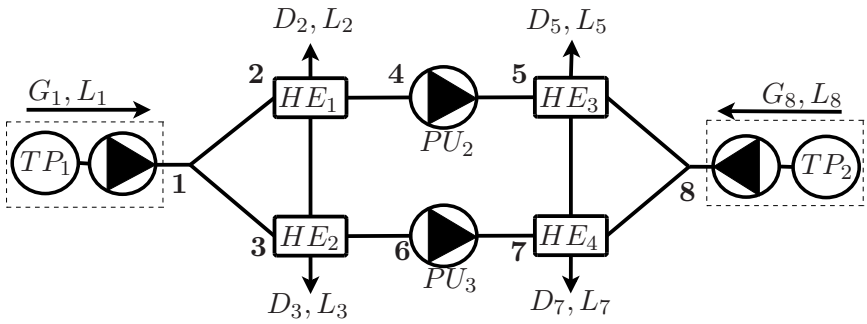

Figure 4.4: Illustration of a district heating system, indicating nodal demand and production in terms of mass flow L, and thermal powers D and G.

Unlike most other hydraulic networks, the DHS consists of both supply and return pipelines. In most cases, the pressure distribution in the supply network does not affect the return network because the flow rates are controlled by the customer's control system. Therefore, simulations of mass flow and nodal pressures are normally carried out only for the supply network [50]. Each aggregated load point requires a certain minimum pressure differential Δp_{min} over its heat exchanger. This requirement was translated to a minimum pressure requirement p_{min} at each aggregated load point.

All thermal power production units have an associated pump responsible for providing flow through the unit and into the supply network. In case this

pump fails, the flow rate through the pump is set to zero. Similarly, in case the production unit fails itself, the flow rate through the associated pump is set to zero. Accordingly, a production unit together with its associated pump may be viewed as one aggregated unit, as indicated by the dotted-line boxes in Fig. 4.4.

Some pumps are operated independently of production units, such as PU_2 and PU_3 in Fig. 4.4. These pumps will usually have the ability to circulate flow in both directions. In case an independently operating pump fails, it is bypassed.

Having predefined the nodal mass flow injections and demands at $N-1$ nodes, the steady-state mass flows and pressures are found by using the method described in Appendix A.

4.7 A Simplified Thermal Power-Flow Model

Based on the mass-flow control principle described in the previous section, it is now possible to define a model which is more accurate and physical than the network flow model presented in Section 4.5. The presented model is suitable for evaluating the steady-state consequences of component failures in DHSs.

Any set of failures $\mathcal{F}$ concerning pump failures or implying the deactivation of pumps are evaluated as described in Algorithm 1. First, a flow simulation, as described in Appendix A, is performed in line 3 of Algorithm 1, to find the vectors of pipeline mass flows $\mathbf{Q_b}$ and load point pressures $\mathbf{p_i}$. Subsequently, pipeline thermal power flows $\mathbf{P_b^t}$ are found in line 4. In case system requirements are not met in line 5, we assume that the DSO will actively curtail load according to a procedure MinCurt in line 6. The objective of this procedure is to meet system requirements while minimising P_{curt}^t as defined in (4.2a).

Partial supply of loads was not considered. Thus, x_i in (4.2a) was treated as a boolean variable. A simple binary GA was used to solve the combinatorial optimisation problem MinCurt. Each binary string in the GA indicates whether a load point is served ($x_i = 1$) or bypassed ($x_i = 0$).

Algorithm 1 Finding min. curtailed thermal power for a failure set $\mathcal{F}$

Ensure: $\mathcal{F}$ contains faulted or deactivated pumps

1: adjust nodal demands and injections according to $\mathcal{F}$
2: $P^t_{curt} \leftarrow 0$
3: $\mathbf{Q_b}, \mathbf{p_i} \leftarrow$ FlowSimualtion
4: $\mathbf{P^t_b} \leftarrow C_p \mathbf{Q_b} \Delta T$ {eqn. (4.1)}
5: **if** any $\left(p_i < p_{min} \parallel P^t_b > P^t_{b,max} \parallel G_i > G_{max,i}\right)$ **then**
6: $\quad P^t_{curt} \leftarrow$ MinCurt
7: **end if**
8: **return** P^t_{curt}

4.7.1 Example: A Simple Test System

The DHS in Fig. 4.4 was used to test the proposed thermal power-flow model, minimising P^t_{curt} subject to some selected failure sets $\mathcal{F}$. Pipeline and nodal data are listed in Tables 4.1- 4.2, along with thermal power flows and pressures for the system in its initial, healthy state. The Hazen-Williams equation was applied as described in [51], using a roughness coefficient of 130. A constant ΔT of 50 °C and an operating pressure of 16 bar was applied. Pumps PU_2 and PU_3 were set to deliver a constant outlet pressure of 1.0 per unit (p.u.), and the minimum pressure requirement was set to $p_{min} = 0.9$ p.u.

Table 4.1: Pipeline parameters and initial thermal power flows.

Nr	**Send. node**	**Rec. node**	**Length** [km]	**Diameter** [m]	**Capacity** [MW]	**Initial Flow** [MW]
1	1	2	1.00	0.20	20	19.00
2	1	3	1.00	0.20	20	19.00
3	2	3	0.50	0.20	20	−0.95
4	2	4	2.00	0.20	20	4.95
5	3	6	2.00	0.20	20	5.05
6	4	5	2.00	0.20	20	4.95
7	5	7	0.50	0.20	20	0.92
8	5	8	1.00	0.15	7	−5.97
9	6	7	2.00	0.15	7	5.05
10	7	8	1.00	0.15	7	−6.03

The minimum consequences for some selected failure sets are presented in

Table 4.2: Nodal demand, supply and initial pressure.

Node	D [MW]	G_{max} [MW]	p_{init} [p.u.]
1	–	50	1.00
2	15	–	0.92
3	13	–	0.92
5	10	–	0.99
7	12	–	0.99
8	–	12	1.02

Table 4.3. Minimum curtailed thermal powers from the thermal power-flow model are compared with results from the network flow model. For this comparison it is assumed that the network flow model is as presented in equations (4.2), but the variable x_i is treated as a binary variable, i.e. partial load supply is not considered. It is indicated which constraints that are violated in the thermal power-flow model for each evaluated failure set, before loads are curtailed. Consider the case where TP_2 fails. The associated pump is deactivated and flow through the unit is set to zero. Mass flow through TP_1 is increased accordingly to fulfil the nodal mass balance, and the new nodal pressures are evaluated. The pressure constraint ($p_2 = p_3 = 0.86$ p.u.) and some pipeline constraints ($P_1 = P_2 = 25$ MW) are violated, as indicated in Table 4.3. The minimum consequences are caused when curtailing load at node 5 for both models, i.e. $P^t_{curt} = 10$ MW. If both TP_2 and PU_2 fail, the pressure constraint is binding in the thermal power-flow model, giving $P^t_{curt} = 12$ MW. Pressures are not considered in the network flow model; hence, the curtailed power does not change from the case where only TP_2 was faulted.

Table 4.3: Minimum curtailed thermal power for some selected failure sets.

Failure set	**Constraint violation**			**Thermal power flow**	**Network flow**
$\mathcal{F}$	p_{min}	$P^t_{b,max}$	G_{max}	P^t_{curt} [MW]	P^t_{curt} [MW]
TP_1	√	√	√	38	38
TP_2	√	√		10	10
PU_2 or PU_3				0	0
PU_2 and PU_3	√			10	0
TP_2, PU_2	√	√		12	10

4.7.2 Applicability of the Simplified Model

Controlling the thermal power flow in a DHS is a complex problem. In this chapter a simplified thermal power-flow model was presented suitable for analysing the steady-state post-contingency flows. However, it should be stressed that this model relies on numerous assumptions, as stated in the text.

In principle, the simplified thermal power-flow model may be applied in reliability evaluation of DHSs considering both node and branch failures, incorporating failure rates and repair times. However, care should be taken as changes in temperature are slow in large DHSs. Thus, assuming steady-state thermal power flow can give misleading results.

Chapter 5

Pipeline Storage

Publication D

This chapter presents a Markov-based method for incorporating pipeline storage in reliability modelling of natural gas pipeline systems. First, it is elaborated how to find the stored amount of energy in a natural gas pipeline. Subsequently, a Markov model is presented, considering pipeline storage as a subsystem with failure and repair rates. Finally, an approach for finding the basic load-point reliability indices in radial natural gas transmission systems is suggested.

The chapter serves as an introduction and supplement to Publication D. Publication D also suggests applying the proposed Markov model to district heating systems. This option is discussed at the end of this chapter.

5.1 Introduction

In contrast to electrical energy, energy transported in pipeline systems does not necessarily require distinctive storage facilities, as the pipelines constituting the network can be used for this purpose. In Chapter 3 we ignored this feature, claiming that energy storage in pipelines is negligible at distribution system level. However, as transportation distances and pipeline dimensions increase, pipeline storage should not be neglected. The material presented in this chapter is primarily relevant for studies concerning natural

gas transmission systems.

Consider a simple natural gas transmission system as illustrated in Fig. 5.1, transporting gas from a source h towards an aggregated load point j through two branches b_{hi} and b_{ij}. In this context the aggregated load point is typically the supply point to a downstream NGDS. Supply to the load point relies on the availability of the two upstream branches and the source. Branch b_{hi} may e.g. be a compressor or a pipeline, whereas b_{ij} is a long pipeline.

If b_{hi} fails, it is isolated by valves v_1 and v_2, and j is no longer connected to the source. However, depending on the amount of energy stored in b_{ij}, j may be supplied yet for a while. At best, the stored energy is sufficient to supply j until b_{hi} has been repaired and connectivity between h and j is restored. In case the stored energy is not enough to fully bridge the repair of b_{hi}, it may still delay and shorten interruption of supply to j and provide useful time for corrective actions in the downstream network.

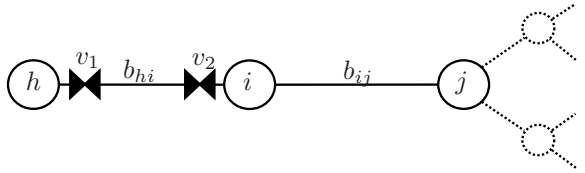

Figure 5.1: A natural gas transmission system.

5.2 Previous Studies

Pipeline storage is often claimed to have a positive impact on the reliability of supply in high-pressure gas systems. However, the modelling and quantification of this impact has been explicitly investigated only in few publications so far. In [52] the critical durations of pipeline storage in a high-pressure nitrogen supply system were computed. The authors combined the critical durations with stochastic simulations of compressor station failure and repair times to find global reliability indices. Focusing on large-scale natural gas transmission systems, [29] presents a procedure combining Monte Carlo simulations with hydraulic transient analysis for the purpose of quantifying system reliability.

In addition to these publications, several studies investigate the transient nature of flow in natural gas transmission systems subject to variations

in demand and availability of sources and compressors, such as in [53, 54]. However, these generally emphasise on selected scenarios rather than finding reliability indices.

5.3 Storage in Natural Gas Pipelines

The storage of natural gas in a pipeline b_{ij} is illustrated in Fig. 5.2. Assume that the pipeline flow is at steady-state, and that the minimum pressure requirement p_j^{min} at the receiving node j and the maximum pressure requirement p_i^{max} at the sending node i should not be violated.

The upper solid-drawn line represents the pressure distribution along the pipeline operating at the maximum inlet pressure p_i^{max}. Conversely, the lower solid-drawn line represents the pressure distribution when meeting the minimum outlet pressure p_j^{min}. In between these curves, the stapled line represents a pressure distribution $p(x)$ associated with an inlet pressure p_i.

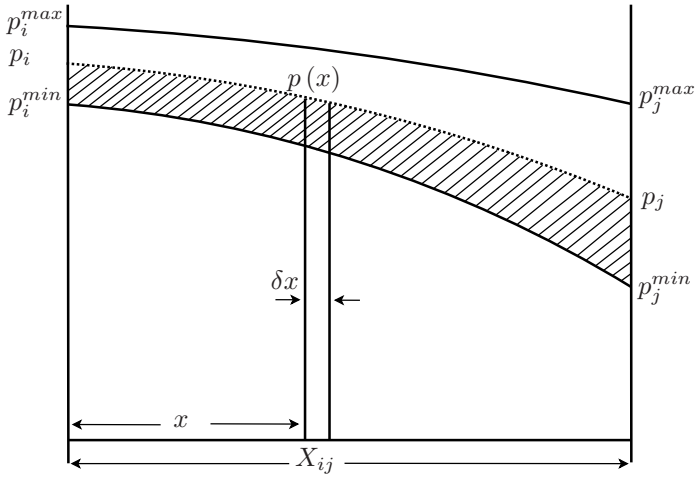

Figure 5.2: Illustration of storage in a pipeline b_{ij} where flow is at steady-state.

For a given inlet pressure p_i it is possible to find the total gas volume V_{ij} contained in pipeline b_{ij} as follows:

$$V_{ij} = \int_0^{X_{ij}} \delta V = \frac{A}{p_b} \int_0^{X_{ij}} p(x)\delta x \tag{5.1}$$

where:

A	= pipeline cross-sectional area
p_b	= base pressure
X_{ij}	= length of pipeline b_{ij}
$p(x)$	= pressure distribution along b_{ij}
x	= distance from pipeline inlet

For the pressure distribution $p(x)$ in Fig. 5.2, V_{ij} is represented as the entire area under the stapled line. Assuming that pipeline flow is at steady-state, V_{ij} can be formulated as in (5.2), as derived and described in [55, 56].

$$V_{ij} = k \left(\frac{T_b}{p_b} \right) \left(\frac{\overline{p} D_{ij}^2 X_{ij}}{\overline{Z}\ \overline{T}} \right) \tag{5.2}$$

where:

$$\overline{p} = \frac{2}{3} \left(p_i + p_j - \frac{p_i p_j}{pi + p_j} \right)$$

and:

k	= numerical constant
T_b	= base temperature
D_{ij}	= diameter of pipeline b_{ij}
$\overline{T}$	= average gas temperature
$\overline{Z}$	= average gas compressibility factor

A certain minimum stored volume V_{ij}^{min} is needed in order to supply node j at p_j^{min}. The extra energy storage, represented by the shaded area in Fig. 5.2 is found as $V_{ij}^s = V_{ij} - V_{ij}^{min}$. In the further discussion, V_{ij}^s is referred to as the pipeline storage.

5.4 Survival Time

The survival time of a pipeline system is an estimate of how long the system is able to serve the connected loads while being fully or partly disconnected from its upstream sources.

In the following we define the survival time ST_{ij} of a single pipeline b_{ij} as the time it takes to fully discharge the pipeline's storage V^s_{ij}, assuming a constant load L_j at node j and no upstream supply:

$$ST_{ij} = \frac{V^s_{ij}}{L_j} \tag{5.3}$$

This is a simplified method for computing the gas pipeline survival time, only considering a steady-state picture of pipeline flow before and after the storage has been discharged. Similar simplified methods are often used in the industry, approximating the transient behaviour of discharging gas from a storage [33, 57, 58].

5.4.1 Example: Survival Time of a Pipeline

Consider a pipeline b_{ij} having a length of 100 km, where the remaining pipeline parameters are as in the case study presented in Publication D. The pipeline's survival time ST_{ij} is found by using (5.3), and is plotted as a function of load L_j for some selected inlet pressures p_i in Fig. 5.3.

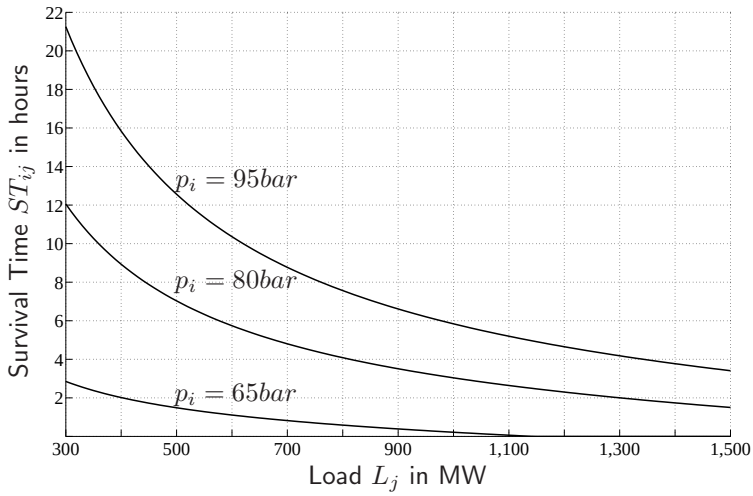

Figure 5.3: Survival time of pipe b_{ij} plotted as a function of load L_j for some selected inlet pressures p_i.

A different approach for finding survival times was applied in Publication D, relying on transient simulations of gas flow. Generally, the survival times found using the two different approaches were relatively close, deviating no more than 30 %.

5.5 Markov Approach for Pipeline Storage

This section presents a basic Markov model suitable for capturing the effect of pipeline storage in reliability analysis of natural gas pipeline systems.

Energy storage in a pipeline can be considered a back-up system being forced into operation in case upstream supply to the pipeline is interrupted. A reliability block diagram illustrating the modelling of storage is shown in Figure 5.4. It should be noted that the storage denoted S_{ij} does not represent a physical connection between nodes h and i, but rather the functionality of the stored energy in pipeline b_{ij} in terms of reliability. Let h be the source node and j the load node. If branch[1] b_{hi} fails, there is no topological connection between the source h and the load j. However, Fig. 5.4 illustrates that j is served from S_{ij}. The storage has a limited capacity described by its survival time ST_{ij}. The Markov model presented in Fig. 5.5 enables us to estimate the basic reliability indices for load point j subject to a failure of the upstream branch (b_{hi}).

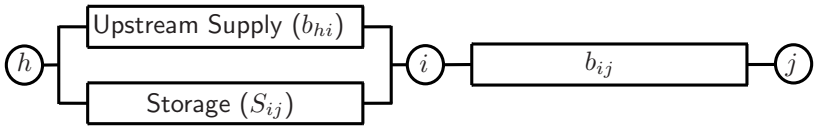

Figure 5.4: Reliability block diagram with respect to energy supply from node h to node j.

5.5.1 Storage Failure Rate

The storage S_{ij} in Fig. 5.4 is defined to have failed once it is fully discharged, i.e. $V_{ij}^s = 0$. Thus, the storage survival time found in Section 5.4 can be

[1]The term branch is used to indicate that b_{hi} may in principle be any network component.

understood as the mean time to failure (MTTF) and the storage failure rate is defined as the inverse of $MTTF_{S_{ij}}$:

$$\lambda_{s_{ij}} = \frac{1}{ST_{ij}} = \frac{1}{MTTF_{S_{ij}}} = \frac{L_j}{V_{ij}^s} \tag{5.4}$$

5.5.2 Markov Model

The state space diagram shown in Fig. 5.5 represents the connection between nodes h and i in the reliability block diagram in Fig. 5.4. Let U denote the upstream supply to node i provided by b_{hi} and S denote the energy storage S_{ij} in pipeline b_{ij}. Failure and repair rates for branch b_{hi} are denoted λ_u and μ_u, respectively. Similarly, failure and repair rates of the storage are denoted λ_s and μ_s. Load point j will experience an interruption if the upstream supply is faulted and the storage is fully discharged. Thus, state 3 in Fig. 5.5 represents the failure state.

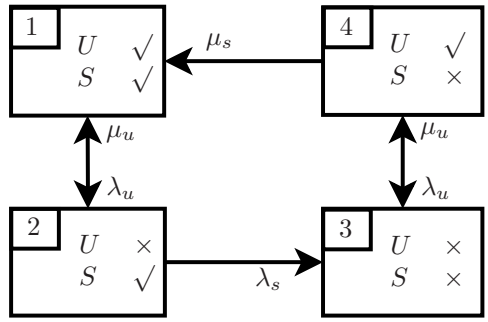

Figure 5.5: A Markov model incorporating upstream supply U and pipeline storage S. Functionality is either operating ($\surd$) or faulted ($\times$).

5.5.3 Assumptions

The state space diagram in Fig. 5.5 represents a continuous and dynamic process as a time-homogeneous Markov process with only four states. A process should show two properties to be considered a time-homogeneous Markov process [59]:

1. **Memoryless** – When the present state of the process is known, the future development of the process is independent of anything that has happened in the past. The process is said to have no memory.

2. **Stationary** – The probability of transition from one state to another is independent of time; the process has stationary transition probabilities.

Thus, for the presented Markov model to be valid, certain assumptions were made, as discussed in detail in Publication D. In short, the major assumptions concern:

Constant load and fixed operator strategy: To fulfil the second property stated above, the storage failure and repair rates should be constant. Thus, load must be considered constant whenever the storage is being discharged and repaired. Alternatively, several load states could be incorporated in the Markov model, as described in Publication D. Furthermore, it is assumed that the operator aims at meeting a predefined upstream pressure corresponding to a given storage level. This assumption guarantees a constant storage repair rate.

Binary storage representation: State 2 represents the system with a faulted upstream supply (U) and a pipeline storage being discharged. If U is repaired before the storage is fully discharged, the system transits back to state 1, representing an operating U and a fully charged storage. However, the storage has been partially discharged while residing in state 2 and its charge level is actually unknown. Therefore, the binary storage representation is an optimistic assumption.

Repair of upstream supply: The repair rate of U has to be path independent and hence, the transition rates from state 2 to 1 and from state 3 to 4 are identical. One could argue that the repairing of the compressor is being started as soon as state 2 is encountered, giving a higher rate from 3 to 4 than from 2 to 1. The assumption of identical repair rates can be understood as a worst case assumption, necessary to guarantee path-independent transition rates.

5.5.4 Reliability Indices

It is possible to derive analytical expressions for the basic reliability parameters of load point j in Fig. 5.4 subject to the failure of upstream supply (b_{hi}). The probability of load point j being interrupted equals the probability of being in state 3 (pr_3):

$$pr_3 = \frac{\lambda_u \lambda_s \left(\lambda_u + \mu_s\right)}{\left(\mu_u + \lambda_u\right)\left(\mu_u \mu_s + \mu_s \lambda_s + \lambda_u \lambda_s\right)} \tag{5.5}$$

The expression in (5.5) can be simplified by making two assumptions. First, it is assumed that $\mu_s \gg \lambda_u$. This assumption is sound given that the operator always aims at keeping a predefined storage level. Second, we assume that $\mu_u \gg \lambda_u$, which is normally the case for the types of repairable components being considered here. The simplified formulation is:

$$pr_3 = \frac{\lambda_u}{\mu_u} \times \frac{\lambda_s}{\lambda_s + \mu_u} \tag{5.6}$$

The average interruption rate λ_j (in interruptions/year) and the average annual outage time U_j (in hours/year) for load point j subject to failure of the upstream unit can be formulated as:

$$\lambda_j = \mu_u \times pr_3 = \frac{\lambda_u \lambda_s}{\lambda_s + \mu_u} = \frac{\lambda_u}{1 + \frac{ST_{ij}}{r_u}} \tag{5.7a}$$

$$U_j = 8760 \times pr_3 = \lambda_j r_u \tag{5.7b}$$

Where $r_u = 8760 \times \mu_u^{-1}$ is the repair time of the upstream unit. All rates are given per year, and r_u and ST_{ij} are given per hour.

For a pipeline b_{ij} with negligible storage, $ST_{ij} \approx 0$. In this case, the basic reliability indices found from (5.7) correspond to the ones described by (2.1) in Chapter 2.

5.5.5 Model Extensions

The basic Markov model presented in Fig. 5.5 was extended to incorporate three load levels and a reserve upstream supply unit in Publication D. These

extensions are not further treated here, and it is referred to Publication D for coverage of these model extensions.

5.6 Modelling Storage in Pipeline Networks

The presented modelling approach can in principle be extended to gas pipeline networks having a radial structural topology. Consider the gas transmission network in Fig. 5.6 transporting gas from a source at node 1 to the load points at nodes 4-6. All transmission pipelines are equipped with remotely operated valves at both ends, to quickly isolate a faulted pipeline.

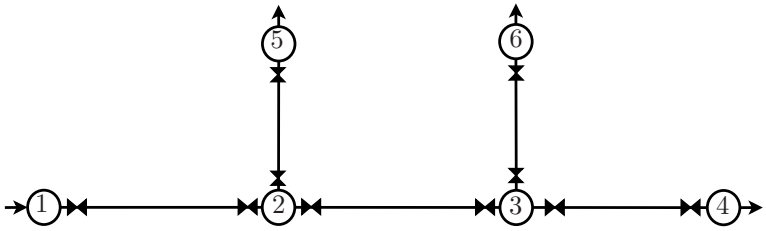

Figure 5.6: A gas transmission network connecting a source and three load points.

Knowing the minimum pressure requirement p_{min} at all load points and the operating pressure p_1 at the source node, it is possible to estimate the storage V_{ij}^s in each pipeline. Assuming constant loads, the steady-state network flows and pressures are easily found. Now V_{ij} can be estimated for each pipeline using (5.2).

Finding V_{ij}^{min} for all branches is more challenging. An approach following the strategy of a depth-first search is suggested below. In a depth-first search, branches are explored out of the most recently visited node which still has unexplored downstream branches. For the network in Fig. 5.6 a depth-first search could e.g. explore the branches in order $\{b_{12}, b_{23}, b_{34}, b_{36}, b_{25}\}$. Each time a node j which does not have unexplored downstream branches is reached, V_{ij}^{min} and p_i^{min} are computed, where i denotes the parent node of j. In case node j is a load point, this computation is straightforward as p_j^{min} was predefined for all load points. Otherwise, if j is not a load point, the highest value of p_j^{min} is used in the further calculations. Consider being at node 3 having visited branches b_{34} and b_{36}. We want to find V_{23}^{min} and p_2^{min}, but there are two different computed values of p_3^{min}

from previous visits to nodes 4 and 6. By choosing the highest value of p_3^{min}, V_{23}^{min} refers to the minimum amount of gas in pipeline b_{23} required to maintain the minimum pressure at both downstream load points. Finally, in accordance with Section 5.3, the storage V_{ij}^s in each pipeline is found as the difference between V_{ij} and V_{ij}^{min}.

In case a pipeline fails, it is isolated by valves at each pipeline end, leaving all load points downstream the faulted pipeline without connectivity to the source. However, the loads are temporarily supplied by the accumulated storage in the pipelines downstream of the faulted pipeline. This feature is illustrated in the reliability block diagram in Fig. 5.7. Each pipeline b_{ij} having a set of downstream pipelines $\mathcal{B}^{ds}$ and downstream load points $\mathcal{N}_L^{ds}$ has been paired with a storage equivalent S_{ij}^{eq}. The storage equivalent S_{ij}^{eq} represents the accumulated storage in the pipelines downstream b_{ij}.

The survival time of the storage equivalent is defined as:

$$ST_{ij}^{eq} = \frac{\sum_{b \in \mathcal{B}^{ds}} V_b^s}{\sum_{k \in \mathcal{N}_L^{ds}} L_k} \tag{5.8}$$

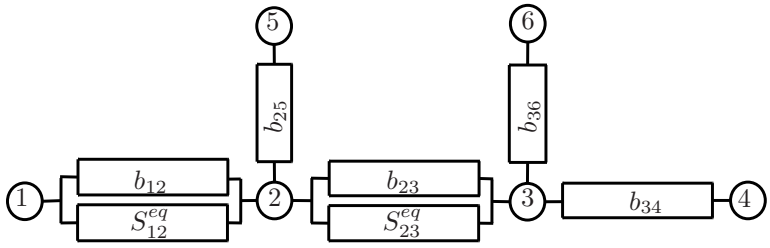

Figure 5.7: Reliability block diagram with respect to energy supply from the source to the load points.

5.6.1 Example: Network Storage

It is possible to extend the application of the analytical simulation procedure applied to gas networks, as described in Publication B, to include the impact of pipeline storage.

A numeric example was performed for the network in Fig. 5.6. It was assumed that each pipeline fails once a year and that it takes 12 hours to

repair the faulted pipeline, hence λ_u =1 year^{-1} and r_u =12 hours. The equivalent survival times were set to:

$$\begin{array}{lll} ST_{12}^{eq} & = \frac{V_{23}^s+V_{34}^s+V_{36}^s+V_{25}^s}{L_4+L_5+L_6} & = 3 \text{ hours} \\ ST_{23}^{eq} & = \frac{V_{34}^s+V_{36}^s}{L_4+L_6} & = 2 \text{ hours} \end{array}$$

To relate these survival times to a physical pipeline, the reader could refer to Fig. 5.3.

Table 5.1 shows how the reliability parameters for the load points are accumulated when considering the failure of each pipeline. Interruption rates are in interruptions/year and outage times in hours/year. For comparison, in case pipeline storage is ignored, the calculated average annual outage time for load points 4 and 5 are 36 hours/year and 24 hours/year, respectively.

Table 5.1: Average interruption rates and annual outage times.

Load pt 4	**Load pt** 4		**Load pt** 5		**Load pt** 6	
Failure	λ_4	U_4	λ_5	U_5	λ_6	U_6
b_{12}	0.800	9.600	0.800	9.600	0.800	9.600
b_{23}	0.857	10.286			0.857	10.286
b_{34}	1.000	12.000				
b_{25}			1.000	12.000		
b_{36}					1.000	12.000
TOT	2.657	31.886	1.800	21.600	2.657	31.886

5.7 Application to District Heating Systems

In resemblance to high-pressure natural gas pipeline systems, energy storage in DHSs is significant and should be considered in reliability studies. This issue was discussed in Publication D, and it was suggested to apply the Markov model in Fig. 5.5 to DHSs.

However, operational differences between the two systems indicate that the Markov model is less suited for the DHS. Unlike the NGS, the DHS is not normally operated with an extra amount of energy in the pipelines. This is not considered a viable option from an operational point of view, since thermal losses increases with increasing flow and supply temperature. Thus, the DHS

The idea presented in Publication D was to continue circulating flow in a pipeline even with no operating upstream thermal power production units. This was also briefly discussed in Chapter 4, illustrated by considering the production unit TP faulted in Fig. 4.3. Although the interruption at the downstream load point will be delayed by continue circulating the water, the transition from state 2 to 1 in Fig. 5.5 may be misleading. While residing in state 2 the load is consuming thermal power, creating a thermal power deficit in the pipeline. In case the system returns to state 1 without visiting state 3, this deficit will continue travelling and eventually reach the load, causing a 'dip' in temperature. For this reason, the Markov model in Fig. 5.5 may provide unrealistic results by overestimating the impact of pipeline storage in the DHS.

Chapter 6

Closure

6.1 Summary

This thesis presents novel methods for assessing reliability of supply and dependency in three different energy distribution systems. Serving as a general framework, conventional network models of the distribution systems were developed. The suggested methods are founded on these network models and were all tested on different test systems or in case studies.

The contributions can be grouped according to their thematic belonging:

Reliability of supply: The contribution described in Chapter 3 (Publication B), concerning reliability evaluation of natural gas distribution systems, is based on state-of-the-art reliability calculations from the electric power domain. Network constraints and the expected operator responses to different failure modes were considered. It is the application area rather than the modelling approach that forms the novel contribution. In contrast, Chapter 5 (Publication D) describes a new modelling approach incorporating pipeline storage in reliability evaluation of high-pressure natural gas pipeline systems. Pipeline storage was considered a subsystem being forced into operation once the upstream supply to a load point fails. The storage failure rate was found, and then the basic reliability parameters were obtained from a Markov model.

Dependency between systems: Two of the contributions concern dependency between systems. First, dependency at load level was modelled in Chapter 2 (Publication A). Introducing a second energy carrier in an area dominated by electric power, will affect the type of energy end-uses served by the electric power system. An optimisation problem was formulated, finding the optimal allocation of switchgear in an electric power distribution system. It was shown how changes in energy end-uses cause changes in the expected customer interruption costs, which in turn affect the optimisation problem. Second, the dependency of district heating systems on electric power was modelled in Publication C. Network models of the two systems were coupled and the consequences of higher-order power system failures were quantified for both systems.

The methods developed in this thesis were all tested on fictitious small-scale test systems. The intention by doing so was to demonstrate the basic functionality, clarify the underlying assumptions and allow for the presented results to be reproduced. In addition, some of the methods were tested on larger test systems presented in the international scientific community, such as [23, 37]. As far as possible, the test system data has been published or referenced.

6.2 Potential Applications

The potential applications of the contributions from this thesis are in the following areas:

- Reliability evaluation of natural gas systems. By using the approaches in Chapters 3 and 5, it is possible to quantify the basic load point reliability indices in natural gas networks, including the impact of pipeline storage.
- Detailed studies of the changes the electric power system faces when introducing a second energy carrier in an area. By using the method in Chapter 2, a network company can analyse whether the allocation of switchgear is appropriate according to the end-uses served by the electric power system.

- Integrated planning of co-existing energy distribution systems. The increasing awareness of integrated planning has resulted in several new tools and methodologies to support the planning process [48, 60, 61]. So far, these mainly concern operational optimisation and do not consider reliability of supply. The reliability evaluation approach for natural gas distribution systems in Chapter 3 and the simplified thermal power-flow model in Chapter 4 could provide useful input in this context.

6.3 Concluding Comments

The main conclusions may be summarised as follows:

- It is possible to include considerations regarding the type of end-uses served by the electric power system when assessing the optimal allocation of switches in the system. A method suitable for this task was presented and applied to test networks.

- Structural and operational similarities between electric power and natural gas distribution systems justify the application of reliability modelling techniques from the electric power domain to the latter.

- The explicit dependency of the district heating system on electric power can be represented by couplings between network models of the two systems. In this way the cascading consequences of power system failures in the district heating system are quantified.

- The impact of pipeline storage on reliability of supply in natural gas pipeline systems can be quantified by means of a Markov model.

These conclusions rely on a number of assumptions, as stated in the publications and throughout the previous chapters. Generally, these assumptions serve to simplify the presented solution procedure and to avoid distracting attention from the novel method or problem formulation.

6.4 Future Work

Some possible subjects for further work are presented below:

Further testing: The contributions described in this thesis were tested on different test systems. A natural step ahead would be to further test the methods in realistic case-studies and discuss the approach, assumptions and results with the relevant stakeholders.

Treatment of constraints: Network constraints are generally treated as absolute in this work. An alternative approach would be to treat these as soft constraints, penalising constraint violations.

Computational performance: Some of the presented algorithms could be improved with respect to computational speed, and in some cases replaced with more efficient algorithms. The topic of computational performance has not been addressed here, but should be considered if further testing and development of the presented methods is desirable.

Accuracy of steady-state assumptions: The models computing thermal power flow in district heating systems and storage in natural gas transmission pipelines, are both steady-state representations of highly dynamic system behaviours. In order to test the accuracy of these models, they could be more thoroughly compared with transient flow simulations.

System couplings: Physical couplings between systems were described for the case of electric power and district heating systems in this work. More sophisticated couplings, allowing back-up systems to act as safety barriers could be included in the presented model. Moreover, other system-couplings, e.g. between electric power and natural gas, could be modelled as well. Inspiring ideas are presented in [62].

Appendix A

Flow in Pipeline Networks

This chapter presents a method appropriate for finding nodal pressures and pipeline flows in meshed pipeline networks comprising various network components. First, two basic ways of formulating the flow problem are presented. Subsequently, a specific method, known as the Newton nodal-loop method is elaborated.

A.1 Introduction

This chapter is basically a compilation of a section in a comprehensive book on analysis of gas networks [63], presenting the Newton nodal-loop method in detail. The method was selected based on its robustness to variations in network topology and nodal input. The presented method has been tested on selected natural gas and water distribution networks in [37, 51, 63].

Equation (A.1) is generally valid[1] for gaseous and liquid flow in a pipeline, assuming isothermal, steady-state flow.

$$Q_b = K_b S_b \left[S_b (p_i^2 - p_j^2) \right]^{\frac{1}{\gamma}} \tag{A.1}$$

[1] Note that a number of modified and specialised equations provide increased accuracy, depending on fluid properties and flow conditions.

where:

Q_b	=	mass flow in pipeline b
K_b	=	pipeline constant for pipeline b (dependent on pipeline dimensions, environmental conditions, fluid properties, etc.)
S_b	=	1 if $p_i \geq p_j$
S_b	=	-1 if $p_i < p_j$
p_i	=	pipeline inlet pressure
p_j	=	pipeline outlet pressure
γ	=	flow exponent (normally ~ 2)

A network comprises a set $\mathcal{N}$ of N nodes and a set $\mathcal{B}$ of B branches. Each node $i \in \mathcal{N}$ may be associated with a certain load L_i, having a positive reference out of the network. For the network in Fig. A.1, nodes 1 and 6 are injecting, whereas nodes 2-5 are consuming mass flow.

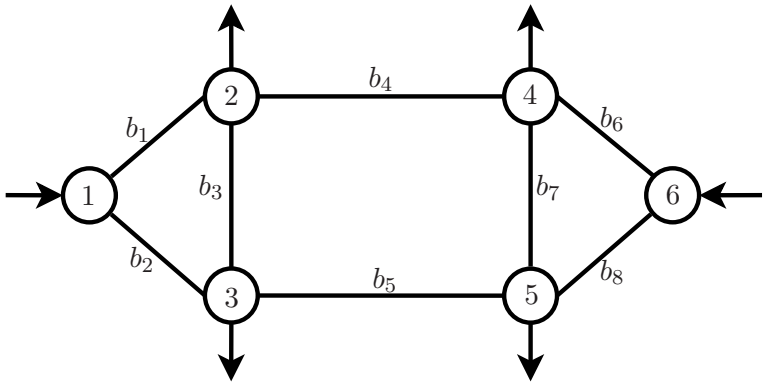

Figure A.1: A network comprising nodes and branches.

A.2 Nodal Formulation

A network, such as the one in Fig. A.1, is described by a branch-nodal incidence matrix $\mathbf{A}$ (dim $N \times B$), where the elements are defined as:

$$a_{ib} = \begin{cases} +1 & \text{if branch } b \text{ enters node } i \\ -1 & \text{if branch } b \text{ leaves node } i \\ 0 & \text{if branch } b \text{ is not connected to node } i \end{cases}$$

The nodal balance is formulated for each node in the network:

$$\mathbf{AQ} = \mathbf{L} \tag{A.2}$$

where:
$\mathbf{Q}$ = mass flow vector, dim B
$\mathbf{L}$ = nodal load vector, dim N

In short, the Newton nodal method finds the pipeline flows based on an approximation of nodal pressures. Then $\mathbf{Q}$ is found from (A.1), before nodal mismatches are found in (A.2). Subsequently, pressure corrections are found with help from a linearised version of (A.1).

A.3 Loop Formulation

It is possible to improve convergence characteristics and make the solution less sensitive to initial conditions by expressing the nodal pressures in a pipeline as a function of flow, and updating flows. Thus, (A.1) can be reformulated:

$$\Delta P_b = p_i^2 - p_j^2 = \hat{K}_b |Q_b| Q_b^{\gamma-1} \tag{A.3}$$

where:
$\hat{K}_b$ = pipeline constant for pipeline b (dependent on pipeline dimensions, environmental conditions, fluid properties, etc.)

The number of loops l in the network is given by $l = B - N + 1$. For the network in Fig. A.1, there are $l = 8 - 6 + 1 = 3$ loops. Note that the loops are not unique. The sum of pressure drops around each loop equals zero, thus:

$$\mathbf{E\Delta P} = 0 \tag{A.4}$$

where:
$\mathbf{E}$ = branch-loop incidence matrix, dim $l \times B$
$\mathbf{\Delta P}$ = vector of pressure drops in branches, dim B

In short, the Newton loop method approximate the loop flows. Then $\mathbf{\Delta P}$ is found from (A.3), before loop mismatches are found in (A.4). Subsequently, loop flow corrections are found with help from a linearised version of (A.3).

A.4 Newton Loop-node Method

The Newton loop-node method as described here, combines the nodal and the loop formulations from Subsections A.2 and A.3. Comparing the Newton loop-nodal to the nodal method, the former has better convergence properties, since (A.3) is linearised rather than (A.1). While (A.3) is nearly quadratic ($\gamma \sim 2$), (A.1) has a near square-root term ($\gamma^{-1} \sim \frac{1}{2}$). Comparing the Newton loop-nodal method with the loop method, the advantage of the former is that loops in the network do not have to be explicitly defined.

Nodal pressures are represented by vector $\mathbf{P}$ (dim N). The branch pressure drops are found in (A.5)

$$\mathbf{\Delta P} = -\mathbf{A^T P} \tag{A.5}$$

By linearising (A.3), the following expression holds true:

$$\mathbf{\Delta P} = \mathbf{\Phi Q} \tag{A.6}$$

where $\mathbf{\Phi}$ (dim $B \times B$) is a diagonal matrix having entries for each branch b:

$$\phi_b = \frac{\partial(\Delta P_b)}{\partial Q_b} = \hat{K}_b |Q_b|^{\gamma-1} \tag{A.7}$$

By combining (A.2),(A.5) and (A.6), $\mathbf{Q}$ can be eliminated to obtain:

$$\mathbf{GP} = -\mathbf{L} \tag{A.8}$$

where:
$\mathbf{G} = \mathbf{A\Phi^{-1}A^T}$

The matrix $\mathbf{G}$ represents the network without non-pipeline elements. Adding U non-pipeline units and setting the flow through each unit as a positive demand at the inlet node and negative demand at the outlet node, (A.8) can be rewritten:

$$\mathbf{GP} = -\mathbf{L} - \mathbf{Kf} \tag{A.9}$$

where the entries in matrix $\mathbf{K}$ (dim $N \times U$) are:

$$k_{iu} = \begin{cases} +1 & \text{if the } u^{th} \text{ unit has its inlet at node } i \\ -1 & \text{if the } u^{th} \text{ unit has its outlet at node } i \\ 0 & \text{otherwise} \end{cases}$$

The vector $\mathbf{f}$ (dim U) describes the flow through each unit.

Equation (A.9) can be reformulated as:

$$\begin{bmatrix} \mathbf{G_N} & \hat{\mathbf{G}} & \mathbf{K^I} \\ \hat{\mathbf{G}}^{\mathbf{T}} & \dot{\mathbf{G}} & \mathbf{K^O} \end{bmatrix} \begin{bmatrix} \dot{\mathbf{P}} \\ \mathbf{P} \\ \mathbf{f} \end{bmatrix} = - \begin{bmatrix} \mathbf{L^I} \\ \mathbf{L^O} \end{bmatrix} \tag{A.10}$$

Consider U units having outlet nodal pressures $p_1, p_2, ..., p_U$. Pressures at the remaining nodes are $\dot{p}_1, \dot{p}_2, ..., \dot{p}_V$, where $V = N - U$. Rows and columns have been permuted from the original matrix $\mathbf{G}$ in (A.9); $\mathbf{G_N}$ (dim $V \times V$) represents pipeline-pipeline connections, $\hat{\mathbf{G}}$ (dim $V \times U$) represents unit-pipeline connections and $\dot{\mathbf{G}}$ (dim $U \times U$) represents unit-unit connections. Furthermore, $\mathbf{K^I}$ (dim $V \times U$) is the inlet part and $\mathbf{K^O}$ (dim $U \times U$) the outlet part of the $\mathbf{K}$ matrix.

In order to solve (A.10), a description of each unit's performance should be incorporated. The flow though a unit and the corresponding inlet and outlet pressures can be formulated as:

$$a\dot{P} + bP + cf = d \tag{A.11}$$

The coefficients a, b, c and d may vary with time. For example, if the outlet pressure is kept constant at P_{set}, then $a = c = 0$, $b = 1$ and $d = P_{set}$. This is the typical performance of a regulator station in a natural gas system. In case the upstream pressure becomes lower than P_{set}, the regulator can turn fully open so that $a = b = 0$, $c = 1$ and $d = f_{upstream}$. Generally (A.11) can be formulated as:

$$\mathbf{C_1}\dot{\mathbf{P}} + \mathbf{C_2}\mathbf{P} + \mathbf{C_3}\mathbf{f} = \mathbf{d} \tag{A.12}$$

where dim $C_1 = (U \times V)$, dim $C_2 = (U \times U)$, dim $C_3 = (U \times U)$ and

dim $d = (U \times 1)$. This gives the final formulation:

$$\begin{bmatrix} \mathbf{G_N} & \hat{\mathbf{G}} & \mathbf{K^I} \\ \hat{\mathbf{G}}^{\mathbf{T}} & \dot{\mathbf{G}} & \mathbf{K^O} \\ \mathbf{C_1} & \mathbf{C_2} & \mathbf{C_3} \end{bmatrix} \begin{bmatrix} \dot{\mathbf{P}} \\ \mathbf{P} \\ \mathbf{f} \end{bmatrix} = - \begin{bmatrix} \mathbf{L^I} \\ \mathbf{L^O} \\ \mathbf{d} \end{bmatrix} \tag{A.13}$$

Equation (A.13) is solved iteratively, until convergence is obtained for the values in $\dot{\mathbf{P}}$, $\mathbf{P}$ and $\mathbf{f}$.

Appendix B

Publications

B.1 Publication A

A. Helseth and A. T. Holen. Impact of Energy End-use and Customer Interruption Cost on Optimal Allocation of Switchgear in Constrained Distribution Networks. *IEEE Transactions on Power Delivery*, accepted for future publication.

Impact of Energy End Use and Customer Interruption Cost on Optimal Allocation of Switchgear in Constrained Distribution Networks

Arild Helseth and Arne T. Holen, *Member, IEEE*

***Abstract*—The introduction of new energy carriers, such as natural gas and district heating, to energy systems dominated by electrical power will certainly relieve stress on the power system. Some of the end uses initially served by the power system will be gradually decoupled and served by alternative energy carriers. As a result, the specific customer interruption costs and load profiles will change. In this paper, we analyze how the optimal level of switchgear in electric power distribution systems is affected by such changes. The proposed optimization method is based on a genetic algorithm and takes into account the constrained network capacity.**

***Index Terms*—Customer interruption cost, genetic algorithms (GAs), network constraints, power distribution protection, power distribution reliability.**

I. Introduction

THE basic function of the power distribution system is to supply customers with electrical energy as economically as possible and with an acceptable degree of reliability. Consequently, obeying the two conflicting objectives of economics and reliability is the main challenge when constructing new or expanding existing distribution systems. Several countries, including Norway, have carried out extensive surveys with the purpose of eliciting the economical losses experienced by different customer groups due to power interruptions. In this way, reliability can be quantified in terms of a monetary value, and the worth of any investment in the power system may be found through a cost-benefit analysis [1].

Electrical power is the dominating energy carrier in the Norwegian energy system. By introducing alternative energy infrastructures, such as natural gas and district heating, some of the energy end uses may be decoupled from the power system. As a result, the electrical load profile will change and the demand for electrical power will decrease.

Will this shift in demand affect the optimal level of investments in reliability-enhancing projects? Intuitively, a relief in demand for electrical power will lead to decreased interruption consequences since less power has to be transported to the customers. Thus, the optimal level of investment in reliability will decrease, compared to the case where electricity serves all end uses. Furthermore, load relief on tightly constrained distribution feeders may improve the ability to restore service through reserve connections in the network, resulting in system reliability improvement without additional investments. On the other hand, consumer surveys reveal that the end use that can only be covered by electricity tends to have a higher associated cost of interruption. These conflicting momentums are all incorporated in an optimization method presented in this paper.

Finding the optimal number and location of switchgear in radial distribution systems is a complex problem which has been approached by several authors [2]–[8]. The problem may be classified as a combinatorial optimization problem having a nonlinear and nondifferentiable objective function. Various techniques have been applied to solve the optimal configuration problem (e.g., dynamic programming [2], binary programming [3], simulated annealing [4], direct search [5], and genetic algorithms (GAs) [6]–[8]).

The presented methodology applies a GA for the purpose of optimizing the number of automated and manual switching devices in a prerouted, radial distribution system. The energy end uses are divided in two categories: those that can only be provided by the power system and those that can be provided by any energy infrastructure. Different interruption costs are applied for these two categories. The impact of reduction in demand and changes in the load profile on the optimization problem is analyzed and discussed. By performing this type of study, a network company may analyze whether the amount and configuration of switchgear is appropriate according to the end-use specific interruption costs and load profiles.

II. Interruption Costs

Different customer sectors apply electricity for different end uses. Surveys from various countries show that each customer sector will evaluate the loss of a service differently, depending on the end uses the customer sector typically covers by electricity and the interruption duration [1]. Customers put more emphasis on the cost and inconvenience associated with the inability to perform their activities due to an interruption rather than the energy which is not supplied.

In Norway, the regulation scheme cost of energy not supplied (CENS) adjusts the revenue of the network companies in accordance with the customers' interruption costs [9]. The expected CENS is calculated as the product of the annual expected energy not supplied (EENS) and a specific interruption cost in NOK/kWh_{ENS} (1 Euro $\approx$ 8 NOK). The applied CENS rate is sector dependent, but independent of interruption duration.

Manuscript received January 29, 2007; revised May 15, 2007. Paper no. TPWRD-00033-2007.

The authors are with the Department of Electrical Power Engineering, Norwegian University of Science and Technology (NTNU), Trondheim 7491, Norway (e-mail: helseth@elkraft.ntnu.no).

Color versions of one or more of the figures in this paper are available online at http://ieeexplore.ieee.org.

Digital Object Identifier 10.1109/TPWRD.2007.909215

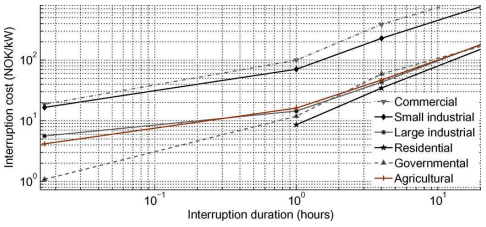

Fig. 1. Sector customer damage functions for Norwegian customers.

TABLE I
RELATIVE CONSUMPTION AND INTERRUPTION COST FOR THE COMMERCIAL CUSTOMER SECTOR

End-use category	Consumption (% of total)	Cost (% of total)
Space heating	26	8
Hot tap water	4	2
Cooling	8	4
Electrical boilers	4	1
Cooking	9	2
Lighting, computers, electric devices etc.	49	83

For more detailed system planning, it is believed that the nonlinear profile of interruption costs as a function of interruption duration should be accounted for. Such profiles are conveniently displayed in sector customer damage functions (SCDFs). SCDFs are created by aggregating the cost functions of individual customers in the same customer sector. The SCDFs for the six different customer sectors used in Norway are shown in Fig. 1, based on an extensive survey conducted by the Institute for Research in Economics and Business Administration (SNF) and SINTEF Energy Research [10]. When studying the SCDFs in Fig. 1, one should keep in mind that the consumers in Norway generally apply electricity to cover all energy end uses.

Additional accuracy may be added by assigning one SCDF for each distinctive end-use category, as represented in (1). Examples on typical end-use categories are shown in the first column of Table I

$$\mathrm{SCDF}_i = \begin{bmatrix} C_{e_1,t_1} & C_{e_1,t_2} & \cdots & C_{e_1,t_n} \\ C_{e_2,t_1} & C_{e_2,t_2} & \cdots & C_{e_2,t_n} \\ \vdots & \vdots & \ddots & \vdots \\ C_{e_m,t_1} & C_{e_m,t_2} & \cdots & C_{e_m,t_n} \end{bmatrix}. \quad (1)$$

Where SCDF_i is the SCDF for customer sector i and $C_{e,t}$ is the cost associated with the inability to serve end-use category e during a period t. In this matrix, m different end-use categories and n different interruption duration periods are displayed. All end-use categories are aggregated in Fig. 1 ($m = 1$), thus every SCDF_i is represented by a $1 \times n$ vector.

Alternative energy carriers, such as district heating and natural gas, are able to cover some of the same end uses as electrical power. An extensive discussion of the different end uses is not within the scope of this paper; thus, we will aggregate end uses in two major categories

End-use category:	Covered by:
Electricity specific	Electric power system
Flexible	Any energy infrastructure

.

Obviously, the category of flexible end uses contains different services depending on the energy carrier. Natural gas may, for example, be used for cooking, but this end use cannot easily be provided by the district heating system. Furthermore, a low supply temperature in a district heating system may exclude the possibility of serving certain thermal end uses.

In the survey described in [10], respondents of some selected customer sectors were asked to estimate the cost associated with the loss of ability to perform activities in selected end-use categories and the annual energy consumption related to each end-use category. These data refer to non-notified interruptions at a given reference time (weekday in January). Data for the commercial customer group are presented in Table I and will be used in the subsequent sections of this paper. The end-use categories of space heating, hot tap water, and electrical boilers are defined as flexible end uses.

It is evident that the inability to perform electricity specific end uses has a higher associated cost than is the case for flexible end uses for the commercial customer sector. Unfortunately, the survey does not give sufficient information to display the end-use specific interruption costs as a function of interruption duration and present accurate corresponding SCDF_i matrices as described in (1) for the two aggregated end-use categories. However, for the purpose of illustrating the suggested method, some new SCDFs were created. The original SCDFs shown in Fig. 1, are now denoted as $\mathrm{SCDF}_i^{\mathrm{old}}$. Based on $\mathrm{SCDF}_i^{\mathrm{old}}$ and the weighting factors α_i and β_i defined in (2), a new SCDF matrix $\mathrm{SCDF}_i^{\mathrm{new}}$, was constructed from (3). For all values of interruption duration, (4) should be fulfilled

$$\alpha_i = \frac{\mathrm{Cost}_i^{EL}(\%)}{\mathrm{Consumption}_i^{EL}(\%)}$$
$$\beta_i = \frac{\mathrm{Cost}_i^{\mathrm{FLEX}}(\%)}{\mathrm{Consumption}_i^{\mathrm{FLEX}}(\%)} \quad (2)$$

$$\mathrm{SCDF}_i^{\mathrm{new}} = \begin{bmatrix} \alpha_i \\ \beta_i \end{bmatrix} \times \mathrm{SCDF}_i^{\mathrm{old}} \quad (3)$$

$$\alpha_i \mathrm{Consumption}_i^{EL} + \beta_i \mathrm{Consumption}_i^{\mathrm{FLEX}} = 100\%. \quad (4)$$

Generally, the services related to the flexible end-use category are less affected by short interruptions than the services related to the electricity specific end use (e.g., due to thermal inertia of buildings and the presence of storage tanks for hot tap water). Consequently, it is likely that the shape of the SCDF for the flexible and electricity specific end-use categories will differ for low values of interruption duration. In order to reflect the differences in shape for the two end-use categories, it is simply assumed that interruptions of the flexible end use having a duration of less than X mins will not be noticeable for the customers.

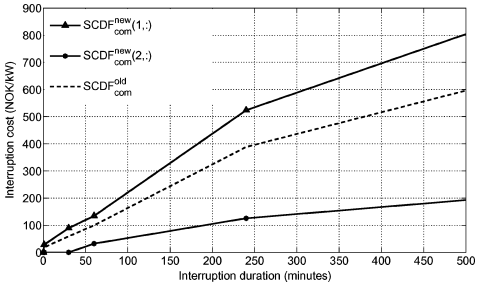

Fig. 2. SCDF for the commercial customer sector.

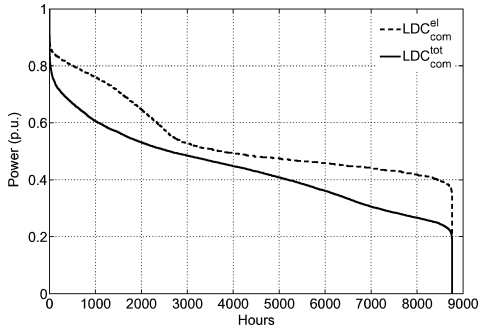

Fig. 3. Load duration curve for the commercial customer sector.

Accordingly, β_i is set to be equal to zero and α_i is changed so that (4) is fulfilled.

A new SCDF matrix for the commercial customer sector $\mathrm{SCDF}^{\mathrm{new}}_{\mathrm{com}}$ was constructed from (3). By using data from Table I, the weighting factors become $\alpha_{\mathrm{com}} = 89/66$ and $\beta_{\mathrm{com}} = 11/34$. $\mathrm{SCDF}^{\mathrm{old}}_{\mathrm{com}}$ and $\mathrm{SCDF}^{\mathrm{new}}_{\mathrm{com}}$ are displayed in Fig. 2, with $X = 30$.

It should be noted that the difference between the electricity specific and the flexible end-use categories shown in Fig. 2 was found to be particularly large for the commercial customer sector and was less evident for the remaining customer sectors.

III. Load Duration Curves

In power distribution networks with constrained capacity, load-flow studies will reveal whether the network constraints are met before system reconfigurations are performed. Estimates of reconfiguration capability are normally based on system peak load and, thus, contributes to a conservative estimate of the reliability of the network. For more detailed reliability studies, load duration curves (LDCs) should be applied. A LDC comprises load data plotted in a descending order of magnitude, where each load level has a corresponding probability of occurrence.

The LDCs for the electricity specific and the flexible end-use categories differ significantly in shape due to different consumption patterns throughout the year. LDCs for the sum of all end uses ($\mathrm{LDC}^{\mathrm{tot}}_{\mathrm{com}}$) and the electricity-specific end uses ($\mathrm{LDC}^{\mathrm{el}}_{\mathrm{com}}$), based on hourly peak load measurements from a typical Norwegian commercial-sector customer, are shown in Fig. 3. In order to analyze the possible influence that the differences in shape have on the optimization problem, two 10-step load duration curves ${}^{10}\mathrm{LDC}^{\mathrm{tot}}_{\mathrm{com}}$ and ${}^{10}\mathrm{LDC}^{\mathrm{el}}_{\mathrm{com}}$ were created based on the data presented in Fig. 3. These curves are used in the subsequent calculations and their corresponding numerical values are shown in Table II.

We now assume that the load duration curve $\mathrm{LDC}^{\mathrm{tot}}_{\mathrm{com}}$ from Fig. 3 is representative for the commercial customers who contributed to the survey in [10].

As previously shown in Table I, the electricity-specific end-use category requires 66% of the total energy demand for the commercial customer group. Assuming that this end-use category adheres to the $\mathrm{LDC}^{\mathrm{tot}}_{\mathrm{com}}$, the maximum power required is 66% as well. However, by using the $\mathrm{LDC}^{\mathrm{el}}_{\mathrm{com}}$ displayed in Fig. 3, the maximum power requirement is only 55% of the total maximum power. Thus, applying the correct load curve may influence the reconfiguration capability of constrained feeders which, in turn, may influence the outcome of the optimization problem.

TABLE II
Numerical Values for 10-Step Load Duration Curves for the Commercial Customer Sector

		${}^{10}LDC^{el}_{com}$	${}^{10}LDC^{tot}_{com}$
Step	Probability	Electricity specific (p.u.)	Total (p.u.)
1	0.0057	1.000	1.000
2	0.1084	0.855	0.755
3	0.1142	0.760	0.605
4	0.1142	0.645	0.531
5	0.1142	0.526	0.484
6	0.1142	0.495	0.448
7	0.1142	0.475	0.410
8	0.1142	0.459	0.360
9	0.1142	0.440	0.305
10	0.0868	0.419	0.268

IV. Problem Formulation

Deciding the optimal level of switchgear in a radial distribution system is a combinatorial optimization problem. The solution space is constrained by the type and amount of switchgear available. We consider two categories of switchgear in this optimization procedure: 1) the automatically operated switch (AOS) and 2) the manually operated switch (MOS). Fuses are also modelled, but their locations have been predefined. The presented optimization procedure treats the switch allocation problem as an independent subproblem, without addressing reinforcement or downsizing of distribution system equipment. It is believed that equipment downsizing should be included for a more detailed analysis, and that this feature may be added modularly to the presented procedure.

A. Switchgear

A short and general description of the functionality of the switchgear applied in the proposed model will follow. An AOS will automatically isolate a faulted section of a distribution circuit once an upstream circuit breaker or recloser has interrupted

the fault current. An MOS is operated manually by a repair crew and is capable of opening and closing a circuit when negligible current is broken or made. The AOS and MOS have no ability to break fault currents; thus, they will not impact the frequency of interruptions experienced by the customers [11]. Fuses are overcurrent protection devices which are usually located at the beginning of distribution laterals. Once a fuse has melted and operated due to a downstream fault, it requires replacement before the protected lateral can carry load again.

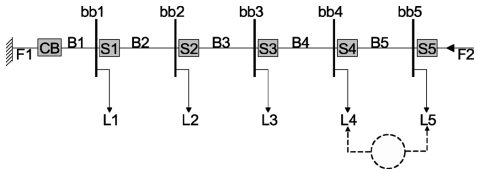

Fig. 4. Simple distribution system radial.

B. Assessing Load-Point Reliability

An analytical simulation approach is applied to assess load-point reliability [12]. Radial distribution systems may be modelled as tree data structures comprising a set of nodes and branches. The failure of each system component is simulated and interrupted load points are classified in distinctive classes depending on interruption time. A two-stage restoration strategy is modelled, as described in [13]. First, a limited set of load points is restored by using the available AOSs. These load points experience an interruption of duration equal to the automatic sectionalizing time and belong to class A. Second, additional load points are restored by using MOSs. These load points experience an interruption duration equal to the manual sectionalizing time and belong to class B. Load points which are not restored before the faulted component has been repaired or replaced belong to class C. In case node voltages drop below a preset minimum level ($V_{\min}$) due to reconfiguration, the solution is rejected and alternative switch operations are sought. This procedure is repeated for all load levels and all contingencies.

The reliability assessment procedure is based on the following assumptions:

- the distribution system is radially operated;
- only first-order contingencies are considered;
- all switchgear is 100% reliable;
- all switchgear is properly coordinated;
- temporary failures are not considered;
- a circuit breaker is always located at the root of each tree (i.e., at the substation of the distribution system).

C. Illustrative Example

The following example illustrates the logic of a two-stage restoration strategy. Furthermore, a discussion on the impact of introducing alternative energy carriers on reliability is given.

Consider the simple radial shown in Fig. 4, comprising five busbars (bb1–bb5), branches (B1–B5), load points (L1–L5), switches (S1–S5), and a circuit breaker (CB). Assume that switches S2, S4, and S5 are AOSs and the remaining switches are MOSs, that S1–S4 are normally closed and that S5 is normally open. The reserve connection through feeder 2 (F2) is capable of supplying L4 and L5 at the given load level. Both flexible and electricity specific end uses are served by the power system.

In case of a permanent fault on branch B2, the restoration algorithm will first request that CB and S2 open to isolate B2. The intention is then to close S5, establish the reserve connection through feeder F2, and restore supply to load points L3–L5. However, due to the feeder constraints, the load-flow study will reveal that the suggested operations result in violated feeder constraints and the algorithm will search for the next AOS downstream S2, which is S4. No constraints are violated this time; thus, CB and S4 are opened to isolate B2 and restore service to L5. Subsequently, the second stage of the restoration is initiated, requesting that the MOSs S1 and S3 open and that CB and S4 close to further limit the isolated area. Again, the network constraints are not violated, and L1 and L4 are restored by performing the requested operations. Load points L2 and L3 will not be restored until B2 has been repaired. Consequently, load point L5 belongs to class A, L1 and L4 to class B, and L2 and L3 to class C.

Assume that the flexible end uses of load points L4 and L5 are detached from the power system and served by a local heat supplier. There is now the possibility that, after a permanent fault on B2, S2 can open so that L3–L5 are restored without violating feeder constraints. Load points L3 and L4 will then belong to class A and, thus, experience improvement in reliability. Both the explicit load reduction and the change in aggregated profile of the feeder load are factors that may trigger the change in reconfiguration capability.

D. Genetic Algorithms

GAs are search algorithms based on the mechanics of natural selection and natural genetics. A GA does not rely on the assumption of linearity, differentiability, continuity, or convexity of the objective function.

A simple binary GA was defined for this optimization problem by using the Java package JGAP [14]. Initially, the GA randomly creates a population of feasible solutions. Each solution is a string of binary variables in which each bit represents the presence (1) or absence (0) of switchgear in a predefined location in the distribution network. The possible locations of switchgear are predefined according to a set of rules. Branches are divided in two types: 1) primary and 2) terminal branches. Terminal branches are directly connected to the load points and are equipped with fuses at their sending ends. Primary branches are not directly connected to load points. A switch may be allocated at the sending end of each primary branch. In Fig. 5, switch S1 on branch B1 is represented by the bits {1,0}. The first bit indicates the presence of the switch and the second bit is the absence of automatic control. Similarly, S2 is present and is controlled automatically. Thus, the primary branches B1 and B2 in Fig. 5 have the presence of an MOS and AOS, respectively.

The next generation of solutions is chosen based on the rules of probability theory and the fitness (objective function) of each

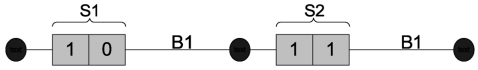

Fig. 5. Possible locations of switchgear on two primary branches.

solution. The further search for an optimal solution is governed by the three basic operators of reproduction, crossover, and mutation. A thorough description of the basic operators of the GA may, for example, be found in [15].

The expected customer outage cost (ECOST) relates the reliability of each solution (s) to a monetary value

$$\mathrm{ECOST}(s) = \sum_{i}^{ni}\sum_{j}^{nj}\sum_{k}^{nk} P_i\lambda_j \left[\gamma_k^1 \mathrm{LDC}_{i,k}^{\mathrm{tot}} \mathrm{SCDF}_k^{\mathrm{old}}(r_{jk}) + \gamma_k^2 \mathrm{LDC}_{i,k}^{el} \mathrm{SCDF}_k^{\mathrm{new}}(1, r_{jk})\right]. \quad (5)$$

ni	number of steps on the LDC;
nj	number of components;
nk	number of load points;
P_i	probability of load step i;
λ_j	average failure rate for component j;
γ_k^1, γ_k^2	Boolean variables for load point k;
$\mathrm{LDC}_{i,k}^{\mathrm{tot}}$	total load at step i of the 10-step LDC for load point k;
$\mathrm{LDC}_{i,k}^{el}$	electricity specific load at step i of the 10-step LDC for load point k;
$\mathrm{SCDF}_k^{\mathrm{old}}(r_{jk})$	specific outage cost related to all end uses for the customer group at load point k given the outage time r_{jk};
$\mathrm{SCDF}_k^{\mathrm{new}}(1, r_{jk})$	specific outage cost related to the electricity specific end use for the customer group at load point k given the outage time r_{jk}.

In case all end uses are covered by electricity at a load point k, $\gamma_k^1 = 1$ and $\gamma_k^2 = 0$ in (5). Conversely, if only the electricity specific end use is covered by electricity, $\gamma_k^1 = 0$ and $\gamma_k^2 = 1$. The optimization procedure can be represented as in (6), where ICOST is the total annualized capital cost for switchgear

$$\text{Minimize}(\mathrm{ECOST} + \mathrm{ICOST}). \quad (6)$$

It should be noted that the GA has no convergence guarantee in arbitrary problems. In order to improve the convergence properties, hybrid GA schemes incorporating local search techniques may be constructed. In this study repeatability of the results was used as a convergence guarantee.

V. System Studies

In order to test the suggested optimization procedure and the impact of shifts in SCDFs and LDCs, the radial distribution system connected to bus 5 of the Roy Billinton Test System (RBTS) was designated as a test system [16], [17]. Failure rates and repair times are given in [16]. Customer data, feeder lengths, and load data are given in [17]. Manual and automatic switching time was set to 1 h and 1 min, respectively. The peak loads given in [17] were all increased by 40%. The annualized capital cost for an AOS and an MOS was set to 12 000 and 8000 NOK/year, respectively. Fig. 6 shows the original version of the test system, where feeders (F1–F4), load points (LP1–LP26), branches (1–43), and normally open switches (NO1–NO2) are labeled.

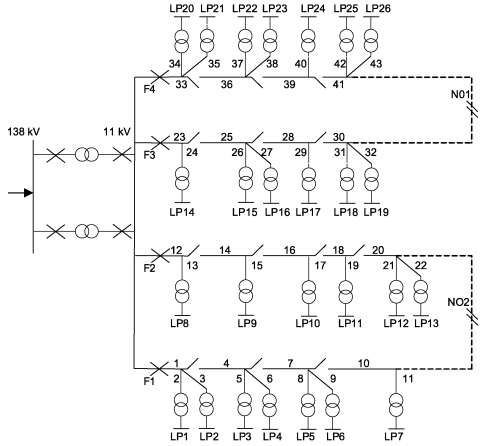

Fig. 6. Distribution system for RBTS bus 5.

The system was tested for five different combinations of SCDFs and LDCs. For all simulations, the minimum voltage $(V_{\min})$ was set to 0.95 p.u. Case 1, which is the base case, assumes that the power system supplies all load. The remaining four cases assume that all of the commercial customers (load points 7, 14, 18, 22, and 24 in Fig. 6) have their flexible end use provided by other energy carriers than electric power. The SCDFs and LDCs used for the commercial customer sector were displayed in Fig. 2 and Table II, respectively. All other load points were associated with the SCDFs shown in Fig. 1 and they were assumed to follow the ${}^{10}\mathrm{LDC}_{\mathrm{com}}^{\mathrm{tot}}$ from Table II.

Table III shows the results of the optimization procedure for the different combinations of SCDFs and LDCs. The character a following the switch number indicates the selection of an AOS, while b indicates an MOS. The corresponding ECOSTs and ICOSTs are shown in Fig. 7.

As expected, the results indicate that the ECOST decreases when the commercial customer–sector load is decoupled from the power system. By using the nonadjusted SCDF and LDC for the commercial customer sector in case 2, this decrease is 15.1%. A further comparison between cases 1 and 2 reveals that although the selected locations of switches in the two cases are essentially the same (except from the switch at branch 41), the number of AOSs is considerably higher in the base case.

TABLE III
OPTIMAL ALLOCATION OF SWITCHGEAR FOR THE PRESENTED CASES

Case	Type of SCDF	Type of LDC	Optimal solution
1	$SCDF_{com}^{old}$	${}^{10}LDC_{com}^{tot}$	7b, 10a, 20a, NO1a, 25a, 28b, 30a, 39a, 41b, N02a
2	$SCDF_{com}^{old}$	${}^{10}LDC_{com}^{tot}$	7b, 10b, 20b, NO1b, 25b, 28b, 30a, 39a, N02a
3	$SCDF_{com}^{old}$	${}^{10}LDC_{com}^{el}$	7b, 10b, 20b, NO1b, 25b, 28a, 30b, 39a, N02a
4	$SCDF_{com}^{new}(1,:)$	${}^{10}LDC_{com}^{tot}$	7b, 10a, 20a, NO1a, 25a, 28b, 30a, 39b, 41a, N02a
5	$SCDF_{com}^{new}(1,:)$	${}^{10}LDC_{com}^{el}$	7b, 10a, 20a, NO1a, 25b, 28a, 30b, 39a, 41b, N02a

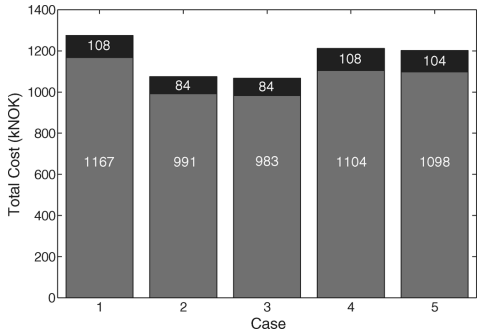

Fig. 7. ECOST (gray) and ICOST (black) for the presented cases ($1\,\mathrm{kNOK} = 1000\ \mathrm{NOK}$).

Marginal changes in ECOST and switch configurations were found when changing the LDC for the commercial customers from case 2 to case 3. The reduction in ECOST, shown in Fig. 7, is a result of the improvement in reconfiguration capability. We also note that the AOS on feeder F3 has changed its location from branch 30 to branch 28.

The optimal allocation and selection of switches is clearly affected by the choice of SCDF. As shown in Table III, the total number of selected switches and the number of AOSs in case 4 is similar to the base case. Taking the final step to case 5, where both the SCDF and LDC have been adjusted, we see that the ECOST decreases compared with case 4, again due to the increased reconfiguration capability. A similar pattern as found when going from case 2 to case 3 is seen from 4 to 5; AOSs are now located more centrally on feeders F3 and F4. By adjusting the SCDF and LDC, the decrease in ECOST from case 1 to case 5 is 5.9%, which is considerably less than the decrease found from case 1 to case 2.

Table IV presents the average annual outage time at some selected load points for the optimal configurations found in cases 1, 2, and 5. It is evident that most load points will experience a reliability improvement in terms of lower expected annual outage time, when going from nonadjusted data in case 2 to adjusted data in case 5.

TABLE IV
AVERAGE ANNUAL OUTAGE TIME FOR SOME SELECTED LOAD POINTS

Load Point	**Case 1** (hr/yr)	**Case 2** (hr/yr)	**Case 5** (hr/yr)
7	3.53	3.64	3.53
12	3.44	3.57	3.44
14	3.53	3.60	3.56
23	3.64	3.64	3.64
26	3.59	3.71	3.58

VI. CONCLUSION

The presented method makes it possible to analyze how the optimal allocation of switchgear in electric distribution systems is affected by decoupling the flexible end use from the system. In particular, the changes in customer interruption costs and load profile have been studied, and it is shown how they influence the optimal allocation of switchgear. This method is useful for configuration studies of distribution networks in areas where alternative energy carriers and sources replace electricity as providers of thermal energy services.

The amount of switchgear allocated in the presented test system was reduced when the flexible end use was decoupled. However, by using customer interruption costs and load duration curves adjusted according to the electricity specific end use, the reduction was not as evident as found when using aggregated data. The test study showed that the choice of SCDF has a more significant impact on the optimization problem than the choice of LDC. In less constrained networks, the impact of adjusting the LDC may be neglected.

ACKNOWLEDGMENT

The authors would like to thank Ph.D. student L. Pedersen at the Norwegian University of Science and Technology for providing detailed information on the load duration curves.

REFERENCES

[1] CIGRE TF 38.06.01, Methods to Consider Interruption Costs in Power System Analysis, CIGRE Publ. 191, 2001.
[2] V. Miranda, A. do Vale, and A. Cerveira, "Optimal emplacement of switching devices in radial distribution networks," in *Proc. CIRED*, Liège, Belgium, 1983, vol. 13, pp. 1–5.
[3] F. Soudi and K. Tomsovic, "Optimized distribution protection using binary programming," *IEEE Trans. Power Del.*, vol. 13, no. 1, pp. 218–224, Jan. 1998.
[4] R. Billinton and S. Jonnavithula, "Optimal switching device placement in radial distribution systems," *IEEE Trans. Power Del.*, vol. 11, no. 3, pp. 1646–1651, Jul. 1996.
[5] P. Wang and R. Billinton, "Demand-side optimal selection of switching devices in radial distribution system planning," *Proc. Inst. Elect. Eng., Gen., Transm. Distrib.*, vol. 145, no. 4, pp. 409–414, 1998.
[6] G. Levitin, G. Mazal-Tov, and D. Elmakis, "Optimal sectionalizer allocation in electric distribution systems by genetic algorithm," *Elect. Power Syst. Res.*, vol. 31, no. 2, pp. 97–102, 1994.
[7] R. E. Brown, S. Gupta, R. D. Christie, and S. S. Venkata, "A genetic algorithm for reliable distribution system design," in *Intelligent Systems Applications to Power Systems*. New York: IEEE, 1996, pp. 29–33.

[8] L. G. W. da Silva, R. A. F. Pereira, and J. R. S. Mantovani, "Allocation of protective devices in distribution circuits using nonlinear programming models and genetic algorithms," *Elect. Power Syst. Res.*, vol. 69, no. 1, pp. 77–84, 2003.

[9] G. Kjolle, A. T. Holen, K. Samdal, and G. Solum, "Adequate interruption cost assessment in a quality based regulation regime," presented at the IEEE Porto Power Tech Conf., Porto, Portugal, 2001.

[10] K. Samdal, G. Kjolle, O. Kvitastein, and B. Singh, Sluttbrukeres kostnader forbundet med avbrudd og spenningsforstyrrelser (in Norwegian) SINTEF Energy Res., 2003.

[11] E. Lakervi and E. J. Holmes, *Electricity Distribution Network Design*, ser. IEE Power Series. Stevenage, U.K.: Peregrinus, 1995, vol. 2.

[12] G. Kjolle and K. Sand, "RELRAD—An analytical approach for distribution system reliability assessment," *IEEE Trans. Power Del.*, vol. 7, no. 2, pp. 809–814, Apr. 1992.

[13] R. E. Brown and A. P. Hanson, "Impact of two-stage service restoration on distribution reliability," *IEEE Trans. Power Syst.*, vol. 16, no. 4, pp. 624–629, Nov. 2001.

[14] JGAP—Java Genetic Algorithms Package. [Online]. Available: http://www.jgap.sf.net.

[15] D. E. Goldberg, *Genetic Algorithms in Search, Optimization, and Machine Learning*. Reading, MA: Addison-Wesley, 1989.

[16] R. N. Allan, R. Billinton, I. Sjarief, L. Goel, and K. S. So, "A reliability test system for educational purposes—Basic distribution system data and results," *IEEE Trans. Power Syst.*, vol. 6, no. 2, pp. 813–820, Apr. 1991.

[17] R. Billinton and S. Jonnavithula, "A test system for teaching overall power system reliability assessment," *IEEE Trans. Power Syst.*, vol. 11, no. 4, pp. 1670–1676, Nov. 1996.

Arild Helseth received the M.Sc. degree in energy and environmental engineering from the Norwegian University of Science and Technology (NTNU), Trondheim, Norway, in 2003, where he is currently pursuing the Ph.D. degree in electrical power engineering.

Arne T. Holen (M'91) received the M.Sc. and Ph.D. degrees from the Norwegian Institute of Technology (NTH), Trondheim, Norway, in 1963 and 1968, respectively.

He is a Professor in the Department of Electrical Power Engineering, Norwegian University of Science and Technology (NTNU), Trondheim.

Dr. Holen is a member of the Power Engineering Society and of the Society of Reliability Engineers.

B.2 Publication B

A. Helseth and A. T. Holen. Reliability Modeling of Gas and Electric Power Distribution Systems; Similarities and Differences. In *Proc. of 9th International Conference on Probabilistic Methods Applied to Power Systems*, Stockholm, Sweden, 2006.

9th International Conference on Probabilistic Methods Applied to Power Systems
KTH, Stockholm, Sweden – June 11-15, 2006

Reliability modeling of gas and electric power distribution systems; similarities and differences

Arild Helseth, Arne T. Holen
Department of Electrical Power Engineering
The Norwegian University of Science and Technology (NTNU)
Trondheim, Norway
{helseth,holen}@elkraft.ntnu.no

***Abstract*— Due to the introduction of alternative energy carriers, such as district heating and natural gas, the Norwegian energy system is becoming more complex. Assessing the reliability of electrical distribution systems is a mature field of research, but limited work has been carried out concerning the reliability of distribution systems for alternative energy carriers. This paper proposes a methodology for assessing the reliability of natural gas distribution systems based on experiences drawn from similar analysis of electrical power distribution systems. A simple test case is presented for illustrative purposes and the basic load-point reliability indices of average interruption rate, average outage time and average annual outage time are found.**

I. Introduction

The energy consumption in Norway is primarily covered by electricity. Introduction of alternative energy carriers in the energy system, such as natural gas and district heating, are supported by the government and is expected to increase in the future.

Planning the coexistence and interconnection of the existing power system and emerging alternative energy infrastructures on a regional level is a complex task involving multiple criteria. Reliable access to energy is one important criterion, but it is not easy to quantify. Traditionally, reliability of supply in electrical power distribution systems (EPDS) has been assessed systematically by models and methodologies [1]. This paper attempts to apply the methodology from the domain of electrical power systems for reliability assessment of natural gas distribution systems (NGDS).

The physical structure of gas networks has several analogies to that of electrical power systems. Natural gas is carried from one or several sources to the consumers through transmission and distribution networks. High transmission pressure ensures efficient and economic transportation of gas to the load centers, where the pressure is reduced stepwise to meet the requirements of the distribution system and the consumers. In resemblance to EPDS, NGDS in urban areas are often meshed structures being operated radially. One feature that differentiate the behavior of electrical power and natural gas systems is the ability of the latter to store energy (gas) both in the pipeline network and in separate storages in order to optimize system performance and reliability. However, since the ability to store gas in the network is limited at lower pressure levels, transient behavior of gas flow is not considered in this work.

Reliability evaluation of natural gas transmission networks has been addressed by several authors [2]–[6]. Inspired by the framework for reliability assessment of electrical power system, [2] suggested dividing the natural gas system into three functional zones, where facilities of gas production, transmission and distribution are evaluated at hierarchical levels. Authors [3]–[5] applied Monte Carlo simulations to assess the availability of sufficient compression facilities in the transmission system to meet the consumer load. In [6] the loss of supply due to transmission pipeline failures was minimized and the security of a gas network was assessed. The criterion of secure operation was fulfilled whenever the pressures at all load points did not fall below their respective minimum levels.

Natural gas and power systems can be coupled, e.g. through gas-fired power plants and compressors based on electricity. A framework for assessing interconnected energy infrastructures was presented in [7]. Impact models of the natural gas transmission network on the electrical power system were presented in [8], [9].

The objective of this paper is to propose a method for assessing reliability of supply in NGDS. An illustrative case study is presented and the basic load-point reliability indices of average interruption rate, average outage time and average annual outage time are found. It is discussed how the results can serve as an input to a reliability assessment of the coupling between NGDS and EPDS.

II. The natural gas system

A. System description

In typical on-shore natural gas systems, gas is transported from the source to the consumers through a network of pipelines comprising many pressure levels. Transmission systems are characterized by few pipelines and high operating pressure. Compressor stations are used to maintain the desired pressure in the transmission network. As an intersection point between the transmission and the distribution system, the measuring and regulating station (MR-station) meters the gas and reduces its pressure so that it is suitable for distribution purposes.

Distribution systems may comprise up to three pressure levels, depending on the design policy of the distribution

company. In this work, only two pressure levels are considered: the high pressure (HPDS) and the medium pressure distribution system (MPDS). Feeder mains carry gas from MR-stations to regulator stations in the HPDS. The pressure is reduced in regulator stations, and the gas is conducted through distribution mains in the MPDS. Service lines are used to connect the consumers to the distribution mains. Large consumers may be connected directly to the HPDS or even the transmission network.

Valves are installed along the distribution system to allow sectionalizing and reconfiguration of the network for maintenance and network expansion. Some valve types also protects against excessive pressure and backflow. Valves are automatically, remotely or manually operated, depending on pressure level and operating philosophy. In case of emergencies in networks with manual valves, the use of clamps for fault isolation may reduce gas escape and the number of affected consumers.

Pressure is reduced from the HPDS to MPDS level by means of a regulator station. Regulators are used to control the pressure of a certain section of the distribution system. If the upstream pressure of the regulator station becomes lower than the preset downstream pressure, the regulator will turn fully open. In addition, the regulator station should protect the downstream distribution system against excessive pressures. Primarily, this is taken care of by the regulator itself, but if this device fails, additional devices, such as shut-off valves and relief valves, are used to lower downstream pressure. The regulator station should be designed to operate independently of other infrastructures. Fig. 1 shows a schematic drawing of a typical regulator station with redundant processing lines. Each processing line comprise the following major components: filter (1), shut-off valve (2), regulator (3) and relief valve (4) [10].

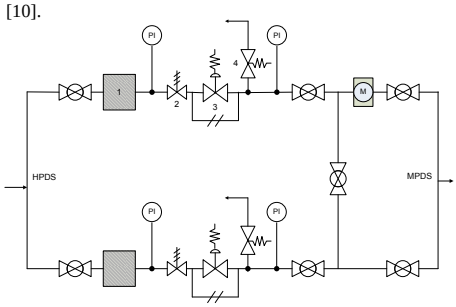

Fig. 1. Regulator station

B. Network flow analysis

Natural gas is a compressible medium and the transmission operator will take advantage of the ability to store gas in the pipelines. This storage capacity, termed line pack, can improve the reliability of the system whenever a source is unavailable or lack of compression facilities occur. The effect of line pack decreases with decreasing operating pressure, and for practical purposes steady-state simulation is a sufficient tool for calculating post-contingency flows and pressures.

For the purpose of calculating pipe flows and nodal pressures in both meshed and radial NGDS, the Newton loop-node method described in [11] is applied. Regulators are modeled to provide a preset downstream pressure.

Unlike the case for power systems, where Ohm's law is valid independently of voltage level, different flow equations applies to different pressure levels in gas networks. For simplicity, the Polyflo flow equation is assumed valid over the range of pressures levels considered.

$$p_i^2 - p_o^2 = KQ_n^{1.848} \tag{1}$$

p_i = pipeline inlet pressure [bar]
p_o = pipeline outlet pressure [bar]
Q_n = pipeline gas flow [m^3/h]
K = constant (function of pipeline length, diameter and friction)

Nodal pressures and pipeline flows must satisfy the appropriate flow equation, and together with the specified values for loads and sources, the first and second of Kirchoff's laws must be fulfilled.

C. Quality of supply

The quality of the gas served to the consumers depends on the following properties:

- Odor
- Chemical properties
- Pressure

Natural gas is colorless, odorless and tasteless and has an odorant added to aid the detection of leaks by making the gas easy to detect by smell. Thus, proper odorization is important for safety reasons, but will not directly affect the reliability of supply. Chemical properties are usually evaluated before the gas is supplied to the transmission network. At distribution level these are considered constant. Different consumers and end-uses require pressure to be within different specified ranges at their respective points of delivery. Experience shows that low-pressure conditions in healthy distribution systems develop gradually, whereas excessive pressures at load points are more of a short-term problem [10]. Only pressure will be used as a measure of the quality of supply in this paper, and only minimum pressure requirements are considered.

D. Power production

Power producing units can either be added to the transmission or distribution system depending on size and purpose.

A cogeneration plant produces both electricity and heat and may be sited in the NGDS. Several cogeneration technologies based on natural gas are available, such as reciprocating engines, turbines and micro turbines. Cogeneration plants are in most cases operated according to the heat demand; thus, the introduction of small cogeneration units in the NGDS will not alter the load profile significantly.

Large gas-fired power plants are sited in the natural gas transmission system and may change the load profile of the system dramatically, as it undergoes the dispatching logic of the power system operator. These plants depend upon high gas pressure at their delivery points and are in general susceptible to pressure drops. The importance of transient simulation for gas network adequacy assessment with the presence of large gas-fired power plant is highlighted in [12].

Integration of distributed generation in the electrical distribution system makes network operation more complicated. As small cogeneration units will not naturally be included in a generation dispatching logic, they may not be relied on alone to serve an electric load. However, they will be running on maximum power in the winter months and may provide a useful relief to any power system under stress [13].

III. Reliability modeling

A. Definitions and assumptions

There are basically two unwanted events in a NGDS:

1) Gas escape
2) Consumer loss of supply

Uncontrolled release of natural gas or loss of pressure in the system can cause unsafe situations due to the potentially explosive mixture of gas and air. This may be contrasted with electricity, where, in the event of loss of supply, the system itself is considered safe. For the purpose of assessing reliability of supply, the event of consumer loss of supply should be quantified.

Generally, interruptions in NGDS can be classified as planned or unplanned. Planned interruptions are related to necessary maintenance or upgrade of the gas system, whereas unplanned interruptions may be caused by various incidents. A thorough treatment of failure causes is outside the scope of this paper, however, examination of past distribution pipeline failure records reveals that exterior mechanical interferences are the main causes of failures in NGDS [6], [14].

The proposed reliability model is based on the following assumptions:

- NGDS are radially operated
- Only pipeline ruptures and regulator station failures are considered
- Only first-order contingencies are considered
- Valves are considered fully reliable
- Each load point requires a minimum pressure P_{req} in order to be supplied sufficiently
- Valves are remotely controlled in HPDS and manually operated in MPDS
- Regulator stations are remotely controlled and can isolate a faulted radial immediately
- A regulator station failure will cause interruption of all downstream consumers

If a failure occurs, reconfiguration of the network requires a sectionalizing time of r_b. Consumers that can not be sufficiently supplied after the reconfiguration will experience an outage time equal to the total time of repair r_c.

Given this set of assumptions, the physical and operational similarity of NGDS and EPDS justifies adoption of techniques from the latter for assessment of reliability in NGDS. An analytical simulation approach as described in [15] has been used as a reference for the proposed method. The effect of constrained network capacity is added.

B. Method description

A method for finding the basic reliability parameters of average interruption rate, average outage time and average annual outage time in a NGDS is proposed and illustrated in Fig. 2. Let $NW|0_k$ describe the network with component k down. All load points connected to the same radial as k loose supply and belongs to class B or C. The remaining load points belongs to class A and are not affected by the failure. If possible, the network is reconfigured and load points can be supplied alternatively while the faulted component is repaired. After reconfiguration, the pressure P_i at each node i is computed. Each load point is characterized by a required pressure $Preq(i)$. If $P_i < Preq(i)$, load point i will not be sufficiently served and will belong to class C. Load points that can be sufficiently fed after reconfiguration belongs to class B. When all network components have been selected, each load point is classified (A-C) for the selected contingency and the reliability parameters are computed and aggregated.

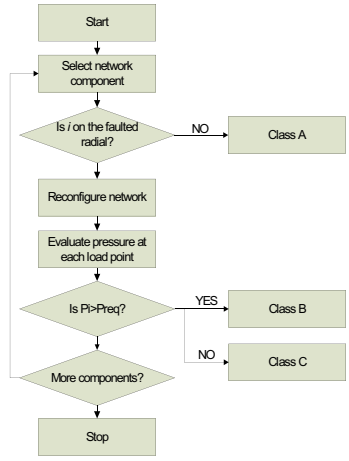

Fig. 2. Classification of load points

If valves are automatically or remotely controlled, consumer interruptions may be avoided for load points belonging to class B due to the effect of line pack. Clearly, this behavior is different from the case of EPDS where no such storage effects can be counted for in reliability analysis.

C. Basic reliability parameters

The basic reliability parameters are first calculated for the HPDS. By considering each regulator station as a load point

with a pressure requirement P_{req}, the reliability parameters can be aggregated to the MPDS. A detailed reliability study of regulator stations is outside the scope of this paper, and for simplicity each regulator station is assigned a failure rate of λ_{RS}. When one regulator station experiences an upstream failure or is faulted itself, all downstream consumers are expected to experience an interruption. Consequently, this procedure gives a pessimistic estimate of load point reliability since load transfer at regulator station level is not accounted for.

For the network analysis at a given pressure level, all load points are evaluated for each contingency. Load point i sited on the radial j will be interrupted each time an failure of component k belonging to j occurs.
Load point average interruption rate [interruptions/year]:

$$\lambda_i = \sum_{k \epsilon j} \lambda_k \tag{2}$$

Load point average annual outage time [h/year]:

$$U_i = \sum_{k \epsilon B} \lambda_k r_B + \sum_{k \epsilon C} \lambda_k r_C \tag{3}$$

r_B - expected time of reconfiguration
r_C - expected time of repair
Load point average outage time [h/interruption]:

$$r_i = \frac{U_i}{\lambda_i} \tag{4}$$

D. Cogeneration

Cogeneration plants are coupling points between the NGDS and EPDS. Generally, cogeneration plants have three failure modes [13]:

1) Unit failure
2) Scheduled maintenance
3) Lack of fuel

The reliability parameters found for a cogeneration load-point can be used as input in reliability studies of the interconnection between NGDS and EPDS.

IV. Case study

A simple illustrative gas distribution network is shown in Fig. 3. The network comprises a MR station which serves as the source, a HP distribution system, two regulator station (R1 and R2) and four load points (A-D). Normally closed sectionalizing valves are black and normally open valves are white. All valves shown in Fig. 3 are remote controlled, except the sectionalizing valve in the MPDS. A cogeneration plant is located in load point C. The operating pressures are 10 and 4 bar at HP and MP distribution levels, respectively. Only pipeline ruptures and regulator station failures are considered. Isolation of ruptures are done with clamps or manual valves in the MPDS and by remote controlled valves at HPDS. HPDS reconfiguration is assumed to occur without delay. Pipeline parameters and load data are listed in Table I and II.

The expected regulator station and pipeline failure rates (λ_{RS} and λ_P), the sectionalizing time (r_B), pipeline repair time (r_C) and regulator station repair time (r_{RS}) are listed below. The resulting reliability parameters are shown in Table III.

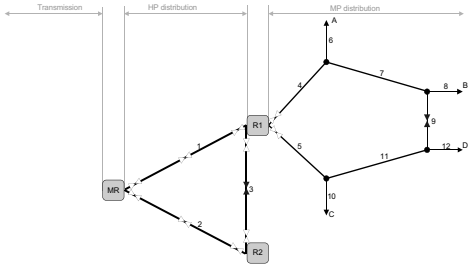

Fig. 3. Gas distribution network

TABLE I
Load and requirements

Load Point	Load[m3/h]	Preq[bar]
R2	3000	4
A	200	2
B	200	2
C	150	3
D	200	2

λ_{RS} = 0.05 /year
λ_P = 0.2 /year·km
r_B = 3 hours
r_C = 48 hours
r_{RS} = 96 hours

Assume now that the sectionalizing valve connected to pipeline 9 in the MPDS is open during normal operation, i.e. the MPDS is operated as a loop. In order to minimize the amount of gas escape due to any pipeline ruptures in the MPDS, regulator station R1 will have to shut off supply to both of the connected distribution mains. Based on this assumption, the reliability parameters for load points A and C in a loop-operated MPDS are calculated and shown in Table IV. The average annual outage time of load points A and C is expected to increase with 23% and 11%, respectively, compared to a radially operated MPDS.

In case the NGDS have abundant capacity, the basic reliability parameters can be found analytically based on the reliability topology and (2)-(4) without evaluating nodal pressures. In capacity constrained networks, evaluation of post-contingency pressures will verify whether the reconfigured network sufficiently supplies each load point.

If pipeline 5 is taken out of service, the reconfigured network will not be able to sufficiently supply the CHP plant (P_C =2.5 bar and $P_{req(C)}$ =3 bar), and it is assumed that the plant has to be disconnected. In this case study, failure of pipeline 5 is the only contingency where a load point which is connected to the source after reconfiguration can not be

TABLE II
PIPELINE DATA

Line	Length[km]	Diameter[mm]
1	10	160
2	10	200
3	3	160
4	5	120
5	5	120
6	3	200
7	3	100
8	5	100
9	2	100
10	3	100
11	5	100
12	3	100

TABLE III
RELIABILITY PARAMETERS

Load point	A			C (CHP)		
Component	λ	r	U	λ	r	U
R1	0.05	96	4.8	0.05	96	4.8
4	1.0	3	3			
7	1.0	3	3			
5				1.0	48	48
11				1.0	3	3
6	0.6	48	28.8			
8	0.6	3	1.8			
10				0.6	48	28.8
12				0.6	3	1.8
Total	**3.3**	**12.7**	**41.4**	**3.3**	**26.6**	**86.4**

served its required pressure. For analysis of complex, capacity constrained gas networks, a load shedding policy should be added to the presented method. Another approach is to apply more than two classes when classifying the faulted load points, e.g. finding if load points are served 100%, 99-50% or 50-0% of its required pressure after reconfiguration, but before any load points are disconnected. Similar reasoning is found in reliability studies of water distribution systems [16].

The remote operation of valves in the HPDS ensures that single contingencies of lines 1-3 will not affect the reliability parameters. In case pipeline 1 or 2 are out of service, pipeline 3 is activated by opening the normally closed valve shown in Fig. 3. Under normal operating conditions, gas is stored in pipeline 3 to avoid loss of pressure in case of outages of pipeline 1 or 2. It should be noted that other operating philosophies may be applied to this case, e.g. when considering the valve status on pipeline 3. The HPDS may be operated as a loop, or pipeline 3 may be depressurized during normal operation of the system. However, none of these changes will significantly influence the calculated reliability parameters.

TABLE IV
RELIABILITY PARAMETERS

Load point	A			C (CHP)		
	λ	r	U	λ	r	U
Total	**6.5**	**7.9**	**51.0**	**6.5**	**14.9**	**96.0**

V. CONCLUSION

A method for reliability assessment of NGDS based on techniques and methodology developed for EPDS is proposed. The rationale behind the comparison of these two systems is founded on the similarity in operating and network expansion philosophy. On the other hand, some essential differences should be counted for in order to find realistic reliability indices. The suggested method is based on an analytical network model taking into account the effect of sequential restoration and constrained network capacity. A simple case is presented for the purpose of calculating the basic reliability parameters in a NGDS with constrained network capacity.

Although limited reliability data are available for studies of NGDS, the importance of quantifying the reliability of these systems separately and in coexistence with other energy infrastructures should be stressed. In this way, the reliability improvements associated with expansions, such as building an extra loop in the network or using remotely controlled valves, could be substantiated.

REFERENCES

[1] R. Billinton, *Reliability Evaluation of Power Systems*. Plenum Press, 2 ed., 1996.
[2] W. Mansell, "Methodology for evaluating natural gas transmission system reliability levels and alternatives," study prepared for the Canadian Petroleum Association, Wright Mansell Research Ltd., 1991.
[3] W. S. Chmilar, "Pipeline reliability evaluation and design using the sustainable capacity method," in *International Pipeline Conference*, vol. 2, (Calgary, Canada), pp. 803–810, The American Society of Mechanical Engineers, 1996.
[4] T. van der Hoeven, T. Fournier, and E. van Meurs, "Planning of the transport system based on reliability figures of the components," in *Pipeline Simulation Interest Group*, (San Francisco, USA), 1996.
[5] M. Mohitpour, J. Szabo, and T. van Hardeveld, *Pipeline Operation & Maintenance - A Practical Approach*. American Society of Mechanical Engineers, 2004.
[6] P. M. Li, "Security assessment of gas networks," *International Journal for Numerical Methods in Engineering*, vol. 11, no. 6, pp. 963–973, 1977.
[7] S. M. Rinaldi, "Modeling and simulating critical infrastructures and their interdependencies," in *Proceedings of the Hawaii International Conference on System Sciences*, vol. 37, (Hawaii, USA), pp. 873–880, 2004.
[8] J. Munoz, "Natural gas network modeling for power systems reliability studies," in *Power Tech Conference*, vol. 4, (Bologna, Italy), 2003.
[9] M. Shahidehpour, Y. Fu, and T. Wiedman, "Impact of natural gas infrastructure on electric power systems," *Proceedings of the IEEE*, vol. 93, no. 5, pp. 1042–1056, 2005.
[10] C. G. Segeler, *Gas Engineers Handbook*. Industrial Press, 1965.
[11] A. Osiadacz, *Simulation and Analysis of Gas Networks*. Gulf Publishing Company, 1987.
[12] R. Wallooppillai and L. My-Linh, "Planning for power: Pipeline design to meet gas-fired power plant needs," in *Pipeline Simulation Interest Group*, (Bern, Switzerland), 2003.
[13] H. L. Willis and W. G. Scott, *Distributed Power Generation - Planning and Evaluation*. Marcel Dekker, 2000.
[14] URS-Corporation, "Safety performance and integrity of the natural gas distribution infrastructure," tech. rep., American Gas Foundation, 2005.
[15] G. Kjolle and K. Sand, "RELRAD - An analytical approach for distribution system reliability assessment," *IEEE Transactions on Power Delivery*, vol. 7, no. 2, pp. 809–814, 1991.
[16] J. Rostum, S. Saegrov, J. Vatn, and G. K. Hansen, "AQUAREL - A computer program for water network reliability analysis combining hydraulic, reliability and failure models," in *CDS - Water network modeling for optimal design and management*, (Exeter, UK), 2000.

B.3 Publication C

A. Helseth and A. T. Holen. Structural Vulnerability of Energy Distribution Systems; Incorporating Infrastructural Dependencies. Accepted for presentation at *16th Power Systems Computation Conference*, Glasgow, Scotland, 2008.

Structural Vulnerability of Energy Distribution Systems; Incorporating Infrastructural Dependencies

Arild Helseth, Arne T. Holen
Department of Electric Power Engineering
The Norwegian University of Science and Technology (NTNU)
Trondheim, Norway
helseth@elkraft.ntnu.no

***Abstract*—In this paper a method for assessing the structural vulnerability of two coupled energy distribution systems is proposed. The co-existing of an electric power distribution system and a district heating system is described and modelled, under the assumption that the operation of the district heating system is directly dependent on electric power. The structural vulnerability of the two systems subject to single failures or a set of simultaneous failures in the power system is found. Thus, the consequences of power system failures for the energy supply as a whole are quantified.**

***Index Terms*—Power distribution, district heating, vulnerability, reconfiguration, network constraints, genetic algorithms (GAs), linear programming**

I. Introduction

Reliability analysis of electric power systems is a rather mature field of study, covering all essential parts of the system [1], [2]. Analysing simultaneous failures in addition to single failures at distribution level will normally not significantly influence the reliability indices, due to low probability of occurrence and modest increase in consequences. Thus, most methods for reliability analysis of distribution systems focus on single failures.

On the other hand, simultaneous failures may be a result of extraordinary circumstances – such as adverse weather, malicious attacks and loss of supporting infrastructures – and will challenge the use of both human and equipment resources. The occurrence of simultaneous failures are not easily predicted and the use of generic failure rates and repair times may not be appropriate for analysing the system impact of these. In this work we emphasise on finding the consequences of multiple simultaneous failures, leaving considerations on probability of occurrence and duration of such failure sets to the judgement of the analyst.

Interruptions of electricity supply may also degrade the performance of parallel energy infrastructures, e.g. district heating and natural gas systems, which are more or less dependent on electricity for proper operation. Consequently, in order to capture the consequences of power system failures for the energy supply as a whole, these parallel infrastructures and their links to the power system should be modelled.

In this paper a method for assessing the structural vulnerability of two coupled energy distribution systems is proposed. The overall aim is to find the vulnerability of the energy system as a whole to single or simultaneous failures in the power system. The structural vulnerability of the systems with respect to failures in the power system is defined as the consequences caused in both systems. Thus, the concept of vulnerability, as defined here, is not related to the probability of such failure sets to occur.

Several recent studies have addressed the concept of vulnerability in electric power systems, ranging from graph theoretical investigations in [3]–[5] to investigations based on more physical models in [6], [7]. These studies all refer to the transmission system, and there is a large gap between the applied definitions of vulnerability. In [8], the vulnerability to failures at distribution level is analysed using a network analytic approach. Here, the electrical properties of the network are neglected and vulnerability is defined as the degree of loss or damage to the system when exposed to a perturbation of a given type and magnitude.

Some studies have been conducted regarding infrastructural dependency modelling. In [9] a general overview of different kinds of interdependencies in critical infrastructures is given. A network analytic approach is presented in [10], identifying vulnerabilities in local distribution systems of electricity, natural gas and water. Furthermore, [11] and [12] describe and analyse the impact of natural-gas system reliability on electric power transmission systems.

The proposed method is described and illustrated for an electric power distribution system (EPDS) co-existing with a district heating system (DHS). The operation of the DHS is directly dependent on electricity. The following section describes the system modelling approach and the corresponding underlying assumptions for both the EPDS and DHS. Section III presents a screening strategy used for finding the most critical failure sets in the EPDS. A limited number of failure sets are fully analysed for both systems. In section IV, a simple example is elaborated, before the method is applied in a case study in section V.

II. System Modelling

Two simple systems, an EPDS and a DHS, are presented below, and a method suitable for finding the systems' vulnerabilities to failures in the EPDS is elaborated. Both the EPDS and the DHS are modelled as networks, comprising a set of

nodes $\mathcal{N}$ and a set of branches $\mathcal{B}$, following an object-oriented modelling approach.

A. Vulnerability Measure

Various indices may be applied for quantification of consequences associated with interruption of energy supply in the two systems. In this study, the frequency and duration of interruptions are not calculated, and the consequences are simply described in terms of interrupted electric and thermal power for the EPDS and the DHS, denoted C_{EPDS} and C_{DHS}, respectively. It should be noted that other relevant system indices, e.g. indices related to the number and type of consumers having their supply interrupted could easily be incorporated in the presented method.

B. Electric Power Distribution System

Fig. 1 resembles a simple EPDS, comprising nodes 1-8 and branches b_1-b_9. The system serves seven load points (nodes 2-8). All branches have switches at their sending and receiving ends, see illustration in the top-right corner of Fig. 1. Branches b_3 and b_9 are load-transfer branches, having normally open switches at both ends. Node 1 represents the energy in-feed point, typically being a HV/MV substation.

Permanent branch and node failures in the EPDS have the potential to interrupt the service to load points. Generally, two distinctive types of interruptions may be classified, depending on interruption duration. Some load points will have their supply restored after a network reconfiguration, while others will have to wait for the repair of one or more of the faulted components. This study only considers the consequences caused by the latter type of interruption. Thus, an idealised system representation with instantaneous network reconfiguration is assumed.

The following assumptions were made when analysing the EPDS:

- temporary failures are not considered;
- all switchgear is fully reliable;
- upstream supply from HV/MV substations is fully reliable;
- load points are either fully supplied or not supplied at all.

Moreover, it was assumed that faulted load-point nodes will be isolated by the operation of a fuse, see illustration in Fig. 1. Thus, only power supply to that particular node will be interrupted. The further studies only consider branch failures in the EPDS.

For each failure set in the EPDS, the following steps are taken to find the system consequences C_{EPDS}:

1) Isolate the faulted branches by using the available switches
2) Run a Genetic Algorithm (GA) to find the optimal use of switches to minimise C_{EPDS} subject to the following constraints:
   a) nodal voltages are not lower than a predefined minimum value at load nodes i; $\forall i \in \mathcal{N} : V_i \geq V_{min}$
   b) branch thermal limits are not exceeded for any branch b; $\forall b \in \mathcal{B} : I_b \leq I_{b,max}$

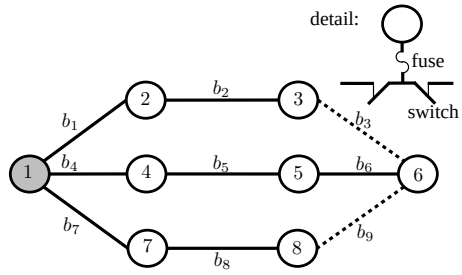

Fig. 1. A simple electric power distribution system.

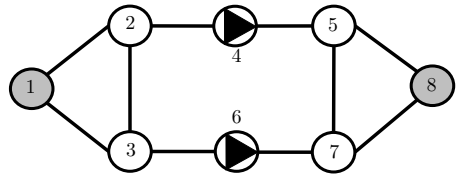

Fig. 2. A simple district heating system.

c) the system is radially operated

The GA was modelled using the simple genetic algorithm, thoroughly described in [13], from the library GAlib [14].

C. District Heating System

A simple DHS is presented in Fig. 2, comprising the following nodes; two thermal power production units (nodes 1 and 8), two pumps (nodes 4 and 6) and four load points (nodes 2, 3, 5 and 7). The system is operated as a meshed system, i.e. water may flow in all pipelines in Fig. 2.

It is possible to formulate the thermal power flow in a DHS as a function of network temperatures and pressures. In order for the system to satisfy consumers' needs, water with adequate temperature and pressure must be circulated to the load points.

In this study, only DHS node failures caused by loss of supply from the EPDS are analysed. DHS pipelines and valves are assumed fully reliable whenever the EPDS has faulted components. Loosing electric power supply to nodes in the DHS may result in insufficient circulating pressure and/or insufficient thermal power production, which in turn may cause interruption of supply to DHS load points. Note that short interruptions of electric power supply to DHS nodes are not treated here, as EPDS reconfiguration is assumed to take place instantaneously. Short electric power interruptions have the potential to trip DHS pumps leading to thermal power interruptions. However, this kind of analysis calls for dynamic system studies and is outside the scope of this paper.

Pressure and temperature distribution studies may be decoupled and performed separately. Changes in pressure are quickly

transferred throughout the whole system, typically taking only a few seconds. Temperature changes are slower and closely related to the speed of the circulating water. However, as this study is not concerned with the duration of interruptions, we do not differentiate between the interruptions caused by lack of pumping capacity and those caused by lack of thermal power production capacity. It is generally assumed that repair of faulted components in the EPDS is slower than the dynamic response of the DHS. Thus, only steady-state considerations of thermal power flow are dealt with in this work.

It is assumed that all DHS nodes can be isolated and bypassed. Consequently, in case a thermal power production unit or pump lacks supply from the EPDS, the hot water is simply bypassed this unit without any increase in temperature or pressure. Furthermore, in case load has to be curtailed in the DHS due to a deficit in thermal power production or pumping capacity, it is assumed possible to bypass any load point in the system. Depending on which node types that are without electric power, different types of analysis are performed, as described below:

1) DHS pump: If supply from the EPDS to a DHS pump is lost, the pump is bypassed and load points in the DHS will experience a drop in pressure. An initial study of pressure distributions reveals whether load point pressures are sufficient, i.e. higher than a predefined minimum value p_{min}. If this constraint is not met, load has to be disconnected. A GA is initiated for the purpose of minimising the consequences (C_{DHS}) of load curtailment in the DHS while meeting the pressure requirement.

2) DHS production unit: If supply from the EPDS to a DHS thermal power production unit is lost, a capacity deficit may occur in the DHS. Rerouting of thermal power flow may also enforce bottlenecks in the DHS. The thermal power flow problem is formulated as a mixed integer programming (MIP) problem using the linear programming library GLPK [15]. The formulation relies on a lossless, steady-state network flow model. The problem formulation is stated as:

MIN.:

$$C_{DHS} = \sum_{i \in \mathcal{N}} (1 - x_i) D_i \tag{1a}$$

S.T.:

$$\sum_{j:(ji) \in \mathcal{B}} P^t_{b(j,i)} - \sum_{j:(ij) \in \mathcal{B}} P^t_{b(i,j)} + G_i - x_i D_i = 0 \tag{1b}$$

$$|P^t_b| \leq P^t_{b,max} \tag{1c}$$

$$G_i \leq G_{i,max} \tag{1d}$$

Where x_i is a boolean variable indicating whether load point i is served or not, and C_{DHS} denotes the total amount of interrupted thermal power. Restriction (1b) describes the nodal thermal-power balance for each node i, where $\mathcal{B}$ is the collection of all branches in the DHS, $P^t_{b(i,j)}$ denotes thermal power flow in branch b connecting nodes i and j, and G_i and D_i are the thermal power production and demand at node i, respectively. Restriction (1c) forces the thermal power flow in each branch not to exceed the capacity constraint $P^t_{b,max}$ for that branch. G_i is constrained by its maximum power $G_{i,max}$ in (1d).

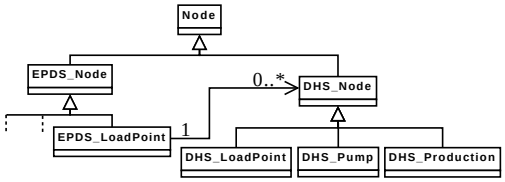

Fig. 3. Class diagram illustrating the node hierarchy.

3) DHS load point: Normally the DHS will interface with aggregated load points trough a heat exchanger, and water is circulated in an underlying secondary circuit supplying smaller loads. Loosing electric power at this location will disable the circulating pumps in the secondary circuit, and consequently the entire aggregated load point will be interrupted. However, the surrounding system is not directly affected by such local effects.

D. Modelling Dependencies

Fig. 3 shows an excerpt of the Unified Modelling Language (UML) class diagram for the node hierarchy applied in the joint modelling of the two systems. Instance variables and functions are omitted for brevity.

Each node in the DHS (DHS Node) has a link to one load point in the EPDS (EPDS LoadPoint) in Fig. 3. Each EPDS load point has an association to zero, one or several DHS nodes. DHS nodes comprise load (DHS LoadPoint), pump (DHS Pump) and production unit (DHS Production) nodes. In case an EPDS load point experiences an interruption, the model checks for associated DHS nodes. If associated DHS nodes are found, the consequences are analysed depending on the type of faulted DHS node(s), as previously described.

III. Failure Set Synergy

Applying the presented method to large scale infrastructures analysing higher-order failure sets is computationally intensive. A screening strategy inspired by [16] was applied in order to fully analyse only the most critical failure sets. Thus, computation time is reduced as well as the number of failure sets to evaluate after the simulation has been performed. The strategy is based on the concept of synergy, as explained below.

Consider the EPDS under study consisting of n components being subject to a failure set $\mathcal{F}^k_i$. The failure set is set number i of order k. The maximum number of failure sets of order k is found by (2).

$$i^k_{max} = \frac{n!}{(n-k)!k!} \tag{2}$$

In case k is larger than 1, it will be possible divide $\mathcal{F}_i^k$ into a certain number of divisions, where each division comprises the same components as in $\mathcal{F}_i^k$. Consider a set of order 3, comprising components a, b and c. There are 4 possible divisions ($d_1 - d_4$) of $\mathcal{F}^3(abc)$, as shown below.

$$\mathcal{F}^3(abc)\begin{cases} d_1 : \mathcal{F}^2(ab) & +\mathcal{F}^1(c), \\ d_2 : \mathcal{F}^2(ac) & +\mathcal{F}^1(b), \\ d_3 : \mathcal{F}^2(bc) & +\mathcal{F}^1(a), \\ d_4 : \mathcal{F}^1(a) & +\mathcal{F}^1(b) + \mathcal{F}^1(c) \end{cases}$$

If $\mathcal{F}_i^k$ gives rise to larger consequences (C_{EPDS}) than the sum of consequences in any of its divisions, $\mathcal{F}_i^k$ is said to be synergistic. In other words; if $\mathcal{F}_i^k$ is the minimum cut set for at least one EPDS load point, it will be synergistic. Thus, the synergy concept relates to network connectivity and reconfiguration capability of the EPDS.

It is possible to screen higher-order failure sets according to their synergy. A failure set of order k may cause large consequences, but if the failure set has no synergy, it indicates that these consequences were counted for when analysing sets of lower order. Thus, running the simulation with an increasing value of k, allows us to emphasise on the synergistic failures sets.

The screening procedure was implemented in the structural vulnerability assessment method as illustrated in Fig. 4. First, the depth of the analysis is set by choosing the highest failure-set order to be considered (k_{max}). Determining k_{max} is the choice of the analyst, depending on how many simultaneous failures that are considered feasible. For each k, i_{max}^k is found from (2). In case the failure set is synergistic and DHS nodes loose supply from the EPDS, one of the steps described in Subsections II-C1 - II-C3 is performed, depending on which DHS node types that are without electricity.

IV. Example

In order to illustrate the proposed method, an example is presented based on the two systems shown in Figs. 1 and 2. The example is limited to EPDS branch failures only, and failure sets comprising three or less branches. As the EPDS has 9 branches, there are 129 failure sets in total. For clarity and simplicity, we assume that the EPDS is unconstrained. The DHS has no pipeline capacity constraints of type (1c), but will have to meet a pressure requirement $p_{min} = 0.9$ p.u. at all load points. All load points in both systems serve a load of 1 MW.

Fig. 5 shows the couplings between EPDS load points and DHS nodes in this example. The thermal power production units do not depend on electric power from the EPDS.

A total of 36 failure sets are synergistic; 27 third and 9 second-order sets. These synergistic sets are treated further in the DHS analysis. A plot of the resulting consequences for the EPDS (C_{EPDS}) and DHS (C_{DHS}) for the synergistic failure sets is presented in Fig. 6. Open circles indicate failure sets of second order and filled circles indicate third-order failure sets. For each circle in Fig. 6, there is a set of failure sets

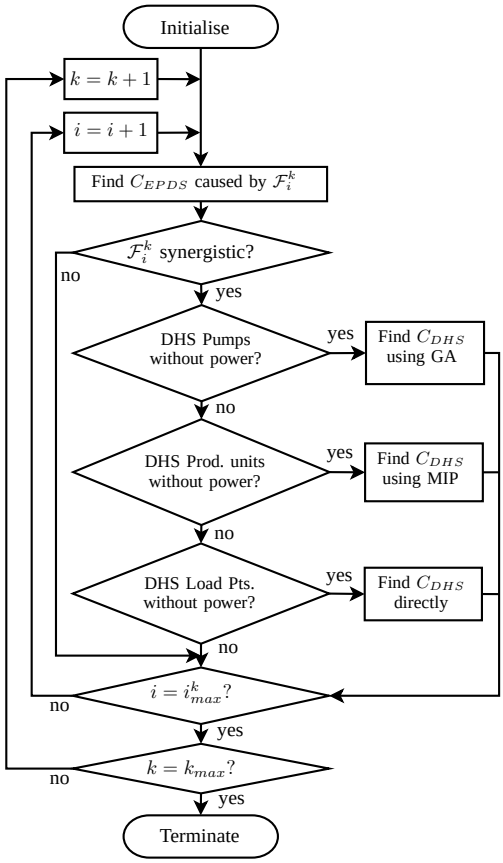

Fig. 4. Flowchart of the structural vulnerability assessment method.

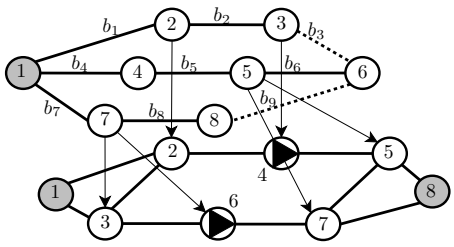

Fig. 5. Dependency of a DHS on electric power. Couplings between EPDS load points and DHS nodes are indicated by arrows.

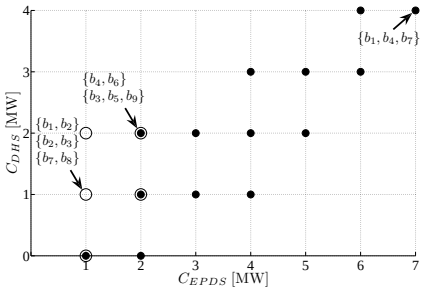

Fig. 6. Interrupted power for both the EPDS (C_{EPDS}) and the DHS (C_{DHS}). Failure sets of second order are marked with ○ and third order with ●.

causing this tuple of consequences. For three of these tuples, the corresponding failure sets are listed in the figure.

As an example, 3 synergistic failure sets will cause the consequence tuple of C_{EPDS} = 1 MW and C_{DHS} = 1 MW, as indicated in Fig. 6. If b_1 and b_2 fail simultaneously, EPDS node 2 will experience an interruption. According to Fig. 5, the load point at node 2 in the DHS looses supply from the EPDS and is interrupted. If b_2 and b_3 fail, EPDS node 3 will experience an interruption. This time, the DHS pump at node 4 in Fig. 2 will loose electric power supply. The GA reveals that the DHS system is only capable of serving 3 out of 4 load points in this state, thus C_{DHS} = 1 MW. Finally, in case b_7 and b_8 fail, both the load at node 3 and the pump at node 6 will loose power. As it is assumed that node 3 in the DHS is bypassed in this situation, the pressure constraints are not violated and no additional load points in the DHS has to be curtailed.

Simultaneous failure of b_4 and b_6 is the most critical second-order failure set in terms of total consequences (C_{EPDS}+C_{DHS}). Furthermore, not surprisingly, the third-order failure set comprising b_1, b_4 and b_7 causes maximum consequences for both systems.

V. Case Study

The presented method was tested on the coupled EPDS and DHS located in the city centre of Trondheim, Norway. A system boundary was defined, including only the central parts of the two systems. Figs. 7 and 8 present the structure of the two systems. It should be noted that both system models are simplified, but still reflect the basic design of the real networks.

The central part of the DHS is shown in Fig. 7. This system comprises 3 pumps, 8 thermal power production units and 11 load points, and the total installed capacity and maximum load is 149 MW and 106 MW, respectively. The surrounding EPDS is a medium-voltage cable network fed by 3 HV/MV substations and serving 34 load points. The voltage and pressure constraints were set to $V_{min} = 0.95$ p.u. and $p_{min} = 0.90$ p.u. Couplings between the two systems are mapped as in Fig. 5, but is not presented here for practical reasons.

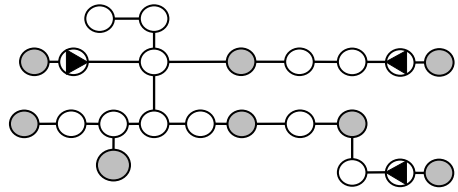

Fig. 7. Overview of the central district heating system.

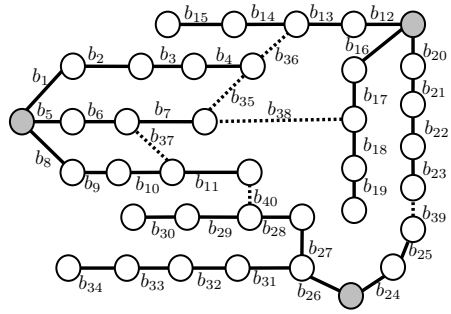

Fig. 8. Overview of the electric power distribution system. Each branch is enumerated.

A simulation was performed for failure sets comprising three or less components, considering only EPDS branch failures. In total there are 40 first, 780 second and 9880 third-order failure sets. From the simulation it was found that 12 first, 64 second and 176 third-order failure sets have synergistic consequences. A scatter plot of the consequence tuples caused by these synergistic failure sets is presented in Fig. 9. Consequences are measured in interrupted electric and thermal power, in percentage of the total load served in each of the two systems.

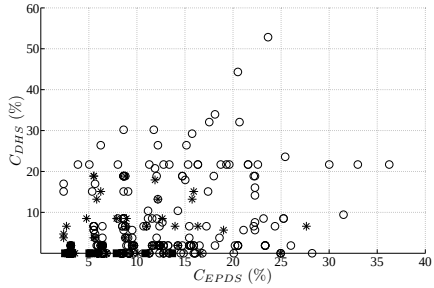

Fig. 9. Interrupted power in percentage of total load for both the EPDS (C_{EPDS}) and DHS (C_{DHS}). Failure sets of first order are marked with ■, second order with ∗ and third order with ○.

In Table I the synergistic failure sets causing maximum consequences, both in terms of C_{EPDS} and C_{DHS}, are listed. The maximum C_{EPDS} in second and third-order synergistic failure sets was found to be 27.6 and 36.3 % of the total load in the EPDS, respectively. For comparison, the maximum C_{EPDS} in second and third-order non-synergistic failure sets was found to be 20.0 and 34.0 %.

At most 1.9 % of the DHS load is interrupted due to single branch failures in the EPDS. This result indicates that the DHS is not particularly vulnerable to single failures in the EPDS. In fact, all the major DHS load points, pumps and thermal power production units can receive power from more than one EPDS feeder.

Studying the two second-order failure sets listed in Table I, it is evident that the set causing the highest value of C_{EPDS} causes only minor consequences in the DHS. On the contrary, if branches b_5 and b_{16} fail simultaneously, violation of EPDS network constraints limits the reconfiguration capability, resulting in EPDS load point interruptions. The system is reconfigured to minimise the interrupted electric power. Cascading consequences in the DHS are not considered when finding the optimal use of switches in the EPDS. For this particular failure set a vulnerable DHS node looses electric power supply, giving a high value of C_{DHS}.

The third-order failure set comprising branches b_1, b_{12} and b_{35} isolates a part of the EPDS which is crucial for proper DHS operation; thus, more than 50 % of the total DHS load is interrupted.

TABLE I
MAXIMUM CONSEQUENCES FOR FIRST, SECOND AND THIRD-ORDER SYNERGISTIC FAILURE SETS.

Order	Maximum	Set	C_{EPDS} (%)	C_{DHS} (%)
1^{st}	C_{EPDS}	b_{26}	13.7	0.0
	C_{DHS}	b_{18}	0.0	1.9
2^{nd}	C_{EPDS}	b_{11}, b_{26}	27.6	6.6
	C_{DHS}	b_5, b_{16}	8.8	18.9
3^{rd}	C_{EPDS}	b_8, b_{26}, b_{37}	36.3	21.7
	C_{DHS}	b_1, b_{12}, b_{35}	23.6	52.8

Although the non-synergistic failure sets are screened out, a thorough interpretation of the remaining synergistic failure sets $\mathcal{F}_{syn}$ can be tedious. Finding the EPDS branches contributing the most to consequences in $\mathcal{F}^k_{syn}$ of a given order k, will provide a measure of component criticality. The contribution R to consequences C (C_{EPDS} or C_{DHS}) of branch b is defined as the ratio between the sum of the consequences caused by synergistic failure sets including branch b and the sum of consequences for all synergistic failure sets:

$$R(b,k) = \frac{\sum_{\mathcal{F}\in\mathcal{F}^k_{syn}, b\in\mathcal{F}} [C(\mathcal{F})]}{\sum_{\mathcal{F}\in\mathcal{F}^k_{syn}} [C(\mathcal{F})]}$$

Table II shows the three components that contributed the most to consequences (in terms of C_{EPDS} and C_{DHS}) caused by second-order synergistic failure sets.

TABLE II
BRANCH CONTRIBUTION TO CONSEQUENCES IN SECOND-ORDER SYNERGISTIC FAILURE SETS.

	$C = C_{EPDS}$		$C = C_{DHS}$	
Rank	**Branch (b)**	**Contr. (R)**	**Branch (b)**	**Contr. (R)**
1	b_{26}	0.090	b_{16}	0.115
2	b_{24}	0.075	b_{20}	0.113
3	b_{20}	0.069	b_{21}	0.076

VI. DISCUSSION

In this study, the frequencies and durations of interruptions were not considered, only the system consequences in terms of interrupted electric and thermal power. Obviously, before drawing final conclusions regarding critical components and possible system reinforcements, one have to somehow evaluate how often interruptions are expected to occur and for how long they are expected to last.

Furthermore, the assumptions regarding the two systems' responses and operations due to failures can be questioned. It is difficult to generalise such behaviour when the failure repair time is unknown. For example, loosing power to a DHS thermal power production unit for a short time, leading to a short-time capacity deficit in the DHS, will rarely be noticed by the average consumer. This work relies on the assumption that electric power interruptions affecting supply to DHS nodes last longer than the time it takes for the thermal power flow to reach steady-state. More detailed system studies could address the dynamic response of the DHS subject to short electric power interruptions, and the sequence of backing up or restarting faulted pumps and production units.

In the presented method, the post-failure system configurations are found in two separate steps. First, the EPDS is reconfigured to minimise interrupted electric power by using the available switches. Subsequently, in case any DHS nodes are without power, curtailed thermal power is minimised while meeting the DHS network constraints. A perhaps more realistic reconfiguration algorithm would integrate the two reconfiguration steps in one procedure. In this way, the cascading consequences in the DHS are considered when finding the optimal use of switches in the EPDS. By integrating the system reconfigurations in this manner, it is likely to expect a reduction in C_{DHS} and a slight increase in C_{EPDS} for some failure sets. In the end, the most representative algorithm will always be the one reflecting the actual communication and cooperation between the distribution system operators.

Finally, it should be noted that simulating the EPDS as a partial system may result in a higher measure of structural vulnerability than in reality, since boundary nodes may be fed by surrounding system parts. These parts are outside the system boundary and are therefore not included in the system model.

VII. Conclusion

A method was proposed, suitable for analysing the structural vulnerability of an electric power distribution system co-existing with a district heating system. The structural vulnerability of these systems with respect to failures in the power system was defined as the consequences caused in both systems. The cascading consequences due to loss of electric power to essential components in the district heating system was discussed and modelled. The method enables the analyst to consider higher-order failure sets in the electric power system and find the consequences caused in both systems. Furthermore, a screening procedure was applied to identify and fully analyse only the most critical failure sets.

The method was applied to a case study, where the failure sets causing the highest consequences were identified. It was briefly discussed and shown how to rank power system components in terms of criticality.

Acknowledgement

The authors would like to thank May Toril Moen and Arnvid Sylte at Trondheim Energi for interesting discussions and for providing data for the case study.

References

[1] J. Endrenyi, *Reliability Modeling in Electric Power Systems*. John Wiley & Sons Ltd., 1978.

[2] R. Billinton and R. N. Allan, *Reliability Evaluation of Power Systems*, 2nd ed. Plenum Press, 1996.

[3] R. Albert, I. Albert, and G. L. Nakarado, "Structural vulnerability of the north american power grid," *Physical review E*, vol. 69, p. 4, 2004.

[4] P. Crucitti, V. Latora, and M. Marchiori, "A topological analysis of the italian electric power grid," *Physica A: Statistical Mechanics and its Applications*, vol. 338, pp. 92–97, 2004.

[5] Å. J. Holmgren, "Using graph models to analyze the vulnerability of electric power networks," *Risk Analysis*, vol. 26, pp. 955–969, 2006.

[6] G. Doorman *et al.*, "Vulnerability analysis of the nordic power system," *IEEE Transactions on Power Systems*, vol. 21, pp. 402–410, 2006.

[7] X. Yu and C. Singh, "A practical approach for integrated power system vulnerability analysis with protection failures," *IEEE Transactions on Power Systems*, vol. 19, pp. 1811– 1820, 2004.

[8] H. Jonsson, J. Johansson, and H. Johansson, "Analysing the vulnerability of electric distribution systems: a step towards incorporating the societal consequences of disruptions," *International Journal of Emergency Management*, vol. 4, pp. 4–17, 2007.

[9] S. M. Rinaldi, "Modeling and simulating critical infrastructures and their interdependencies," in *Proceedings of the Hawaii International Conference on System Sciences*, vol. 37, Hawaii, USA, 2004, pp. 873–880.

[10] G. E. Apostolakis and D. M. Lemon, "A screening methodology for the identification and ranking of infrastructure vulnerabilities due to terrorism," *Risk Analysis*, vol. 2, pp. 361–376, 2005.

[11] J. Munoz, "Natural gas network modeling for power systems reliability studies," in *Power Tech Conference*, vol. 4, Bologna, Italy, 2003.

[12] M. Shahidehpour, Y. Fu, and T. Wiedman, "Impact of natural gas infrastructure on electric power systems," *Proceedings of the IEEE*, vol. 93, no. 5, pp. 1042–1056, 2005.

[13] D. E. Goldberg, *Genetic Algorithms in Search, Optimization, and Machine Learning*. Reading, MA: Addison-Wesley, 1989.

[14] M. Wall, "GAlib: A C++ library of genetic algorithm components," [online]. Available: http://lancet.mit.edu/ga/.

[15] A. Makhorin, "GLPK (GNU Linear Programming Kit)," [online]. Available: http://www.gnu.org/software/glpk/glpk.html.

[16] H. Jonsson, J. Johansson, and H. Johansson, "Identifying critical components in electric power systems: A network analytic approach," in *Proceedings of the European Safety and Reliability Conference (ESREL)*, Stavanger, Norway, 2007.

B.4 Publication D

A. Helseth and G. Koeppel. Pipeline Storage and its Impact on Reliability of Supply in Pipeline Energy Systems. *Reliability Engineering & System Safety*, in review.

Pipeline Storage and its Impact on Reliability of Supply in Pipeline Energy Systems

Arild Helseth [a,*] Gaudenz Koeppel [b]

[a] *Department of Electric Power Engineering, Norwegian University of Science and Technology, Trondheim, Norway*
[b] *Power Systems Laboratory, Swiss Federal Institute of Technology ETH Zurich, Switzerland*

Abstract

This paper presents a novel Markov-based approach for modelling and analysing the impact of pipeline storage on the reliability of supply in pipeline energy systems. It is described how to calculate the survival time for both natural gas and district heating systems subject to upstream failures. Storage failure and repair rates are introduced and incorporated in a Markov model. These rates reflect the system aspect of having storage capacity available, not technical failure and repair of the storage. The approach is tested on a simple natural gas transmission system, and the results are compared with Monte Carlo simulations. The comparisons indicate that the model is capable of capturing the impact of pipeline storage on reliability of supply.

Key words: Reliability Modelling, Pipeline, Storage, Natural Gas, District Heating

1. Introduction

In the context of reliability, stored energy can be used for two purposes. It is used to either provide back-up energy in case of a supply outage or to provide additional energy in peak demand periods. In contrast to electrical energy, energy carriers transported in pipeline systems do not necessarily require distinctive storage facilities, as the pipelines constituting the network can be used for this purpose. This is common and well established in the gas industry, often referred to as line pack.

Reliability evaluation of natural gas and district heating systems has been adressed by several authors. Some studies place emphasis on the overall system reliability, as e.g. in [1] for natural gas and [2] for district heating applications. A Markov-based methodology was applied in [3], analysing the probability of the natural gas system's supply capacity falling short of the load demand. In [4] the minimum reduction in load in a gas network due to pipeline failures was found. The corresponding criterion for secure operation was met if pressure levels at all load points did not fall below the respective minimum levels. None of these studies address pipeline storage, they however all refer to and apply reliability evaluation methods well established in the power system domain [5].

Pipeline storage is often claimed to have a positive impact on the reliability of supply in both natural gas and district heating systems. However, the modelling and quantification of this impact has been addressed only in few publications so far. In [6] the critical durations of pipeline storage in a high- pressure nitrogen supply system subject to compressor failures were analysed. Focusing on large-scale natural gas transmission systems, [7] presents a procedure combining Monte Carlo simulations with hydraulic transient analysis for the purpose of quantifying system reliability.

The most important operational characteristics of pipeline energy systems are shortly outlined in the following paragraphs, focusing on gas systems. Due to the physical characteristics of the transmission media, i.e. natural gas and hot water, a pressure or temperature increase at the inlet of the pipeline requires a certain travelling time to reach the outlet. Put differently, an unexpected load increase at the pipeline outlet, cannot be satisfied immediately by operator action at the pipeline inlet. Thus, in order to prevent such load increases to be faced with a delayed system response, the pipeline operator can prepare for such events by building up an appropriate storage in certain pipeline segments [8]. This stored energy is then used to bridge the time required for the system and the

* Corresponding author. Tel.: (+47) 73597295 Fax: (+47) 73594279
Email addresses: helseth@elkraft.ntnu.no (Arild Helseth), g.koeppel@alumni.ethz.ch (Gaudenz Koeppel).

media to respond in case of a load increase.

In natural gas systems, gas is stored by increasing the inlet flow relative to the outlet flow. The additional gas accumulated in the pipeline results in a pressure increase at both inlet and outlet. The higher inlet pressure requires the compressor to inject at a higher pressure level, consequently consuming more power. Hence, both the temporarily increased inflow rate for building the line pack and, after having done so, the operation of the pipeline at the higher pressure level lead to increased operational costs. Therefore, the system operator is faced with a trade-off between risking a delayed response to load increases and higher expenses for possibly unnecessarily prepared line pack.

However, operating with an additional amount of gas in the pipeline or at a higher temperature can also have a positive impact on the reliability of supply, even if no unexpected load increases occur. In case of an outage of the pipeline inlet supply, e.g. a compressor station failure or loss of heat source, the inflow is not sufficient anymore to meet the load demand. The energy stored in the pipeline is then used to maintain the supply of the load until either the minimum supply pressure or the minimum supply temperature is reached.

This paper only focuses on the latter operation mode, presenting a model that allows to generally analyse and quantify the impact of pipeline storage on reliability of supply in case of an upstream failure. A Markov model is presented, suitable for analysing a basic pipeline energy system, including different load levels.

The following section illustrates the pipeline system's layout and discusses the elements of the Markov model. Section 3 discusses the physical properties of the two pipeline systems. In section 4, a case study is elaborated, and the reliability of a natural gas system under different operating conditions is quantified. Finally, Monte Carlo simulations are performed in order to test the accuracy of the Markov model.

2. Markov Modelling Approach

2.1. *A Basic Markov Model*

This section presents a basic approach for modelling storage in pipeline energy systems. The storage in such systems can be considered to be an assisting system, taking over or supplementing in cases of emergencies. The storage is charged whenever the supply exceeds the demand and it is discharged whenever the supply falls short of the demand.

Consider the natural gas and district heating systems illustrated in Fig. 1. There are generally two upstream failure modes in these systems: loss of energy supply and loss of compressor facilities. The term energy supply is system dependent and may refer to heat sources, gas reservoirs or even a set of upstream pipelines. Compressors are necessary to maintain the required pressure and flow rates in order to meet the load demand in both systems depicted in Fig. 1. In the case of district heating, an outage of the compressor results in an almost immediate supply outage due to the incompressibility of water. In order to focus on the benefits of energy storage, compressor failures are not considered in the district heating case.

In the following paragraphs, the simple natural gas transmission system in Fig. 1a is used as an illustrative example. It should be noted that the reliability model also applies to district heating system in Fig. 1b.

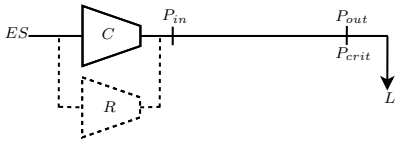

Figure 1a. A gas transmission system with an energy supply ES, an operating compressor C and a reserve compressor R, with pipeline inlet pressure P_{in}, outlet pressure P_{out}, critical pressure P_{crit} and load L.

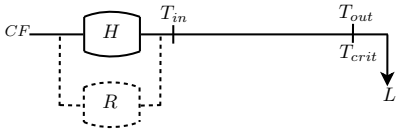

Figure 1b. A district heating transmission system with compressor facilities CF, an operating heating unit H and a reserve heating unit R, with pipeline inlet temperature T_{in}, outlet temperature T_{out}, critical temperature T_{crit} and load L.

The compressor station is located at the inlet or sending end of the pipeline, comprising two compressors: the main operating compressor (C) and the reserve compressor (R). For the basic Markov model, only compressor C will be considered and it is assumed that the energy supply (ES), being e.g. a gas reservoir or a set of upstream pipelines, is 100 % reliable. The influence and required dimension of the reserve compressor will be discussed later-on. By adjusting the pipeline inlet pressure (P_{in}) at the compressor station, the pipeline operator can control the amount of stored gas in the pipeline. In case C fails to operate, the constant load (L) at the receiving end will start discharging gas from the pipeline. It is assumed that the consumers will not experience an outage as long as the pressure at the load (P_{out}) is higher than a predefined critical pressure (P_{crit}) at the load.

The state space diagram representing the systems in Fig. 1 is shown in Fig. 2. The systems are considered to behave as stationary Markov processes, with the corresponding assumptions being discussed below. For the natural gas system, both the compressor and the pipeline storage are represented with binary models, i.e. the compressor can be either in an operating state (up) or in a failed state (dn), whereas the storage is either charged and ready for discharge (up) or it is fully discharged (dn). The supply of the load fails as soon as the system enters state 3, with both

the compressor having failed and the storage having been discharged subsequently.

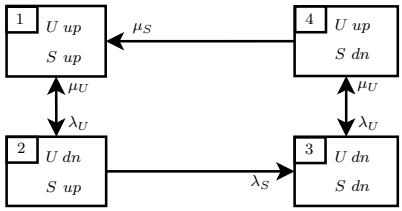

Figure 2. A 4-state Markov model incorporating an upstream unit U (either a compressor or a heating unit) and the pipeline storage S, assuming a constant load.

As the storage is defined to have failed once it is discharged, the failure rate of the storage (λ_S) can be defined as the inverse of the time to discharge [9]. This time can be understood as the mean time to failure (MTTF) and depends on the available compressor capacity, the load level and the available pipeline storage. Consequently, the failure of the storage only concerns the system aspect of having energy available or not – technical failures involved with the storage are not considered. In order to satisfy the conditions for a stationary Markov process, the load is assumed constant during the discharge. A detailed description on how to find the system's survival time for a given load and supply scenario is presented in section 3, both for gas and district heating pipeline systems.

The model in Fig. 2 assumes that the storage is only discharged in case of an outage of the compressor. Likewise, the storage can only be recharged once the compressor is operating again. The repair rate of the compressor (μ_U) not only includes the physical repairing of the compressor, but also the time required to re-establish the necessary flow rate to reach steady state supply of the load.

The state space diagram represents a continuous and dynamic process as a Markov process with only 4 states. For this model to be valid, certain assumptions were made. It is important to note here that the purpose of the model is to analyse the major system aspects of pipeline storage. The repair rate of the compressor has to be path-independent and hence, the transition rates from state 2 to 1 and from state 3 to 4 are identical. One could argue that the repairing of the compressor is being started as soon as state 2 is encountered. Thus, the repair rate from state 3 to state 4 should be comparatively higher, considering a background repair of the compressor while discharging the storage. However, it is possible to experience another compressor outage when being in state 4, transiting back to state 3. The necessary repair rate μ_U then again corresponds to the total necessary repair duration including the time required for re-establishing the appropriate flow rate. Therefore, the assumption of identical repair rates can be understood as a worst case assumption, necessary to guarantee path-independent transition rates.

Some assumptions are also necessary to justify the system's behaviour while residing in state 2, with a failed compressor and discharging the pipeline storage. If the compressor is repaired before the storage is fully discharged, the system transits back to state 1, representing an operating compressor and a fully charged storage. However, the storage has been partially discharged while residing in state 2 and its charge level is actually unknown. It is therefore a matter of mapping the continuous charge level to a binary model. One approximation is to use discretised charge levels for the storage, allowing to keep track of the momentary charge state. As discussed in [9], this measure albeit improves the accuracy of the calculations, it however does not change the general findings and considerably increases the number of states. Another possibility would be to have a transition from state 2 to state 4, representing an operating compressor but defining any not fully charged storage to be empty. Including this transition would constitute a worst case representation of the system.

2.2. *Model Extension*

Natural gas and district heating systems are subject to large variations in load throughout the day. In particular, this holds true for natural gas pipelines serving gas-fired power plants. This load behaviour is represented with a load model consisting of 3 different load levels, as described in [10]. All three load levels L_1, L_2 and L_3 are equally likely and satisfy $L_1 > L_2 > L_3$. Load level changes are defined to happen on an hourly basis and the different load levels L_1, L_2 and L_3 occur daily during α, β and γ hours, respectively.

Given that $\alpha + \beta + \gamma = 24$, the following transition rates may be derived:

$$\lambda_{L21} = \lambda_{L31} = \frac{\alpha}{23}$$
$$\lambda_{L12} = \lambda_{L32} = \frac{\beta}{23}$$
$$\lambda_{L13} = \lambda_{L23} = \frac{\gamma}{23}$$

Combining the 3-state load model with the 4-state pipeline model from Fig. 2, gives the 12-state Markov model shown in Fig. 3.

According to Fig. 1, the main upstream unit is supported by a reserve unit that is defined to be in cold stand-by, to be switched into operation with an ideal switch. In order to have a realistic representation of the setup, the model in Fig. 3 is complemented with such a cold stand-by unit. This allows us to investigate the relation between the capacity of the reserve unit, the amount of prepared pipeline storage and the reliability of supply. The resulting 24-state model is not displayed here, but follows the same pattern as the 12-state model in Fig. 3. All further calculations are based on the 24-state model.

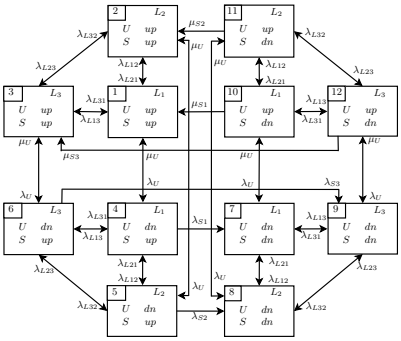

Figure 3. A 12-state Markov model representing one upstream unit U (either a compressor or a heating unit), the pipeline storage S and three load levels $L1 - L3$.

3. Physical Characteristics

In order to find a measure of the pipeline storage survival time and the corresponding storage failure rate, the dynamic responses of both a natural gas and a district heating pipeline system are simulated. Introductory descriptions of the physical characteristics of the two systems are given below.

3.1. *Natural Gas Systems*

Natural gas is a compressible medium, and the compressibility may be used by the pipeline operator to store extra amounts of gas in the pipeline system.

Under isothermal conditions, the governing set of equations for transient flow in natural gas pipelines comprise the state (1a), continuity (1b) and momentum (1c) equations. The numerical method known as the method of characteristics was applied for solving (1). The method is thoroughly described in [11].

$$B = \sqrt{zRT} \tag{1a}$$

$$\frac{B^2}{A}\frac{\partial m}{\partial x} + \frac{\partial p}{\partial t} = 0 \tag{1b}$$

$$\frac{\partial p}{\partial x} + \frac{1}{A}\frac{\partial m}{\partial t} + \frac{pg}{B^2}\sin(\theta) + \frac{fB^2m^2}{2DA^2p} = 0 \tag{1c}$$

where:

B = acoustic wavespeed in $\frac{m}{S}$

z = compressibility factor

R = gas constant in $\frac{m^2}{S^2K}$

T = temperature in K

A = cross-sectional area of pipe in m^2

m = mass rate of flow in $\frac{sm^3}{S}$

x = position along pipeline in m

p = pressure in bar

t = time in S

g = gravity in $\frac{m}{S^2}$

θ = angle between pipe and horizontal plane

f = friction factor

Consider a natural gas transmission pipeline as illustrated in Fig. 1a, working at steady state where the supply and demand are balanced. The initial relative mass flow (m) and pressure (p) distributions along the pipeline are shown in Fig. 4, step 1. A sudden loss of upstream compressor facilities was simulated, and the steps 2-4 in Fig. 4 show the dynamic response of the system at different time steps. Eventually, the pressure at the pipeline outlet falls below the critical pressure P_{crit} and the system has reached a failed state. In case $P_{crit} = 0.8$ for the system simulated in Fig. 4, the system's survival time and failure rate for this particular contingency is 1.68 $hours$ and 0.59 $hours^{-1}$, respectively.

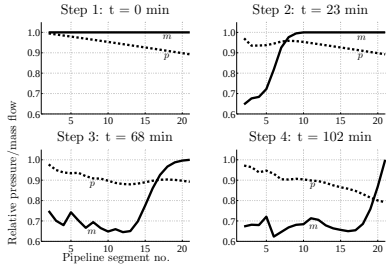

Figure 4. Dynamic response of a gas transmission pipeline experiencing a partly loss of supply. The solid-drawn line shows the relative mass flow (m) and the stapled line shows the relative pressure (p) in different pipeline segments. The pipeline is divided into 20 segments.

3.2. *District Heating System*

Studying the dynamics of energy flow in district heating systems involves both mass flow and temperature dynamics. Changes in flow are quickly transferred throughout the whole system in the form of pressure waves, typically taking only a few seconds. Temperature dynamics, on the other hand, is closely related to the speed of the circulating water

and the travelling time from the heat producing unit to the load may take hours. Consequently, this study only considers the loss of heat producing units, assuming that loss of compressor facilities may be added as an independent module in the reliability model. Temperature dynamics may be decoupled from the flow dynamics in a quasi-dynamic procedure, as described in [12]. Transient temperature distributions in district heating pipelines may be found by applying a convective transport equation, presented in (2).

$$\frac{\partial \phi}{\partial t} + v\frac{\partial \phi}{\partial x} + a\phi = 0 \tag{2}$$

where:

$\phi =$ relative temperature (the difference between temperature in the pipe and temperature of the ground) in $^{\circ}C$

$t =$ time in S

$x =$ position along pipeline in m

$v =$ flow velocity in $\frac{m}{S}$

$a =$ heat loss term in S^{-1}

Fig. 5 illustrates the response of a 10 km district heating transmission pipeline after partially loosing heat supply at the inlet, decreasing the inlet temperature from $100^{\circ}C$ to $60^{\circ}C$. The circulating speed of water was set to 1 $\frac{m}{S}$. Eventually, the temperature at the pipeline outlet falls below the critical temperature T_{crit} and the system has reached a failed state. In case $T_{crit} = 80^{\circ}C$, the system's survival time and failure rate for this particular contingency is 2.67 $hours$ and 0.38 $hours^{-1}$, respectively.

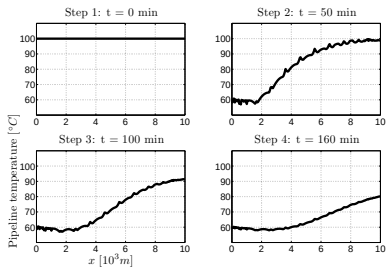

Figure 5. Dynamic response of a district heating pipeline experiencing a partly loss of supply. The figures show the pipeline temperature (in $^{\circ}C$) as a function of pipeline length (in 10^3 m) at different time steps.

4. Case Study

The presented modelling approach was applied to a simple, but practical natural gas transmission system. It should be noted that, once the survival times have been calculated, the procedure is essentially the same for the district heating system in Fig. 1b.

4.1. *A Natural Gas Case Study*

A natural gas transmission system as illustrated in Fig. 1a was analysed. The system has one compressor which is normally operating, and one compressor serving as reserve. Three load states were considered. Initially, a reserve unit with installed capacity of 1100 MW was considered, which is sufficient to meet the demand of load states 2 and 3, but not state 1. The physical and model parameters are given in Table 1. Based on these parameters, the corresponding storage failure rates were found as shown in Table 2. The results are not significantly sensitive to the storage repair rates (μ_{s1}, μ_{s2} and μ_{s3} in Fig. 3), and it was assumed that the storage cannot be charged as long as the main compressor is not operating.

Table 1
Natural gas system parameters.

Physical Parameters			**Model Parameters**		
Symbol	**Data**	**Unit**	**Symbol**	**Data**	**Unit**
P_{in}	80	bar	α	3	-
P_{crit}	60	bar	β	9	-
L_1	1500	MW	γ	12	-
L_2	1100	MW	λ_U	2	failures/year
L_3	700	MW	λ_R	2	failures/year
Length	100	km	μ_U	0.10	$hours^{-1}$
Diameter	0.46	m	μ_R	0.10	$hours^{-1}$
f	0.013	-			

Table 2
Storage failure rates for the natural gas system.

Symbol	**Capacity [MW]**	**Load [MW]**	**Rate [$hour^{-1}$]**
λ_{S1}	0	1500	0.53
λ_{S2}	0	1100	0.33
λ_{S3}	0	700	0.26
λ_{S4}	1100	1500	0.21

Four failure states are recognised. Obviously, the three states where both compressors are down together with an empty storage are failure states. Furthermore, in case only the reserve compressor is operating and the load is at its maximum (L_1), supply does not meet demand, and the storage will be discharged at a rate λ_{S4} presented in Table 2. When the storage has been fully discharged, the fourth failure state is reached.

Solving the 24-state Markov model, the annual expected time residing in one of the four failure states is 0.78 hours/year and the corresponding frequency of being in a failed state is 0.78 $year^{-1}$.

The reliability of the system is sensitive to the frequency of peak-load hours. By varying the number of peak-load occurrences per day (α), the average annual outage time and the average failure rate varied as shown in Fig. 6.

It was also of interest to investigate the impact of reserve unit size on the system's reliability. In Fig. 7 the average annual outage time is presented for some reserve unit sizes. The ability of the reserve unit to sufficiently serve the

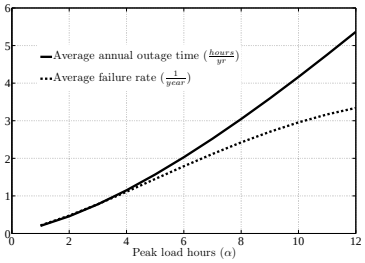

Figure 6. Average annual outage time and average failure rate as functions of the number of peak load hours (α).

three load states was clearly influential on the outage time. In addition, by increasing the reserve unit size in between load steps, e.g. from 700 to 800 MW, the survival time was improved, giving an improvement in reliability, as seen in Fig. 7.

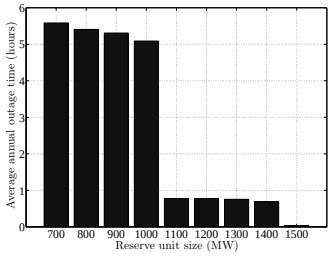

Figure 7. Average annual outage time for different reserve unit sizes.

4.2. *Model Verification*

In order to evaluate the error introduced by considering the states in Fig. 3 as memoryless, Monte Carlo simulations following the system state transition sampling approach described in [13] were performed. Transitions from a system state depends randomly on the state duration of the component or load level which departs earliest from its present state. The data from Table 1 was applied and the continuous pipeline storage level, represented as vectors of mass flow and pressure distributions, was continously mapped throughout the simulations.

Two simulations were run and their convergence processeses are shown in Fig. 8 together with a horizontal line indicating the analytical result. First, the reserve unit capacity was set to 1100 MW, which is enough to cover load states 2 and 3, but not load state 1. Running the Monte Carlo simulation with a total simulation time of 3000 hours gave an outage time of 0.98 hours/year, which is approximately 26 % higher than the analytical result. The system state comprising a non-operating main compressor, an operating reserve compressor and a charged storage will experience storage discharge in load state 1, but not in load states 2 and 3. As the continuous charge level is not mapped in the Markov model, switching from load state 1 to any of the other load states will in this case reset the storage to a fully charged state. Thus, the analytical result gave a slightly optimistic estimate of average annual outage time.

Second, a fully redundant reserve compressor was considered. Applying a total simualtion time of 80000 years, the gap between the simulated and the analytical result was negligible, as shown in the lower part of Fig. 8.

For comparison, in case the effect of pipeline storage is ignored, i.e. all storage failure rates are set equal to zero, the resulting average annual outage time is 2.53 hours/year in the first case and 0.046 hours/year with a fully redundant reserve compressor.

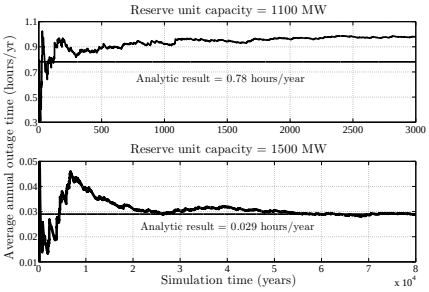

Figure 8. Average annual outage time as a function of number of simulated years. The top figure refers to reserve compressor capacity of 1100 MW, and the bottom figure to a fully redundant reserve compressor.

5. Conclusions

The presented model serves the general purpose of addressing pipeline storage and its impact on reliability of supply in energy pipeline systems. A Markovian approach was chosen to quantify pipeline system reliability, and the concepts of storage failure and repair times of a pipeline storage were introduced.

A simple example from the natural gas domain was presented, and the average annual outage times and the average failure rates were calculated for different system configurations. It was discussed how the model can be applied to district heating systems as well. The results indicate the significant impact of storage on reliability in large energy pipeline systems. Comparing the analytical results from the Markov model with Monte Carlo simulations indicated that, altough a bit optimistic, the presented approach captures the impact of pipeline storage on reliability of supply.

References

[1] R. L. Mansell, Methodology for evaluating natural gas transmission system reliability levels and alternatives, Tech. rep., Wright Mansell Research Ltd. (1991).

[2] A. Carpignano, M. Piccini, M. Gargiulo, A. Ponta, Reliability and availability evaluation of highly meshed network systems: status of the art and new perspectives, in: Annual Reliability and Maintainability Symposium, 2002.

[3] W. S. Chmilar, Pipeline reliability evaluation and design using the sustainable capacity method, in: Proceedings of the International Pipeline Conference, 1996.

[4] P. M. Li, Security assessment of gas networks, International Journal for Numerical Methods in Engineering 11 (1977) 963–973.

[5] R. Billinton, R. N. Allan, Reliability Evaluation of Power Systems, 2nd Edition, Plenum Press, 1996.

[6] P. Massee, J. T. M. Van Kempen, The operation and reliability of a gas production and distribution system, in: Proccedings of International Centre for Heat and Mass Transfer, 1990.

[7] M. Mohitpour, J. Szabo, T. Van Hardeveld, Pipeline Operation and Maintenance: A Practical Approach, ASME Press, 2005.

[8] R. G. Carter, H. H. Rachford, Optimizing line pack management to hedge against future load uncertainty, in: Pipeline Simulation Interest Group, 2003.

[9] G. Koeppel, Multi-carrier systems and the effect of energy storage, Ph.D. thesis, Swiss Federal Institute of Technolgy ETH Zurich (2007).

[10] R. Ringlee, A. Wood, Frequency and duration methods for power system reliability calculations: II – demand model and capacity reserve model, IEEE Transactions on Power Apparatus and Systems PAS-88 (4) (1969) 375–388.

[11] E. B. Wylie, V. L. Streeter, Fluid Transients in Systems, Prentice Hall, 1993.

[12] H. Pálsson, H. V. Larsen, B. Böhm, H. F. Ravn, J. Zhou, Equivalent models of district heating systems, Tech. rep., Department of Energy Engineering, Technical University of Denmark and Systems Analysis Department, Risö National Laboratory (1999).

[13] R. Billinton, L. Wenyuan, Reliability Assessment of Electric Power Systems Using Monte Carlo Methods, Plenum Press, 1994.

Bibliography

[1] J. Endrenyi, *Reliability Modeling in Electric Power Systems.* John Wiley & Sons, 1978.

[2] R. Billinton and R. N. Allan, *Reliability Evaluation of Power Systems*, 2nd ed. Plenum Press, 1996.

[3] R. E. Brown, *Electric Power Distribution Reliability.* Marcel Dekker, 2002.

[4] R. Billinton, M. Fotuhi-Firuzabad, and L. Bertling, "Bibliography on the application of probability methods in power system reliability evaluation 1996-1999," *IEEE Transactions on Power Systems*, vol. 16, no. 4, pp. 595 – 602, 2001.

[5] G. Kjølle *et al.*, "Adequate interruption cost assessment in a quality based regulation regime," in *Proc. of IEEE Porto Power Tech Conference*, Porto, Portugal, 2001.

[6] R. Billinton and R. Allan, "Power system reliability in perspective," *IEE J. Electron. Power*, vol. 30, pp. 231–236, 1984.

[7] E. Lakervi and E. J. Holmes, *Electricity Distribution Network Design*, 2nd ed. Peter Peregrinus Ltd., 1995.

[8] M. E. Baran and F. F. Wu, "Network reconfiguration in distribution systems for loss reduction and load balancing," *IEEE Transactions on Power Delivery*, vol. 4, no. 2, pp. 1401–1407, 1989.

[9] R. N. Allan, E. N. Dialynas, and I. R. Homer, "Modelling and evaluating the reliability of distribution systems," *IEEE Transactions on Power Apparatus and Systems*, vol. PAS-98, no. 6, pp. 2181–2189, 1979.

[10] G. Kjølle and K. Sand, "RELRAD - An analytical approach for distribution system reliability assessment," *IEEE Transactions on Power Delivery*, vol. 7, no. 2, pp. 809–814, 1992.

[11] R. E. Brown and A. P. Hanson, "Impact of two-stage service restoration on distribution reliability," *IEEE Transactions on Power Systems*, vol. 16, no. 4, pp. 624–629, 2001.

[12] CIGRE TF 38.06.01, "Methods to consider interruption costs in power system analysis," 2001.

[13] K. Samdal *et al.*, "Sluttbrukeres kostnader forbundet med avbrudd og spenningsforstyrrelser," SINTEF Energy Research, Tech. Rep., 2003 [in Norwegian].

[14] L. Pedersen, "Load modelling of buildings in mixed energy distribution systems," Ph.D. dissertation, Norwegian University of Science and Technology, 2007.

[15] A. Helseth and A. T. Holen, "Impact of energy end-use on optimal allocation of switchgear in radial distribution networks," in *Proc. of International Symposium on Modern Electric Power Systems*, Wrocław, Poland, 2006.

[16] V. Miranda, A. do Vale, and A. Cerveira, "Optimal emplacement of switching devices in radial distribution networks," in *Proc. of CIRED'83*, vol. 13, Liège, Belgium, 1983.

[17] F. Soudi and K. Tomsovic, "Optimized distribution protection using binary programming," *IEEE Transactions on Power Delivery*, vol. 13, no. 1, pp. 218–224, 1998.

[18] R. Billinton and S. Jonnavithula, "Optimal switching device placement in radial distribution systems," *IEEE Transactions on Power Delivery*, vol. 11, no. 3, pp. 1646–1651, 1996.

[19] P. Wang and R. Billinton, "Demand-side optimal selection of switching devices in radial distribution system planning," *IEE Proceedings - Generation, Transmission and Distribution*, vol. 145, no. 4, pp. 409–414, 1998.

[20] G. Levitin, S. Mazal-Tov, and D. Elmakis, "Optimal sectionalizer allocation in electric distribution systems by genetic algorithm," *Electric Power Systems Research*, vol. 31, no. 2, pp. 97–102, 1994.

[21] R. E. Brown *et al.*, "A genetic algorithm for reliable distribution system design," in *Proc. of Intelligent Systems Applications to Power Systems*, Orlando, USA, 1996, pp. 29–33.

[22] L. G. W. da Silva, R. A. F. Pereira, and J. R. S. Mantovani, "Allocation of protective devices in distribution circuits using nonlinear programming models and genetic algorithms," *Electric Power Systems Research*, vol. 69, no. 1, pp. 77–84, 2003.

[23] R. N. Allan *et al.*, "A reliability test system for educational purposes - Basic distribution system data and results," *IEEE Transactions on Power Systems*, vol. 6, no. 2, pp. 813–820, 1991.

[24] R. Billinton and S. Jonnavithula, "A test system for teaching overall power system reliability assessment," *IEEE Transactions on Power Systems*, vol. 11, no. 4, pp. 1670–1676, 1996.

[25] W. Mansell, "Methodology for evaluating natural gas transmission system reliability levels and alternatives," Wright Mansell Research Ltd., Study prepared for the Canadian Petroleum Association, 1991.

[26] P. M. Li, "Security assessment of gas networks," *International Journal for Numerical Methods in Engineering*, vol. 11, no. 6, pp. 963–973, 1977.

[27] W. S. Chmilar, "Pipeline reliability evaluation and design using the sustainable capacity method," in *Proc. of International Pipeline Conference*, vol. 2, Calgary, Canada, 1996, pp. 803–810.

[28] T. van der Hoeven, T. Fournier, and E. van Meurs, "Planning of the transport system based on reliability figures of the components," in *Proc. of the PSIG Annual Meeting*, San Francisco, USA, 1996.

[29] M. Mohitpour, J. Szabo, and T. van Hardeveld, *Pipeline Operation & Maintenance - A Practical Approach*. American Society of Mechanical Engineers, 2004.

[30] URS-Corporation, "Safety performance and integrity of the natural gas distribution infrastructure," American Gas Foundation, Tech. Rep., 2005.

[31] European Gas Pipeline Incident Data Group, "Gas pipeline incidents: 6th report 1970-2004," European Gas Pipeline Incident Data Group (EGIG), Tech. Rep., 2005.

[32] M. Scarrone, N. Piccinini, and C. Massobrio, "A reliability data bank for the natural gas distribution industry," *Journal of Loss Prevention in the Process Industries*, vol. 2, no. 4, pp. 235–239, 1989.

[33] S. C. Erichsen, "Gas distribution," in *Workshop on Reliability in Energy Distribution Systems*, Trondheim, Norway, 2005.

[34] M. Paty, "Security and gas distribution network structures," in *Proc. of International conference on natural gas technologies: Energy security, environment and economic development*, Kyoto, Japan, 1993.

[35] I. C. Campell, "Fail-safe control for gas distribution systems: The need for gas protection in the urban environment," in *Proc. of the High Consequence Operations Safety Symposium II*, Albuquerque, USA, 1997.

[36] J. Røstum *et al.*, "AQUAREL - A computer program for water network reliability analysis combining hydraulic, reliability and failure models," in *Proc. of Water Network Modelling for Optimal Design and Management*, Exeter, UK, 2000.

[37] A. J. Osiadacz and M. Gorecki, "Optimization of pipe sizes for distribution gas network design," in *Proc. of the PSIG Annual Meeting*, Albuquerque, USA, 1995.

[38] A. Andersson and C. Mattson, "Leveranssäkerhet i fjärrvarmesystem," Värmeforsk, Tech. Rep., 1989 [in Swedish].

[39] B. G. Dahlman *et al.*, "Leveranssäkerhet," Värmverksföreningen, Tech. Rep., 1992 [in Swedish].

[40] G. Ballocco, A. Carpignano, and M. Gargiulo, "Merging cut sets methods and reliability indexes for reliability and availability analysis of highly meshed networks," in *Proc. of European Safety and Reliability Conference (ESREL)*, Maastricht, The Netherlands, 2003.

[41] A. Ponta, C. Tripodi, and S. Bertocci, "Reliability analysis of Torino sud district heating system," in *Proc. of Reliability and Maintainability Symposium*, Washington DC, USA, 1999.

[42] A. Carpignano *et al.*, "Merging FT approach with the indexes approach to assess the reliability and availability of heating distribution networks," in *Proc. of European Safety and Reliability Conference (ESREL)*, Torino, Italy, 2001.

[43] ——, "Reliability and availability evaluation for highly meshed network systems: status of the art and new perspectives," in *Proc. of Reliability and Maintainability Symposium*, Philadelphia, USA, 2002.

[44] ——, "Monte Carlo method application for reliability and availability of highly meshed network systems," in *Proc. of European Safety and Reliability Conference (ESREL)*, Berlin, Germany, 2004.

[45] P. Valdimarsson, "Modelling of geothermal district heating systems," Ph.D. dissertation, University of Iceland, 1993.

[46] H. Pálsson *et al.*, "Equivalent models of district heating systems for online minimization of operational costs of the complete district heating system," Risö National Laboratory, Tech. Rep., 1999.

[47] H. V. Larsen *et al.*, "Aggregated dynamic simulation model of district heating networks," *Energy Conversion and Management*, vol. 43, no. 8, pp. 995–1019, 2002.

[48] A. M. Quelhas, E. Gil, and J. D. McCalley, "Nodal prices in an integrated energy system," *Int. J. Critical Infrastructures*, vol. 2, no. 1, pp. 50–69, 2006.

[49] M. Geidl and G. Andersson, "A modeling and optimization approach for multiple energy carrier power flow," in *Proc. of IEEE PES PowerTech*, St. Petersburg, Russian Federation, 2005.

[50] B. Böhm *et al.*, "Simple models for operational optimisation," IEA District Heating and Cooling, Tech. Rep., 2002.

[51] R. W. Jeppson, *Analysis of Flow in Pipe Networks*. Ann Arbor Science, 1977.

[52] P. Massee and J. T. M. V. Kempen, "The operation and reliability of a gas production and distribution system," in *Proc. of Mathematical Modelling and Computer Simulation of Processes in Energy Systems*, 1990.

[53] S. Ohanian and R. Kurz, "Transient simulation of the effects of compressor outage," in *Proc. of the PSIG Annual Meeting*, Palm Springs, USA, 2003.

[54] R. G. Carter and H. H. Rachford, "Optimizing line pack management to hedge against future load uncertainty," in *Proc. of the PSIG Annual Meeting*, Palm Springs, USA, 2003.

[55] T. R. Weymouth, "Problems in natural gas engineering," *Transactions of the ASME*, vol. 34, pp. 185–234, 1912.

[56] E. S. Menon, *Gas Pipeline Hydraulics*. Taylor & Francis, 2005.

[57] C. Chauvelier-Alario, B. Mathieu, and C. Toussaint, "Decision making software for Gaz de France distribution network operators: CARPATHE," in *Proc. of 23rd World Gas Conference*, Amsterdam, The Netherlands, 2006.

[58] M. P. Nowak and M. Westphalen, "A linear model for transient gas flow," in *Proc. of Intnl. Conf. on Efficiency, Costs, Optimization, Simulation and Environmental Impact of Energy Systems (ECOS)*, Copenhagen, Denmark, 2003.

[59] M. Rausand and A. Høyland, *System Reliability Theory; Models, Statistical Methods and Applications*, 2nd ed. Wiley-Interscience, 2004.

[60] B. H. Bakken, H. I. Skjelbred, and O. Wolfgang, "eTransport: Investment planning in energy supply systems with multiple energy carriers," *Energy*, vol. 32, no. 9, pp. 1676–1689, 2007.

[61] M. Geidl and G. Andersson, "Optimal power flow of multiple energy carriers," *IEEE Transactions on Power Systems*, vol. 22, no. 1, pp. 145–155, 2007.

[62] G. Koeppel, "Multi-carrier systems and the effect of energy storage," Ph.D. dissertation, Swiss Federal Institute of Technolgy ETH Zürich, 2007.

[63] A. Osiadacz, *Simulation and Analysis of Gas Networks*. Gulf Publishing Company, 1987.